ABSTRACT

Title of dissertation: PHENOMENOLOGICAL ASPECTS OF HEAVY QUARK SYSTEMS

Paul M. Hohler, Doctor of Philosophy, 2008

Dissertation directed by: Professor Thomas D. Cohen
Department of Physics

The systems of heavy quarks are particularly interesting because they lend themselves to effective field theory techniques. Typically this involves considering an expansion about the limit of infinitely heavy quarks. In this limit, the phenomenology of heavy quark systems differs qualitatively from light quark systems; this provides a window into the workings of QCD. However, in the real world, heavy quarks have a finite mass. This dissertation will examine a number of heavy quark systems and describe the associated phenomenology It will also probe the extent to which realistic systems are well approximated by expansions about the heavy quark limit. This will be done with direct comparison with experimental data and models with a finite heavy quark. In the end, this study will show that, many of the systems considered here, it is unlikely that realistic heavy quarks can be accurately described by such expansions.

PHENOMENOLOGICAL ASPECTS OF HEAVY QUARK SYSTEMS

by

Paul M. Hohler

Dissertation submitted to the Faculty of the Graduate School of the
University of Maryland, College Park in partial fulfillment
of the requirements for the degree of
Doctor of Philosophy
2008

Advisory Committee:
Professor Thomas D. Cohen, Chair/Advisor
Professor Paulo F. Bedaque
Professor Elizabeth Biese
Professor Lyle Isaacs
Professor Stephen J. Wallace

Acknowledgments

A dissertation such as this and progress through a Ph.D. program cannot be done alone. There are many people who I would like to acknowledge for their support of me during the past five years.

First, I would like to thank my advisor Tom Cohen. I have greatly enjoyed working with him and learning from him. We have spent countless hours discussing physics together. So thank you Tom, for your time, your knowledge, and your interest in my well being.

I also appreciate all of the assistance that the TQHN group has provided. There is a real warmth in the group which makes all of us happy to be here and produces an environment which fosters a healthy exchange of ideas and encourages learning and questioning from their students.

I need to acknowledge the contribution of my additional collaborators, Richard Lebed and Aleksey Cherman.

My parents have always been supportive and encouraging throughout my life, so thanks Mom and Dad.

My life as a graduate student would have been a lot less interesting and rewarding if it hadn't been for my girlfriend Melinda Wilson. In addition to the fun and excitement that we have shared, I thank her for the compassion and companionship which she has shared with me.

Finally, I would like to that the D.O.E. for supporting this work through grant DE-FGO2-93ER-40762.

Table of Contents

List of Tables

List of Figures

Chapter 1

Introduction

1.1 Overview

Quantum Chromodynamics (or QCD) is believed to be the fundamental theory describing hadronic physics. One key goal of nuclear and hadronic physics is to use the fundamental principles of QCD to explain nuclear and hadronic phenomena. However, QCD is a non-linear theory which makes the task of understanding hadronic phenomena extremely difficult from first principles. To gain insights into the complexity of QCD, one often must resort either to models which are intended to capture specific aspects of QCD or derive effective theories in particular limits of QCD and to develop expansions about them. In either method, it is always important to relate the models and the effective theories back to QCD and experimental physics.

One important subset of QCD physics is the examination of heavy quark systems. Hadronic systems which contain heavy quarks provide unique and interesting phenomenology compared with their lighter counterparts. The heavy quark, in these systems, provides an additional handle for understanding QCD because the heavy quark has a typical energy scale which is different from the light quarks. The presence of two scales in heavy quark systems naturally leads to the construction of an effective theory and a small parameter out of which a peturbative expansion can be

made.

This dissertation will examine the phenomenology of a variety of different heavy quark systems. The systems were chosen because of their connection to hadronic states beyond the naïve quark model. In each of the systems considered, the phenomenology of systems where the heavy quark mass is taken to be arbitrarily large (this is known as the heavy quark limit) is examined. This limit may be well justified for these systems since the heavy quark mass is much heavier than any other energy scale in the problem. However, much of the work presented here will investigate how close these systems are in practice to this extreme limit for realistic systems. In other words, does one expect to be able to experimentally detect some of the unique features of the heavy quark limit in these particular systems?

The systems that will be examined here include: the formation of heavy pentaquark states from heavy meson-nucleon interactions in a potential model, the examination of heavy baryon states in the context of the Skyrme model, and the use of an emergent symmetry of QCD to relate doubly heavy diquarks to heavy antiquarks. A final system considered is very different from the others as it pertains to understanding the ratio of viscosity to entropy density as a universal property of fluids. This is related to the other chapters as gas of heavy mesons (mesons containing a single heavy quark) plays a central role. Furthermore, the theme of trying to understand one's expectations of QCD is again revisited for these fluid systems.

What makes QCD so difficult? QCD is constructed as a non-abelian gauge theory based upon the group $SU(3)_C$ [1, 2, 3]. This group structure is due to the belief that quarks have an intrinsic degree of freedom, called color, which comes in

three types, red, blue, and green. In the theory, the interactions between quarks is mediated by particles known as gluons which are represented by the gauge fields. The gauge structure of the theory leads to a relatively simple Lagrangian,

$$\mathcal{L}_{\text{QCD}} = \sum_{\text{flavors}} \bar{q}(i\not{D} - m_f)q - \frac{1}{4}G^A_{\mu\nu}G^{\mu\nu}_A, \tag{1.1}$$

where q are the quark fields, D_μ is the covariant derivative, m_f is the bare mass of each flavor of quark, and $G^A_{\mu\nu}$, the field strength of the gluon fields, is defined as $G^A_{\mu\nu} \equiv \partial_\mu A^A_\nu + \partial_\nu A^A_\mu + if^{ABC}A^B_\mu A^C_\nu$ with f^{ABC} as the $SU(3)$ structure constant and A^A_μ as the gluon field. The covariant derivative is defined as $D_\mu = \partial_\mu + igt^C A^C_\mu$ where t^C is a matrix of the fundamental representation of $SU(3)$, and g is the QCD bare strong coupling constant.

At first glance the structure of the QCD Lagrangian does not appear to be very complicated. There are terms for the kinetic energy for both quarks and gluons as well as interaction terms stemming from the covariant derivative. The difficulties begin when one expands out the field strength term, $-\frac{1}{4}G^A_{\mu\nu}G^{\mu\nu}_A$, in terms of the gluon fields. From this expansion, one discovers that there are three and four gluon interaction terms. These additional three and four gluon interactions expand the number of Feynman diagrams for a particular process. These added diagrams inherently lead to complications. A critical one is that when one attempts to determine the running of the strong coupling constant, these added interactions cause the coupling to grow at low energies. This running is exactly opposite to that of the couplings for the electro-magnetic and weak forces where at low energies their couplings are weak. This phenomenon, where the strong coupling constant is small

at high momenta, is called asymptotic freedom and was first derived in the context of QCD in Refs. [1, 4, 5, 6]. At low momenta, one expects the opposite, *i.e.*, large couplings. The large couplings prevent a meaningful perturbative expansion in powers of the strong coupling constant for low energy hadronic physics. This lack of a perturbative expansion greatly complicates hadronic calculation from the fundamental principles of QCD and necessitates the use of non-perturbative techniques in dealing with QCD.

There are many non-perturbative techniques which have been useful in studying QCD. The technique which when applicable captures QCD is lattice QCD. By using different computation techniques, one can approximate QCD path integrals numerically. In the future, this technique should allow physicists to numerically solve QCD with increasing accuracy. Currently simplifying approximations are needed for many observables due to computational power.

The most important non-perturbative technique for this dissertation is the use of effective field theories. In general, effective field theory is a technique which is useful when a theory has a clean separation of at least two scales. For the case of two distinct scales, these two scales can be thought of as a high energy and a low energy scale. Typically, the low energy scale would control the long-distance effects while the high energy scale is needed to probe short-distance effects. In certain problems, these two energy scales do not influence one another. In these cases, an effective field theory is a very practical tool. Instead of describing the system in terms of the original degrees of freedom, effective field theory is based on effective degrees of freedom which incorporate the short-distance physics in a non-perturbative manner.

For example, in chiral perturbation theory, the bare quark mass is assumed to be small. This allows one to integrate out the short-distance effects of the light quarks and the gluons and describe a theory of light mesons. Chiral perturbation theory can investigate the meson interactions and hadronic effects without the complication associated with forming the meson states which is included in the full theory of QCD. Effective field theory techniques are especially important because they can be applied to any system in which a separation of scale is seen.

Effective field theories are particularly powerful in the context of QCD because they can convert a theory without a naïve perturbative expansion into one with a well-defined expansion. However, the perturbative expansion produced by effective theories is still susceptible to the standard problems of expansions. The expansion, and thereby the effective theory, will break down when either the expansion parameter can no longer be treated as small or the coefficients of the expansion, which are assume to be $O(1)$, are unusually large. In this study, when it is shown that the chosen effective theory is no longer applicable, it will be due to one of these two problems.

Heavy quark physics lends itself very well to the effective field theory approach to QCD because of the scale separation between the heavy quark mass, m_Q, and the hadronic scale, Λ_H. In the next section, the heavy quark effective theory (HQET) will be discussed. The section following that introduces the large N_c limit. This is another technique (though not an effective theory) which can translate QCD into a systematic expansion. Though it may not be immediately obvious at the outset, the large N_c limit and the $1/N_c$ expansion play a critical role in this work. This chapter

concludes with a historical introduction to exotic particles, or hadrons not derivable from a naïve quark model. These sections are intended to provide the theoretical backbone as well as the context for the other chapters.

The remaining chapters in this dissertation are structured as follows. Chapter 2 investigates the existence of heavy pentaquark states and attempts to construct such states from the binding of a heavy meson and a nucleon through a one-pion exchange potential. Chapter 3 extends this work in the context of a Skyrme type model. The investigation there focuses on the binding of regular heavy baryons with some insights into heavy pentaquark states. Lastly this chapter analyzes the Isgur-Wise function using the framework of the Skyrme model.

Chapter 4 investigates an emergent symmetry of QCD, namely the doubly heavy quark – anti-quark symmetry. This chapter compares the hadronic spectrum expected from the heavy quark limit with that observed in nature, and examines the possibility that this symmetry may be relevant in understanding the physical spectrum. The last chapter of this dissertation, Chapter 5, is somewhat different from the work in the other chapters. This chapter investigates the claim that a universal bound on the ratio of shear viscosity to entropy density exists. A heavy quark system, that of a heavy meson gas, plays a critical role in examining this claim. A specific counterexample to the claim of a universal bound is examined.

The research presented here is based upon the work in Refs. [7, 8, 9, 10] and borrows substantially from them.

1.2 Heavy Quark Effective Theory

The heavy quark limit and heavy quark effective theory (HQET) play important roles in the work presented here. Therefore a thorough introduction of these topics will be presented. The concept of a heavy quark limit was considered by Isgur and Wise [11, 12], while the development of HQET had contributions from Refs. [13, 14, 15] along with others.

When considering heavy quark physics, one immediately observes the natural presence of two scales; the mass of the heavy quark m_Q and the hadronic scale Λ_H, which is typically taken to be $\Lambda_{\rm QCD}$ or a few times this. The heavy quark limit considers the case when $m_Q \gg \Lambda_H$, or equivalently, $m_Q \to \infty$ while Λ_H remains finite. In this limit, one can formulate an effective field theory with the expansion parameter $\frac{\Lambda_H}{m_Q}$. This effective theory is Heavy Quark Effective Theory (HQET).

To formulate HQET consider the following. In the heavy quark limit, though the mass of the quark is very large, the momentum of the particle may be finite. Because of this, it is conventional to label the states not by their momentum, but by their velocity. This transformation is simply achieved by having $\vec{p} = m_Q \vec{v}$. Furthermore, the large quark mass suppresses the pair creation of heavy quarks. To understand this suppression, remember that one can always describe the heavy quark's on shell momentum as $\vec{p} = m_Q \vec{v}$. If the particle is off shell, it can only be off shell by an amount of order Λ_H because this is the natural scale of the dynamics. Therefore, the off shell energy is not sufficient to create a second heavy quark.

Using these ideas, HQET can be formulated as in Ref. [16]. To begin, consider

the Fourier decomposition of a heavy quark field:

$$q = e^{-im_Q \mathbf{v}\cdot\mathbf{x}} h_v^{(Q)}(\mathbf{x}), \tag{1.2}$$

where $h_v^{(Q)}$ is the field which destroys the heavy quark with velocity v and heavy quark flavor Q. Again note that the creation of a heavy anti-quark is not possible with this field due to pair creation suppression. The heavy quark field, h_v, also satisfies the relation,

$$\not{v} h_v^{(Q)} = h_v^{(Q)}. \tag{1.3}$$

Inserting this field into the quark term in the QCD Lagrangian, Eq. (1.1), the HQET Lagrangian to leading order becomes

$$\mathcal{L}_0^{\text{HQET}} = \bar{h}_v^{(Q)}(i\not{D} - m_Q(1 - \not{v}))h_v^{(Q)} \tag{1.4}$$

which can be reduced using Eq. (1.3) to

$$\mathcal{L}_0 = \bar{h}_v^{(Q)} iv \cdot D h_v^{(Q)}. \tag{1.5}$$

Note a few observations about this Lagrangian. This Lagrangian does not depend on the spin of the heavy quark; this in turn suggests that at leading order HQET has an emergent $SU(2)$ spin symmetry [11, 12]. This spin symmetry implies that hadronic states which differ only in the heavy quark spin, such as the D and D^* or B and B^* mesons, should be degenerate. As will be shown, this degeneracy will be broken at next-to-leading order. The leading order Lagrangian also has a $SU(N_f)$ flavor symmetry where N_f is the number of heavy quark flavors. This is because the derived Lagrangian is independent of heavy quark flavor, so each quark flavor

which is massive enough to consider HQET will lead to this same leading order Lagrangian.

The $1/m_Q$ corrections to this leading order Lagrangian can be easily formulated. There are two sources for $1/m_Q$ corrections. The first comes from extending the kinetic energy terms. This can be done by considering the first correction to the h_v field. That is, the Fourier decomposition of Eq. (1.2) can be written as

$$q = e^{-im_Q \mathbf{v}\cdot\mathbf{x}}[h_v^{(Q)} + \chi_v^{(Q)}] \tag{1.6}$$

where the field χ_v is $1/m_Q$ suppressed from h_v and has the property that

$$\not{v}\chi_v = -\chi_v. \tag{1.7}$$

Furthermore, one can express χ_v in terms of h_v by using Eq. (1.6) in the equation of motion for the q field,

$$(i\not{D} - m_Q)q = 0. \tag{1.8}$$

This leads to

$$\chi_v^{(Q)} = \frac{1}{2m_Q} i\not{D}[h_v^{(Q)} + \chi_v^{(Q)}] \rightarrow \frac{1}{2m_Q} i\not{D} h_v^{(Q)} + O(1/m_Q). \tag{1.9}$$

Using this expression for the χ field and Eq. (1.6) in the original QCD Lagrangian leads to the leading order heavy quark Lagrangian of Eq. (1.5) and the $1/m_Q$ correction,

$$\mathcal{L}_1^{\text{kin}} = \bar{h}_v^{(Q)} \frac{(iD)^2}{2m_Q} h_v^{(Q)}. \tag{1.10}$$

The second $1/m_Q$ correction to the heavy quark Lagrangian comes from considering the color magnetic moment couplings. This is $O(1/m_Q)$ because the color magnetic

moment is proportional to $1/m_Q$ as with normal quarks. This leads to the term

$$\mathcal{L}_1^{\rm cmm} = -\alpha_2(\mu)\bar{h}_v^{(Q)} g \frac{G_{\alpha\beta}\sigma^{\alpha\beta}}{4m_Q} h_v^{(Q)}, \tag{1.11}$$

where g is the strong coupling constant, G is the color field strength, and $\alpha_2(\mu)$ is the color magnetic coupling which can be renormalized. Examining the two $1/m_Q$ corrections in Eqs. (1.10) and (1.11) reveals that neither term preserves the flavor symmetry of the leading order Lagrangian (because both depend on flavor dependent quark mass) while only Eq. (1.10) preserves the spin symmetry. In the end, the HQET Lagrangian through $O(1/m_Q)$ reads:

$$\mathcal{L}_{\rm HQET} = \bar{h}_v^{(Q)} iv\cdot D h_v^{(Q)} + \bar{h}_v^{(Q)} \frac{(iD)^2}{2m_Q} h_v^{(Q)} - \alpha_2(\mu)\bar{h}_v^{(Q)} g \frac{G_{\alpha\beta}\sigma^{\alpha\beta}}{4m_Q} h_v^{(Q)}. \tag{1.12}$$

Further corrections to this Lagrangian can be derived in a manner similar to that described here.

In addition to expressing HQET at the level of heavy quarks, one can consider the physics from the hadronic level [17]. Here instead of investigating the dynamics of heavy quarks, the relevant degrees of freedom become heavy mesons. Since the heavy and light quarks decouple within the heavy mesons in the heavy quark limit, the structure of the effective theory of mesons should be similar to the structure of the heavy quark theory. When coupling the heavy mesons to the light hadrons, it is important that the light hadrons exhibit chiral symmetry. This is incorporated in the standard way for chiral perturbation theory. Here the light mesons with two light quark flavors are treated as the pseudo-Goldstone bosons creating by breaking the $SU(2)_L \times SU(2)_R$ chiral symmetry into the $SU(2)_V$ vector subgroup. These

pseudo-Goldstone fields can be expressed as

$$\Sigma = \exp\Big(\frac{2iM}{f_\pi}\Big) \tag{1.13}$$

where M is the meson mass matrix, defined for two light flavors as,

$$M = \begin{bmatrix} \sqrt{\frac{1}{2}}\pi^0 & \pi^+ \\ \pi^- & -\sqrt{\frac{1}{2}}\pi^0 \end{bmatrix}, \tag{1.14}$$

and f_π is the pion decay constant. In addition to the Σ field, it is also useful to define

$$\xi = \sqrt{\Sigma}. \tag{1.15}$$

It is equivalent to describe the mesons in terms of either the Σ or the ξ fields. However, it may be more convenient to use one or the other for different systems.

In addition to the chiral symmetry of the light mesons, the effective theory should exhibit the symmetries associated with the heavy quark limit, namely the spin symmetry. As mentioned before, this symmetry creates a degeneracy between the pseudoscalar D meson and the vector D^*. To incorporate this symmetry into the effective Lagrangian, a new heavy meson field which combines these two spin states into one field can be defined;

$$H_a = \frac{(1+\not{v})}{2}[P^*_{a\mu}\gamma^\mu - P_a\gamma_5], \tag{1.16}$$

where $P^*_{a\mu}$ destroys the vector state, P_a destroys the pseudoscalar state, v is the velocity of the heavy meson, and a is a flavor label of the light quark in the meson. Just as with the heavy quark fields, the operators only destroy heavy particles, and never create heavy anti-particles. The vector field is also subject to the constraint

$v_\mu P_a^{\mu *} = 0$. Furthermore, the field conjugate to H can also be introduced as,

$$\bar{H}_a = \gamma_0 H_a^\dagger \gamma_0 = [P_{a\mu}^{*\dagger}\gamma^\mu + P_a^\dagger \gamma_5]\frac{(1+\not{v})}{2}. \tag{1.17}$$

The effective Lagrangian which can be formed from these fields can be constructed by writing the most general Lagrangian coupling the two sets of fields.

$$\begin{aligned}\mathcal{L} = &- i\mathrm{Tr}\bar{H}_a v_\mu \partial^\mu H_a + \frac{i}{2}\mathrm{Tr}\bar{H}_a H_b v^\mu [\xi^\dagger \partial_\mu \xi + \xi \partial_\mu \xi^\dagger]_{ba} \\ &+ \frac{ig}{2}\mathrm{Tr}\bar{H}_a H_b \gamma_\nu \gamma_5 [\xi^\dagger \partial^\nu \xi - \xi \partial^\nu \xi^\dagger]_{ba} + \cdots ,\end{aligned} \tag{1.18}$$

where the ellipse denotes terms with more derivatives, terms which are $1/m_Q$ suppressed, or which explicitly break some of the symmetries. The trace in each of the terms is over spin states. One can show that this Lagrangian explicitly respects both the heavy quark symmetry as well as chiral symmetry. The first term in Eq. (1.18) is the kinetic energy of the heavy meson fields and has a similar structure to the kinetic term for heavy quarks. The second term couples the H field to the vector current of light mesons, $V^\mu = \frac{i}{2}(\xi^\dagger \partial^\mu \xi + \xi \partial^\mu \xi^\dagger)$, while the last term couples the H field to the axial current $A^\mu = \frac{i}{2}(\xi^\dagger \partial^\mu \xi - \xi \partial^\mu \xi^\dagger)$. The coupling to the vector current is fixed based upon the covariant derivative, while the axial coupling is not theoretically fixed by other symmetries and is given by g in Eq. (1.18).

It can also be useful to express the same Lagrangian rather in terms of the Σ fields. With the proper substitution the Lagrangian reads,

$$\mathcal{L} = -i\mathrm{Tr}\bar{H}_a v_\mu \partial^\mu H_a + \frac{i}{2}\mathrm{Tr}\bar{H}_a H_b v^\mu (\Sigma^\dagger \partial_\mu \Sigma)_{ba} + \frac{ig}{2}\mathrm{Tr}\bar{H}_a H_b \gamma^\nu \gamma^5 (\Sigma^\dagger \partial_\nu \Sigma)_{ba} + \cdots . \tag{1.19}$$

These Lagrangians can be used in the standard way to formulate an effective theory of heavy mesons and light hadrons. As will be shown, depending on the assumptions

going into the light quark ansatzes, the physical description of the effective theory will differ.

1.3 Large N_c and the $1/N_c$ expansion

The large N_c limit and the $1/N_c$ expansion plays a critical role in some calculations in this dissertation. A brief introduction of what is large N_c is therefore useful.

Unlike in QED, the coupling constant for QCD is not small enough for a perturbative expansion to be constructed in the hadronic energy regime. Therefore, it has long been an outstanding problem to determine if QCD had another intrinsic parameter for which a systematic expansion could be constructed. To this end, 't Hooft noted [18, 19] that if one replaced the QCD $SU(3)_c$ gauge group with $SU(N_c)_c$ then QCD could be written as an expansion in $1/N_c$. This change in the group structure is based on the replacement of the three colors associated with QCD with N_c colors. By allowing the number of colors to become large, the proposed $1/N_c$ expansion can become useful. Many key results of the large N_c limit which were first described by 't Hooft and Witten [18, 19, 20], are summarized in Table 1.1. For an understanding of the work in this study, the N_c dependence of the strong coupling constant, the baryon mass, and the three types of interactions listed in Table 1.1 are important and thus will be discussed in some detail here.

Many of the features of large N_c are due to the scaling of the strong coupling constant scales. To understand why g scales like $1/\sqrt{N_c}$, consider the leading

Quantity	**Large N_c scaling**
Strong coupling constant	$\frac{1}{\sqrt{N_c}}$
Closed color loops	N_c
Meson mass	N_c^0
Baryon mass	N_c
Meson-meson interaction	$\frac{1}{N_c}$
Baryon-baryon interaction	N_c
Baryon-meson interaction	N_c^0
Meson creation vertex	$\sqrt{N_c}$
Vertex of k mesons	$N_c^{-(\frac{k-2}{2})}$

Table 1.1: Large N_c scaling relations.

contribution to gluonic vacuum polarization.

This diagram has a single gluon loop with two copies of the coupling, g^2. Inside the loop, there is an unspecified color label; thus the diagram should be proportional to N_c. However, it is quite unreasonable to believe that this diagram (and higher loop diagrams as well) would be more dominant than the gluon propagator or that it would be divergent in the large N_c limit. This divergence can be absorbed by allowing the coupling constant to depend on N_c. Since the diagram is proportional to $g^2 N_c$, by choosing g to scale like $g \sim g_0/\sqrt{N_c}$, the overall dependence of the diagram to N_c becomes N_c^0 (for fixed values of the N_c independent parameter g_0.). This choice not only resolves the possible inconsistent divergences for the gluon vacuum polarization, but it also creates a consistent power counting scheme to evaluate the N_c dependence of other diagrams. This scheme gives rise to the $1/N_c$ expansion.

To understand how the mass of the baryon depends on N_c, remember that

a baryon is a composite object consisting of N_c quarks. Each of the N_c colors is represented exactly once to ensure the color neutrality of the baryon. As Witten first described [20], the baryon mass has three factors: the rest mass of the constituent quarks, their kinetic energy, and the interaction potential;

$$\text{Baryon Mass} = \text{Quark masses} + \text{Quark kinetic energy} - \text{Potential energy}. \quad (1.20)$$

The individual quark mass and kinetic energy should be independent of N_c. The combination of the N_c constituent quarks in the baryon causes both of these terms to scale like N_c. But what about the interaction potential? For a complete understanding, one must consider a many-body Hartree-Fock calculation, but the general N_c dependence can be obtained from examining the most naïve two-body interaction between quarks. This is dominated by the single gluon exchange which should be proportional to g^2, or scale like $1/N_c$. Additionally, there is a combinatorics factor because the gluon exchange can be between any two of the baryon's N_c quarks. This gives a factor of $\frac{1}{2}N_c(N_c-1)$, or N_c^2 for large N_c. Therefore, the interaction potential of the baryon also scales like N_c. Combining the rest mass, kinetic energy, and interaction potential dependence, one concludes that the baryon mass scales as N_c.

From the N_c dependence of the strong coupling constant, it is straightforward to formulate the N_c dependence on meson-meson interactions. Meson-meson interactions are dominated by gluon exchange, with the leading order attributed to a single gluon exchange. Such interactions are proportional to the coupling constant squared, g^2; thus, from before, the meson-meson interaction scales like $1/N_c$. This

implies that in the large N_c limit, mesons do not interact with one another.

The baryon-baryon interaction is a little more complicated than the meson-meson interactions. The baryon interactions are dominated by the diagrams which includes the exchange of a single quark with or without the accompaniment of a gluon exchange. The baryon interaction through a quark exchange without a gluon scales like N_c. One can choose to exchange any of the N_c quarks from one of the baryons, but to ensure that the final baryon states are color neutral, there is only one possible quark in the other baryon with exactly the same color as the initial exchanged quark. Hence the overall dependence of N_c. When the quark exchange is accompanied by a gluon exchange, the gluon can restore the color neutrality if the exchanged quarks have different colors. Therefore, the interaction depends on the combinatorics factor, N_c^2, from choosing a single quark from each of the two baryons. There is also a factor of $1/N_c$ from the coupling constants associated with the gluon exchange. Therefore the overall dependence of the baryon-baryon interaction is N_c. It may seem unusual that the interaction might diverge in the large N_c limit, but remember that since the baryon mass also scales like N_c, the interaction is only $O(1)$ relative to this mass.

The final relevant interaction to consider is between baryons and mesons. This will be mediated by either gluon exchange or by quark exchange (the combination will be $1/N_c$ suppressed). The gluon exchange has the typical $1/N_c$ dependence for the coupling constant. This gluon can be exchanged between only N_c unique pairs of quarks, coming exclusively from the different quarks in the baryon. Thus, the baryon-meson interaction depends as N_c^0. The quark exchange has a similar

dependence because there is only one quark in the meson which could be exchanged and only one quark in the baryon with the same color as the one from the meson. Since the baryon-meson interaction scales like N_c^0, the baryon is unaffected by the interaction (since its mass is of $O(N_c)$) while the meson is strongly influenced.

This has been a sampling of some of the effects in hadronic physics at the large N_c. A comprehensive review would require more space than is given here, but such a review is not needed to make the work in this dissertation accessible. Over the years the predictions of the large N_c limit have been examined with physical systems with a variety of success. For some systems, the $1/N_c$ expansion is useful as a qualitative or semi-qualitative tool in understanding aspects of QCD, while for others it works poorly.

1.4 Exotic hadrons

When the naïve quark model was introduced, it was believed that all hadrons came in one of two varieties; baryons constructed from three quarks, and mesons constructed from a quark and an anti-quark. This distinction was not derivable from the model, but rather imposed based upon the phenomenological evidence at the time. However, since the inception of QCD, it has always been a goal to determine whether this fundamental theory restricts the hadron spectrum to these states, or if more exotic hadrons are allowable by QCD. Since, to date, a complete solution to QCD has not been achieved, any insight, either theoretically or experimentally, into the type of allowable hadronic states within the context of QCD or some limit

of the theory is interesting.

The simplest forms of exotic particles can be classified as either tetraquarks (mesons with two quark and two anti-quarks), pentaquarks (baryons with four quarks and one anti-quark), or hybrids (hadrons constructed from quark and gluon degrees of freedom). One could even envision hadrons composed of even more quarks (say six or seven or 1 million), but tetraquarks, pentaquarks, and hybrids constitute the simplest extension to the naïve baryon and meson states.

Throughout the years there have been thousands of theoretical papers devoted to describing these exotic particles. With such a large number, it is not possible, nor useful, to attempt to provide a synopsis of this extensive research here. Though it is important to note that all exotic spectra are dependent on the model or the considered limit of QCD.

Experimentally, to date there has not been a single confirmed observation of a particle with unequivocal exotic quantum numbers. Many have claimed that the light scalar meson, such as a_0 or f_0, or certain nucleon resonances might be exotic. However, it is difficult to ascertain whether these states have an exotic quark content because they have the same quantum numbers as other non-exotic hadrons. This type of hidden exoticness is a key feature which has obscured light quark exotic identification.

Other popular candidates of experimentally observed states which may be a four quark state are seen in the unexplained excitation of J/Ψ. There have been a number of J/Ψ excitations which have not corresponded to a typical excitation suggested by previous models. The most studied one is the $X(3872)$. This state

has been seen to decay into J/Ψ and either $\pi^+\pi^-$ [21, 22, 23, 24] or $\pi^+\pi^-\pi^0$ [25, 26] as well as decay into D^0D^{*0} [27]. Since its mass does not fall nicely into the expected charmonium levels, and because it is close to the DD^* threshold, there has been much speculation whether this is a threshold effect, an unusual charmonium state, a D meson molecule, or a tetraquark state. However, the $X(3872)$, like its lighter cousins, has hidden exotic quantum numbers requiring further evidence to distinguish between the different scenarios.

The only identified particle which is suggestive of a tetraquark state and nearly has exotic quantum numbers is the recently observed $Z(4430)^+$. This state has been identified by Belle [28] to decay into Ψ', an excited charmonium state, and a single pion, π^+, which happens to be charged. If one believes that the $c\bar{c}$ of the Ψ' is also present in the $Z(4430)^+$, then the decay into a single charged pion would imply that this is indeed at least a four-quark state. Further confirmation needs to be established before any definitive identification of $Z(4430)^+$'s quark content is made. Should the identity of this state be confirmed, it would be a major discovery as it would constitute the first unequivocal observation of a four-quark meson.

The experimental history of pentaquark states is even a more convoluted story. Ten groups performing a variety of experiments [29, 30, 31, 32, 33, 34, 35, 36, 37, 38] have reported the appearance of the pentaquark state now called Θ^+, a resonance with baryon number +1, strangeness +1, and a mass in the vicinity of 1540 MeV. However, these experiments were all performed with relatively limited statistics and significant cuts, raising the possibility that the reported resonance is due to nothing more than statistical fluctuations. One ground for skepticism arises from a series

of experiments that did not find a Θ^+ resonance [39, 40, 41, 42, 43, 44, 45, 46, 47, 48, 49, 50]. Of course, it is unclear whether some of the experiments with negative results should be sensitive to such an observation, since there is no reliable theoretical framework for predicting the Θ^+ production rate. The Θ^+ width generates another source of doubt: $\Gamma(\Theta^+)$ must be exceedingly narrow (in the range of 1–2 MeV or smaller), or it would have been detected long ago [51, 52, 53, 54, 55, 56], and to many it strains credulity that such a narrow state exists in this kinematic range.

One common thread in these early reports of detection (or non-detection) of the Θ^+ is the fact that the analysis came from experiments designed for other purposes and the appearance of the signal only after the imposition of various cuts. Given the limited size of the data sets, all of the studies yielded spectra with very limited statistics, creating the possibility of narrow peaks due to statistical fluctuations. The need for high-statistics experiments became very clear. Special-purpose experiments designed to look for pentaquarks with high statistics have been performed at Jefferson Lab; the CLAS Collaboration has analyzed the high-statistics data from photons on both a proton target [57] and a deuterium target [58], and finds no evidence for a Θ^+ peak. While these experiments alone do not rule out the Θ^+, they show that at least two of the previous claims of evidence for the state, the SAPHIR γp result [37] and the CLAS γd result [38], were indeed statistical fluctuations. Though this is countered by the persistent identification of the Θ^+ by the LEPS collaboration of SPring8 [59].

Because of the lack of detection of the Θ^+ by the higher statistical experiments, much of the field has come to believe that there are no reliable signals indicating

the existence of a pentaquark. Further higher statistical experiments are needed to resolve the outstanding questions. However, the lack of confirmation of the Θ^+ does not imply that pentaquark states are not possible within the context of QCD, only that a light pentaquark state is unlikely to be found at 1540 MeV.

Experimental confirmation of a hadron state with exotic quantum numbers remains an elusive goal. Such observation would provide a fascinating new handle to approach hadron physics. Without such experimental evidence, physicist are left with speculation when it comes to these exotic states. In this vein, this dissertation examines the implications of exotic hadrons with the context of different models. The knowledge that exotic hadrons exist or don't exist can be a useful tool in constraining hadronic models.

Chapter 2

On the existence of heavy pentaquarks in the large N_c and heavy quark limits

2.1 Introduction

The first heavy quark system which will be investigated pertains to heavy pentaquarks. These particle states can be considered exotic from the context of the naïve quark model. As discussed in the introduction, an understanding of any quark model exotic state provides insight into the structure of QCD. In this chapter, it will be demonstrated that a heavy pentaquark state must exist in the combined heavy quark and large N_c limits. Furthermore, models which were designed to represent aspects of the physics in the extreme limits will be utilized with physically relevant parameters. These models are important because if it could be shown that phenomenological significant models would lead to heavy pentaquarks in a robust manner, one could assert that heavy pentaquarks would be expected to exist in physical systems. Unfortunately, as will be demonstrated in this chapter, the formation of a heavy pentaquark away from the extreme heavy quark and large N_c limits is highly model dependent. Thus the existence of strongly interacting, stable, heavy pentaquarks remains an open question.

The experimental landscape of the possible observation of light pentaquark

states was discussed in the previous chapter. To highlight, a possible pentaquark resonance, called Θ^+, with the quantum numbers of baryon number +1 and strangeness +1 was identified in ten experiments [29, 30, 31, 32, 33, 34, 35, 36, 38, 37] with a mass near 1540 MeV. This state was not observed in other experiments [39, 40, 41, 42, 43, 44, 45, 46, 47, 48, 49, 50]. The identifications which were made relied on the examination of low statistical experimental data. It is known that this type of identification method is susceptible to the possible enlargement of random fluctuations, particularly if no protocol for selecting cuts is made prior to the attempts to find a peak in the data. Furthermore, higher statistical experiments were subsequently performed [57, 58] without identifying the desired resonance.

The theoretical landscape for pentaquarks has been just as murky. A paper by Diakonov, Petrov, and Polyakov [60] was seminal in focusing attention on the pentaquark in that it predicted a narrow state at almost exactly the mass where the Θ^+ was later reported. However, that paper is based upon an approximation later shown to be inconsistent with the large N_c assumptions implicit in the model [61, 62, 63, 64, 65, 66, 67, 68, 69]. After the experimental claims of pentaquarks appeared, a vast literature of models for the Θ^+ followed. In all of these models, the existence of the Θ^+ depends upon *ad hoc* assumptions; thus they cannot be used reliably to predict the existence of the state, and accordingly are not reviewed here. Ultimately one may hope for lattice QCD eventually to resolve the theoretical question of whether the state exists. However, current lattice simulations for both heavy and light pentaquarks [70, 71, 72, 73, 74, 75, 76, 77, 78, 79], while improving, remain inconclusive.

Given this morass, it is sensible to ask whether one can find a regime in which the question of the pentaquark's existence is more tractable. It has been noted previously in the context of various models [80, 81] that heavy pentaquarks, states in which the $\bar{s}$ quark in Θ^+ is replaced by a $\bar{c}$ or a $\bar{b}$ quark, are more likely to be bound than the $\bar{s}$ type. The principal purpose of the analysis in this chapter is to explore the possible existence of heavy pentaquarks. This chapter shows in a particular limit of QCD, the combined large N_c and heavy quark limits, that heavy pentaquarks must exist, and that they are stable under strong interactions. The critical question of whether $1/N_c$ and $1/m_Q$ corrections are sufficiently small for this qualitative result to survive in the physical world is then explored. There are no known analytic methods starting directly from QCD to answer this last question; thus, this question must be investigated in the context of models.

Models which treat the heavy pentaquark as a bound state of a heavy meson and a nucleon interacting via pion exchange are employed. Although similar models have been considered previously [82], the present work expands on them and is done in the context of the combined heavy quark and large N_c limits. Such models have two principal virtues: First, as is shown below, the combined large N_c and m_Q limit mandates the existence of bound pentaquarks. Indeed, this demonstration is based on the fact that QCD in the combined limit can be reduced to a model of this form. Second, the long-distance behavior of the model is well known empirically (up to experimental uncertainties in the pion-heavy meson coupling constant). If the long-distance attraction due to pion exchange were sufficient to bind the pentaquark for any reasonable choice of short-distance dynamics (as happens in the combined limit)

then one would have a robust prediction that heavy pentaquarks exist (although their detailed properties would still depend on uncontrolled short distance physics). Unfortunately, it is found that this is not the case.

Before proceeding it is useful to clarify a semantic point. This discussion relies heavily on the large N_c limit of QCD; as N_c becomes large, the minimum number of quarks in a baryon containing a heavy antiquark is not 5, but rather N_c+2. Nonetheless, such states are still denoted as "pentaquarks," to make the obvious connection to the $N_c=3$ world.

This chapter is organized as follows. In Sect. 2.2, a brief background on heavy pentaquarks is provided. Section 2.3 presents a rigorous argument for the existence of heavy pentaquarks in the combined large N_c and large m_Q limits. Then Sect. 2.4 explores the question of whether this qualitative result survives in the real world of $N_c = 3$ and finite m_Q by studying simple models based on a pion exchange between nucleons and heavy mesons. Finally, Sect. 2.5 presents a brief discussion of the implications of this chapter and concludes.

2.2 Heavy Pentaquarks: Background

The experimental situation involving reports of heavy pentaquarks remains obscure. The H1 Collaboration at HERA has reported [83] a narrow resonance Θ_c appearing in $D^{*-}p$ $[(\bar{c}d)(uud)]$ and $D^{*+}\bar{p}$ $[(c\bar{d})(\bar{u}\bar{u}\bar{d})]$ states produced in inelastic ep collisions, with a mass of $3099\pm3\pm5$ MeV and a width of 12 ± 3 MeV. It should be noted that the Θ_c, even if it withstands further experimental scrutiny, is *not* the

type of heavy pentaquark discussed in this chapter, since it is a resonance unstable against strong decay. Moreover, subsequent evidence argues against its existence: The FOCUS Collaboration [84], using a method similar to that of H1 but with greater statistics, finds no evidence for Θ_c. The experimental situation for heavy pentaquarks remains in a state as unsatisfactory as with their lighter cousins.

On the theoretical side, much of the heavy pentaquark research to date has been performed in the context of different variants of the quark model [80, 85, 86, 87, 88, 89, 90]. The purpose here is not to review this work in any detail, but to stress one of its key points: Heavy pentaquarks occur far more naturally than light pentaquarks in such models, simply because a heavy quark is drawn more closely than a lighter quark to the bottom of any potential well. At the time much of the theoretical analysis was performed, many researchers assumed that light pentaquarks were experimentally firmly established, and so such models seemed to make rather robust predictions of stable pentaquarks. Now that the existence of the light pentaquarks has become more questionable, the reliability of heavy pentaquark predictions can also be questioned. Nevertheless, the tendency of heavy pentaquarks to bind more tightly than light ones remains generically true, a simple fact that continues to play a crucial role in the analysis presented here.

Stewart, Wessling, and Wise [80] also raise a critical issue in the context of a diquark type model, namely, whether heavy pentaquarks could prove stable against strong decays. They argue that negative-parity heavy pentaquarks should have the lowest energy (in contrast to the positive-parity Θ^+ of the Jaffe-Wilczek model [91, 92]) since this involves s-wave interactions between the diquarks. They suggest that

the additional attraction in such negative-parity states might be sufficient to render the states stable against strong decays. This chapter will argue that pentaquarks do in fact exist, at least in an artificial world in which the combined large N_c and large m_Q limits of QCD are well satisfied.

Since the large N_c limit plays a critical role in the argument, it is useful to remark upon previous work on heavy pentaquarks as $N_c \to \infty$. References [85, 86, 93, 94] impose large N_c counting rules in the context of a quark picture as a way to implement large N_c QCD. Such a picture suggests a Hamiltonian and asymptotically stable eigenstates. However, *generic* excited baryons at large N_c are broad resonances with $O(N_c^0)$ widths and require an approach respecting their nature as poles occurring at complex values in scattering amplitudes. Such a "scattering picture" has been developed previously [95, 96, 97, 98, 99, 100, 101]. While obtainable through a generalization of the large N_c treatment for the stable ground-state band of baryons [102], the scattering approach naturally allows a proper treatment of resonant behavior such as large configuration mixing between resonances of identical quantum numbers [103]. Even for pentaquarks of $O(N_c^0)$ widths, the scattering approach predicts multiplets degenerate in both mass and width [104, 105]. But this technology, while generally true, is not required in the current work; as is now shown, the heavy pentaquarks discussed in this paper are stable against strong decay, at least in the combined formal limit $N_c \to \infty$, $m_Q \to \infty$.

2.3 The Existence of Heavy Pentaquarks

It will now be shown that heavy pentaquarks exist in the combined large N_c and large m_Q limits, and indeed they are stable against strong decay. An appropriate parameter to describe the limiting procedure must first be chosen. Here, the natural choice is the λ expansion, where

$$\lambda \sim 1/N_c \ , \ \Lambda_H/m_Q \ , \tag{2.1}$$

Λ_H is the hadronic scale, and m_Q is the mass of the heavy quark. It should be noted that the natural expansion turns out to be in powers of $\lambda^{1/2}$ [106, 107], instead of λ^1 for a pure $1/N_c$ expansion.

Consider the states in the QCD Hilbert space that have energy less than $M_N + M_H + m_\pi$ (M_H is the mass of the lightest hadron containing heavy antiquark $\overline{Q}$), and have baryon number $+1$ and heavy quark Q number -1. These conditions exactly describe potentially narrow heavy pentaquarks Θ_Q (assuming no symmetry forbids the one-pion decay). Now consider further states with energy less than M_N+M_H; any pentaquark state appearing here must be a bound state as no hadronic decay can occur. However, scattering states which have the appropriate quantum numbers and which have low enough energies clearly occur between the nucleon and the heavy meson. Therefore states that can be labeled Θ_Q exist.

The key point is that in the regime under consideration an effective potential for the nucleon and the heavy meson can be described. First note that momenta in the scattering states scale as λ^0. Since the N, H reduced mass μ scales as λ^{-1}, the kinetic energy scales as λ^1, which is much smaller than $m_\pi = O(\lambda^0)$. One may

therefore construct an effective theory in which all scatterings with >2 final-state hadrons are integrated out.

However, these states naively appear nonlocal, which would prevent the construction of a local potential. The range of the nonlocality scales as the inverse of momenta p associated with the smallest kinetic energy T which one integrates out. In this case, $T \sim m_\pi$. Therefore, the range scales like $1/p = (2\mu m_\pi)^{-1/2} \sim \lambda^{1/2} \to 0$ as $\lambda \to 0$: The nonlocality disappears.

Next, one must ensure that the potential that binds the pentaquark does not vanish in the combined limit. From Witten's original N_c counting [20], one finds that indeed $V(\vec{r}) \sim \lambda^0$, preventing its disappearance relative to the kinetic energy. Noting that the heavy quark coupling scales as $g_s \sim N_c^{-1/2}$, the nucleon coupling is of order $g_A/f_\pi \sim N_c^{1/2}$, and the pion propagator is of order $m_\pi \sim N_c^0$, one combines these ingredients to find the desired λ^0 scaling for the potential.

The existence of stable heavy pentaquarks can now be easily proven. Having established the locality and scaling of the potential between heavy hadrons, a quantum field theory problem has been reduced to one of nonrelativistic quantum mechanics. It is well understood in this context that a potential with an attractive region has an infinite number of bound states as $\mu \to \infty$ (see Appendix A for details). In the present case, $\mu \sim \lambda^{-1} \to \infty$ while $V(\vec{r}) \sim \lambda^0$. Thus, proving the existence of heavy pentaquarks in the combined limit requires only that $V(\vec{r})$ is attractive in at least some region. Fortunately, the form of $V(\vec{r})$ at large distances is known: It is given by a one-pion exchange potential (OPEP), because π is the lightest hadron that can be exchanged between H and N. It is moreover known that, regardless of

the relative signs of the coupling constants, attractive channels appear in the OPEP. Thus, $V(\vec{r})$ necessarily has attractive regions, serving to bind the heavy pentaquark.

2.4 Bound States and the One-Pion Exchange Potential

Now that stable heavy pentaquarks have been shown to exist in the combined large N_c, large m_Q limit, the critical question becomes whether they also occur in our $N_c = 3$, finite m_Q world. Currently, this question cannot be answered in a model-independent way without solving QCD. To get insight one can resort to models for enlightenment.

Effective potential models based upon one-pion exchange at long distance will be focused on here. As discussed in Sect. 2.3, such models are clearly useful not only because they represent physically correct phenomenology, but also guarantee stable pentaquarks in the combined limit. But it is also noted that the argument does not depend upon the particular short-distance behavior of the effective potential. If the real world is sufficiently close to the combined-limit world for the argument to remain valid, all models of this sort must yield (multiple) stable pentaquarks. Note that the masses of the various pentaquark states can depend sensitively upon the details of the short-distance interaction, but their existence cannot. The question then becomes whether models of this type predict bound pentaquarks in a robust way, independent of the details of the short-distance physics. If so, one has a strong reason to believe that the states are, in fact, bound in nature.

A "realistic" potential that has the correct long-distance behavior (OPEP)

and an *ad hoc* short-distance part constrained only by the natural scales of strong interaction physics is constructed. This potential acts between a nucleon and a heavy meson (D or B). The nucleon-pion interaction is well understood; its interaction Lagrangian reads

$$\mathcal{L}_{NN\pi} = -\frac{g_A}{f_\pi\sqrt{2}}\bar{N}\tau^a\gamma_\nu\gamma_5 N\,\partial^\nu\pi^a\ , \tag{2.2}$$

where the axial coupling constant $g_A \simeq 1.27$, and the pion decay constant $f_\pi \simeq$ 131 MeV.

The heavy meson-pion interaction can be derived from the HQET effective Lagrangian, Eq. (1.18) in Sect. 1.2. The interaction is based upon the coupling of the heavy meson fields to an axial current. The axial current in Eq. (1.18) can be re-expressed by expanding the field ξ in powers of M, the meson matrix, and noting that M can be written as

$$M = \sqrt{\frac{1}{2}}\tau^a\pi^a. \tag{2.3}$$

Combining this with the expansion of the ξ, the interaction term of the Lagrangian can be written in a form similar to the nucleon interaction,

$$\mathcal{L}_{\rm int} = -\frac{g_H}{f_\pi\sqrt{2}}{\rm Tr}\bar{H}H\gamma_\mu\gamma_5\tau^a\,\partial^\mu\pi^a\ . \tag{2.4}$$

Recall, that the field H in the Lagrangian is a composite field of both the pseudoscalar and vector mesons. Of course, the pseudoscalar and vector mesons are *not* degenerate in the real world due to $1/m_Q$ corrections. This mass difference must be included in realistic models.

Both the nucleon and heavy meson interactions with the pion can be expressed

in terms of the spin and isospin of the particles:

$$\mathcal{L}_{NN\pi} = \frac{2\sqrt{2}g_A}{f_\pi}(\vec{S}_N \cdot \vec{\partial}\pi^a)I_N^a \ , \tag{2.5}$$

$$\mathcal{L}_{\rm int} = \frac{2\sqrt{2}g_H}{f_\pi}(\vec{S}_l \cdot \vec{\partial}\pi^a)I_H^a \ , \tag{2.6}$$

where $\vec{S}_N$ and $\vec{I}_N$ are the spin and isospin of the nucleon, $\vec{S}_l$ is the spin of the light quark in H, and $\vec{I}_H$ is the isospin of the H field. These constructions can be simultaneously justified because the heavy meson rest frame can be chosen as the relevant dynamical frame, while the nucleons can be treated non-relativistically. Combining Eqs. (2.5) and (2.6), treating the nucleon and heavy meson in the static limit (*i.e.*, ignoring recoil, which is suppressed in the combined limit) and Fourier transforming yields the OPEP in position space:

$$\begin{aligned} V_\pi(\vec{r}) &= \vec{I}_N \cdot \vec{I}_H \left[2S_{12}V_T(r) + 4\vec{S}_N \cdot \vec{S}_l V_c(r)\right] \\ &= (I^2 - I_N^2 - I_H^2)[S_{12}V_T(r) + (K^2 - S_N^2 - S_l^2)V_c(r)] \ , \end{aligned} \tag{2.7}$$

where the central part of the potential (r measured in units of $1/m_\pi$) is

$$V_c(r) = \frac{g_A g_H}{2\pi f_\pi^2}\frac{e^{-r}}{3r} \ , \tag{2.8}$$

and the tensor part is

$$V_T(r) = \frac{g_A g_H}{2\pi f_\pi^2}\frac{e^{-r}}{6r}\left(\frac{3}{r^2} + \frac{3}{r} + 1\right) \ . \tag{2.9}$$

I is the total isospin of the combined system, while $\vec{K} \equiv \vec{S}_N + \vec{S}_l$, and

$$S_{12} \equiv 4\left[3\,(\vec{S}_N \cdot \hat{r})(\vec{S}_l \cdot \hat{r}) - \vec{S}_N \cdot \vec{S}_l\right] . \tag{2.10}$$

It remains unknown whether g_A and g_H are of the same sign or of different signs, so the potential could have an additional overall negative sign.

Clearly, the OPEP dominates the interaction at large r since the π is the lightest hadron. At shorter ranges, the OPEP is no longer dominant and the effective potential is qualitatively different. The value of r at which the OPEP ceases to dominate the effective potential is presumably of order $1/\Lambda_{\rm QCD} \sim 1$ fm, the characteristic range in strong interactions. Therefore, for distances less than some cutoff value $r_0 \sim 1$ fm, a purely phenomenological potential is used. Note that such a short-range potential is not simply added to the OPEP at short distances, but one entirely replaces the OPEP by this new potential: The $1/r^3$ behavior of the tensor part of the OPEP at short ranges is unphysical and would completely dominate the potential if not removed. The short-distance potentials used are taken to be either (central) constants or quadratic functions, and their strengths are allowed to vary. If the logic of the underlying argument based upon the combined limit also holds for realistic m_Q values and $N_c = 3$, then the precise details of the potentials should be irrelevant to whether the pentaquark states bind.

The OPEP of Eq. (2.7) is used in a nonrelativistic Schrödinger equation and solved for bound states. Since the tensor term in the potential allows mixing between L states, L is not a good quantum number. However, S_{12} commutes with the parity operator, making P a good quantum number. Therefore, states labeled by J, S (total spin $\vec{S} \equiv \vec{S}_Q + \vec{K}$), and P are used as eigenstates. Treating states mixed under L requires a coupled-channel calculation; the coupled equations are obtained by including all possible states labeled by L and K that are consistent with a given set of J, S, and P.

Lastly, since this potential is intended to be "realistic", in principle B-B^* and

D-D^* mass differences can affect the results. Of course, these differences are $1/m_Q$ effects and vanish in the heavy quark limit. Since the principal reason for the model calculation is to test qualitatively whether the physical world lives in the regime of validity of the combined $1/N_c$ and $1/m_Q$ expansion, it makes sense to include this difference. However, in practice the effect of this mass difference is entirely repulsive, making the states less likely to bind. Thus, if the states do not bind in the equal-mass case, they do not bind at all. Accordingly, equal masses are used and the effect of the mass splitting is only investigated in cases where binding occurs.

One attempts to make this model as realistic as possible, given the rather simple forms assumed for the short-distance potential. To this end, the heavy-meson coupling constant g_H is chosen to be $\approx \pm 0.59$ (extracted from $D^* \to D\pi$ decay [108]) and the values for other observables [109] are collected in Appendix B, Table B.1. As an initial guess, the parameters of the short-range potential were constrained such that this potential combined with a OPEP between nucleons gives the correct 2.2 MeV deuteron binding energy. This choice is not necessary, but it has the virtue of ensuring that the potential parameters are not completely unreasonable from the point of view of hadronic physics. The potentials are summarized in Table B.2. Ultimately, many of the parameters may be varied in order to probe the robustness of the qualitative results.

The coupled differential equations are then solved using standard numerical methods. Bound-state solutions are sought for all $J = \frac{1}{2}$ and $J = \frac{3}{2}$ states using both a constant and a quadratic form for the short-distance potential, for $I = 0$ and $I = 1$, and with either sign of g_H relative to g_A. Initially (as discussed above), it is assumed

that the pseudoscalar and vector mesons masses are degenerate. A complete set of tables of bound states appears in Tables B.3 and B.4. Here some key features of these results will be discussed.

For constant and quadratic potentials constrained by matching to the deuteron energy, bound states of the pentaquark are uncommon. No channel supports a bound state with a D meson. The B meson is able to bind weakly in the channels with negative parity, but only with $I=0$. Binding in these states is relatively weak, around 1.3 MeV for the constant potential and around 3.9 MeV for the quadratic potential, and binding energies are consistently the same between these channels (Table B.3, Cols. A and B). It should be noted that both Ref. [80] and our calculations have the negative parity states being more stable. The greater binding for the quadratic (versus the constant) potential is natural since it is significantly deeper.

The case in which the short-distance potential is simply set to zero is also analyzed. For this case, the OPEP does not bind a pentaquark for any channel. In order for this potential to bind without the aid of short-distance potential, g_H would need to be raised to unreasonably high levels, near 1 (approximately double the extracted value), and in some cases larger than 2. When realistic mass differences between the vector and pseudoscalar mesons are introduced, binding becomes weaker. This mass splitting eliminates binding for all channels with either type of potential considered.

The heavy-meson coupling constant g_H used in this analysis is motivated by the results of a recent experiment by the CLEO Collaboration that measured [108] the width of the $D^{*\pm} \to D^0\pi^\pm$ decay. The value of g_H is extracted from the width

and found to be $\pm 0.59 \pm 0.07$. The analogous decay process is energetically forbidden in the B sector, preventing a direct extraction; therefore, heavy quark symmetry is exploited and the same value of g_H is used for the B sector. Note, however, the uncertainty in the bottom sector is due to possible $1/m_Q$ corrections. Accordingly, a range of heavy-meson couplings is also investigated and the same qualitative results are found.

These results depend upon the strength of the short-distance potential. Clearly, as these potentials become more strongly attractive, the states are more likely to bind. As the potential needed to bind deuterium may by anomalously small, a deeper constant potential was also considered. Table B.3, Col. C and Table B.4, Col. A show the results when the constant potential is decreased from the depth needed to bind deuterium, -62.79 MeV, to about 4 times as deep, -276 MeV. The deeper well produces both more bound states and causes previously unbound states to bind (in particular, the D meson can form a bound state in the deeper potential).

The choice of OPEP cutoff at $r = 1$ fm is arbitrary. One does not expect the OPEP to be valid for $r < 1$ fm, but the effective cutoff might occur at somewhat larger r. Table B.3, Col. D and Table B.4, Col. B present the binding of states with a cutoff of 1.5 fm (the potential depth is -62.79 MeV). The negative-parity states remain the only bound ones, but the binding is now stronger, and the D meson binds. These fluctuations in strength of binding indicate the importance of the short-distance physics to the heavy pentaquark formation.

2.5 Discussion

Despite the general argument of Sect. 2.3 that by using the large N_c and large m_Q combined limit the long-range OPEP is sufficient to bind pentaquarks, it is observed in a class of models that if a heavy pentaquark binds at all due to one-pion exchange, it does so weakly in a few channels and depends in a nontrivial way upon the details of the short-range interaction. The main implication is obvious: In the real world, $1/N_c$ and $1/m_Q$ corrections can be substantial. Indeed, they are large enough to render unreliable qualitative predictions about heavy pentaquarks based upon the combined limit.

Given this somewhat unhappy result, the most important question is whether or not heavy pentaquarks do in fact bind to form stable states under strong interactions, and if so, whether only very weakly-bound states occur, such as the ones seen here. Both of these questions remain open. The short-distance part of the effective potential is simply not known sufficiently enough to provide a definitive answer. An optimistic view is that the short-distance interaction between the heavy meson and the nucleon is likely to be more attractive than that between nucleons, which has a strong repulsive core. This argument is particularly plausible if one views at least part of the repulsive core between nucleons to arise due to the Pauli principle between overlapping nucleon wave functions; this effect is greatly reduced in the interaction between a nucleon and a heavy meson. If it is true that the short-range effective potential between the heavy meson and the nucleon is significantly more attractive than the analogous nucleon-nucleon case, then it is quite likely that heavy

pentaquarks form stable, tightly-bound states.

Finally, the question of why the qualitative prediction of the combined large N_c and large m_Q limits is insufficient is addressed. At first sight this may seem surprising since both the $1/N_c$ and $1/m_Q$ expansions have proven to be predictive in many situations. One must remember, however, that the quality of a systematic expansion depends on coefficients as well as the expansion parameter, and the size of these coefficients depends on the observable being studied. If some observable has "unnaturally" large coefficients, then the expansion can easily fail unless the expansion parameter is extremely small. This view is echoed in Ref. [110]. The relevant question is whether one ought to expect "unnaturally" large corrections to the leading behavior.

In retrospect, it is perhaps not so surprising that combined expansion is insufficient here. One can make an analogous argument, based entirely upon $1/N_c$ counting, that both the deuteron and the ${}^1S_0$ two-nucleon channel ought to be deeply bound and have a large number of bound states: Both the effective interaction between nucleons and the masses of the two nucleons grow as N_c^1. However, as has been stressed elsewhere [111], this argument fails for smaller values of N_c. Similarly, numerous doubly-heavy strongly-bound tetraquarks ought to exist in the heavy quark limit: The effective interaction between heavy mesons is independent of the heavy quark mass and scales as $1/(N_c m_Q)$. However, as discussed in Ref. [112] and based upon models similar to those studied here, it is questionable whether they are bound for physical m_Q. Evidently, the coefficients describing interactions between hadrons can in some qualitative way be sufficient to weaken significantly re-

sults one would naively expect directly from the $1/N_c$ or $1/m_Q$ expansions, yielding very large corrections to the leading-order results for real-world parameters. Why this is so is one of QCD's more intriguing mysteries.

In conclusion, this chapter has shown that heavy pentaquarks must exist in combined large N_c and large m_Q limits. A one-pion exchange potential between a nucleon and a heavy meson was constructed, and the coupled non-relativistic Schrödinger equations were solved, obtaining bound states. Some weakly-bound states do exist in some models, but their existence depends sensitively on unknown short-distance physics. The lack of binding emphasizes that the real world is too far from the idealized world of large N_c and large m_Q to render the expansions robust for these observables. In order to deduce whether or not heavy pentaquarks exist requires a more complete understanding of the short-distance physics than is presently known.

To address some of the limitations associated with the short-distance physics, another model, namely the Skyrme model, which has a set prescription on how one should handle the short-distance physics, will be examined in the next chapter.

Chapter 3

Heavy baryons in the Skyrme model

3.1 Introduction

In the previous chapter, heavy pentaquarks were considered in the context of one-particle phenomenological models. In this chapter, a different phenomenological model, namely the Skyrme model of chiral solitons in large N_c, will be used to describe nucleon states. In addition to heavy pentaquarks, this model can be extended to study all forms of heavy baryons, both exotic and ordinary. Though this model does provide some insights into the heavy pentaquark states previously considered, this chapter will focus on the properties of the regular heavy baryons.

It has been known for a number of years that heavy baryons can be modeled in the heavy quark and large N_c limits from the binding of heavy mesons with light chiral solitons [113, 114, 115, 116, 117]. In these limits, both the heavy meson and the chiral soliton have large masses, and it is legitimate to describe the system in terms of a collective degree of freedom between the heavy meson and baryon. The large masses drive the particles to the bottom of an effective potential. In most cases considered, this minimum occurs at the origin of the relative coordinate, causing both particles to be situated on top of one another. Previous attempts at describing heavy baryon physics within this model assumed that particles would experience small harmonic perturbations in the potential away from their minimum.

The previous works showed that the channels which constituted physical heavy baryons had attractive potentials while those channels which did not correspond to physical particles had repulsive potentials [113, 114, 115]. Since the physical world does not correspond to the extreme heavy quark and large N_c limits which guided the previous work, it is interesting to ask the extent to which realistic masses drive the particles to the bottom of the potential (as expected in the combined limit) when the harmonic approximation to the effective potential is replaced by the leading order potential to all distances. In this chapter, a class of corrections to this picture is examined. Similar issues have arisen for nucleon-nucleon forces in large N_c [118, 119]. The assumption that the heavy quark mass and N_c are large enough to enable us to describe the dynamics in terms of a collective degree of freedom which is describable as a non-relativistic effective potential is continued. However, it is not automatically assumed that the masses are so large as to drive the particles into the vicinity of the the minimum of the potential. Instead, the consequences of considering the complete potential with realistic particle masses on heavy baryon physics will be examined. As this chapter will show, the physics is qualitatively quite different from what one would expect if the world were close to the idealized limit.

Baryons described as solitons in a chiral Lagrangian were first considered by Skyrme [120]. These chiral solitons have the correct quantum numbers as baryons in the large N_c limit [121] when the Wess-Zumino term is included [122]. While the extensive early calculations [123] focused on $SU(2)$ solitons, the theory was also extended to include baryons with strange quarks. This was done by either

considering the strange quark as light, and extending the $SU(2)$ chiral fields to $SU(3)$ [124, 125], or by considering the strange quarks as heavy, compared to the lighter quarks, and strange baryons as bound states of the $SU(2)$ soltion and K-mesons [126, 127].

To extend the theory to include even heavier quarks, such as charm and bottom, the former approach of extending the soliton group structure is not reasonable since the mass of the heavy quarks is vastly different from the lighter three quarks. Therefore, the appropriate manner is the latter, put forth in the strange case by Callan and Klebanov, where the heavy baryon states are considered bound states of light quark chiral solitons and heavy mesons. For simplification, this chapter will focus its attention on models made from $SU(2)$ chiral solitons, as was done in previous work [113, 114, 115]. Furthermore, the theory must also exhibit heavy quark symmetry [17, 128, 129]. Thereby, the heavy meson is treated by chiral heavy quark effective theory (HQET). Chiral HQET treats the heavy mesons as the dynamical degrees of freedom and provides a systematic expansion, in powers of the hadronic scale, Λ, over the heavy quark mass, m_Q, to examine the Lagrangian and subsequent interactions, as discussed in Sect. 1.2.

This method can also be used to bind heavy anti-mesons with chiral solitons to form pentaquark states. Such calculations have been performed previously for the case of strange quarks [63]. That work showed that the light pentaquark channel was not sufficiently attractive to yield bound light pentaquark states or prominent resonances. The previous chapter argued on general model-independent grounds that in the extreme heavy quark and large N_c limits, bound heavy pentaquark states must

exist, primarily because the heavy particles fall to the bottom of the potential well. However, it was shown that unlike in the extreme heavy quark and large N_c limits in which the long-range one-pion-exchange potential automatically binds heavy pentaquarks regardless of the details of the short distance interactions, for physical masses the existence of bound pentaquarks was highly sensitive to the details of the short distance interaction. The Skyrme type chiral soliton models provide one framework for treating the short-distance physics, and thus it is interesting to determine if such theories could support heavy pentaquark binding. More significantly, the experience with the exotic channels suggests the possibility that the behavior in the non-exotic channels may also be substantially different from the limit on which the standard Skyrme analysis is based.

The interest in determining the heavy baryon energy spectrum and wave function within a chiral soliton model has also led to studies of the Isgur-Wise function for transitions between heavy baryons. Formally, the Isgur-Wise function describes the non-perturbative physics associated with the form factor of the semileptonic weak decay of $\Lambda_b \to \Lambda_c e^- \bar{\nu}_e$ [11, 12]. Traditionally it is expressed as a function of the transfer velocity rather than the momentum transfer. If the dynamics of the heavy baryons are known exactly, this function can be calculated for all velocities. The Isgur-Wise function has been calculated previously when the effective potential was approximated as harmonic both in the context of the Skyrme model [115] and in a model-independent context [116, 117]. This chapter considers the longer range effects of the interaction between the heavy and light degrees of freedom and leads to a non-universal form of the Isgur-Wise function dependent on the details of the

interaction.

This study is by no means the first study to consider applying the Skyrme model to attempt to explain either heavy baryons or exotic particles. In addition to Refs. [113, 114, 115], heavy baryons spectroscopy within the Skyrme model has been previously considered by the work of Oh and his collaborators [130, 131, 132, 133, 134, 135, 136].

The overall goal of this chapter is to explore the properties of heavy baryons in the Skyrme model in which the collective degree of freedom between the heavy meson and the remainder of the system is beyond the harmonic region of the ideal heavy quark and large N_c limits. In the next section, the complete effective potential is derived, and it is shown that when the full potential is considered, for realistic parameters, the heavy baryon wave function extends well beyond the region where the harmonic approximation is applicable. This will be followed by a demonstration that the simplest type of interactions do not create bound states with realistic binding energies for the heavy baryons–indeed, they give the same mass for ordinary heavy baryons and pentaquarks. This motivates the inclusion of additional terms in the potential which allow for the correct binding energies and distinguish between heavy baryon and heavy pentaquark states. The consequences of these new potentials will be considered. Lastly, the influences upon the Isgur-Wise function by these newly calculated wave functions for the heavy baryons will be examined.

3.2 Derivation of the effective potential

The framework of this section is based on the standard treatment of heavy baryons in the Skyrmion in terms of a collective degree of freedom between the heavy meson and the remainder of the system [113, 114, 115]. To begin the analysis of heavy baryons, the effective potential for this degree of freedom needs to be determined. The relevant Lagrangian for this purpose can be divided into the soliton sector and the HQET sector,

$$\mathcal{L} = \mathcal{L}_{\text{Skyrme}} + \mathcal{L}_{\text{HQET}}. \tag{3.1}$$

The soliton portion determines the dynamics of the ordinary baryons. For concreteness only the simplest such model will be considered: the one originally proposed by Skyrme:

$$\mathcal{L}_{\text{Skyrme}} = \frac{1}{16} f_\pi^2 \,\text{Tr}[\partial_\mu \Sigma^\dagger \partial^\mu \Sigma] + \frac{1}{32e^2} \,\text{Tr}[(\partial_\mu \Sigma)\Sigma^\dagger, (\partial_\nu \Sigma)\Sigma^\dagger]^2 + \frac{1}{8} m_\pi^2 f_\pi^2 \,(\text{Tr}[\Sigma] - 2), \tag{3.2}$$

where f_π is the pion decay constant, e is the Skyrme parameter, m_π is the pion mass, and Σ is the chiral soliton field [120]. The last term provides the pion with a mass and fixes it to its physical value. As will be demonstrated below, this simplest model is not adequate phenomenologically. However, the analysis will begin with this model, and more sophisticated models will subsequently be considered.

Conventionally, the chiral soliton is treated classically as a first approximation and the ansatz taken for the form of the chiral field is,

$$\Sigma_0(\vec{x}) = \text{Exp}[i\vec{\tau} \cdot \hat{x}\; F(r)], \tag{3.3}$$

where $F(r)$ is the profile function determined by minimization of the soliton mass. Since this solution breaks both rotational and isorational invariance, any rotation within the isospin space will lead to a degenerate classical solution. That is,

$$\Sigma(\vec{x}) = A\,\Sigma_0(\vec{x})\,A^{-1} \tag{3.4}$$

where A is an $SU(2)$ matrix of the form $A = a_0 + i\vec{\tau}\cdot\vec{a}$ where different values of a_0 and $\vec{a}$ (constrained by $a_0^2 + \vec{a}\cdot\vec{a} = 1$) lead to a degenerate solution. This classical degeneracy is lifted when a_0 and $\vec{a}$ are promoted to quantum collective variables leading to baryons with the physical quantum numbers [123].

However, there is a subtlety concerning the use of the quantization scheme of Ref. [123] for the regime considered here. There are two types of collective motion—the rotational/isorotational degrees of freedom of Ref. [123] and the collective vibration of the heavy meson off of the light baryon. Provided that the natural time scales for these types of motion are very different, they decouple. Formally, in the large N_c and heavy quark limits, when the collective vibrational degree of freedom resides near the bottom of the potential well and vibrates harmonically, its natural time scale goes as $\lambda^{-1/2}$ [106, 107] while the time scale of the [123] collective coordinate is λ^{-1}, where λ is an overall counting parameter for the combined limit:

$$\frac{1}{N_c} \sim \frac{\Lambda_H}{m_Q} \sim \lambda \tag{3.5}$$

and Λ_H is the characteristic hadron mass scale. Formally, in the ideal limit, $\lambda \to 0$ and the two scales decouple. However, in the present study where effects beyond the $\lambda \to 0$ limit are explicitly examined, the situation is more problematic.

As a practical matter, in order to proceed, it will be assumed that the motions do decouple. This can be justified in part on empirical grounds. The splitting between the Σ_c and the Λ_c in the extreme limit would be ascribed to a rotation excitation and hence of order λ. The splitting between the first negative parity Λ_c (the $\Lambda_c(2593)$) and the Λ_c is vibrational (in the ideal limit) and hence is of order $\lambda^{1/2}$ which is parimetrically higher than the rotational excitation. In practice $M_{\Sigma_c} - M_{\Lambda_c} \approx 170$ MeV while $M_{\Lambda_c(2593)} - M_{\Lambda_c} \approx 320$ MeV. Thus, the ordering is what one expects. However, it is by no means obvious that one can legitimately take 320 MeV to be considered to be qualitatively large compared to 170 MeV.

There is another reason why it is reasonable to treat the motions as though they decouple for certain qualitative purposes. If the goal is to assess whether the standard Skyrmion treatment for charmed and bottom baryons (which implicitly works in the neighborhood of the combined limit) is self consistent, two issues arise. The first is whether the rotational and vibrational motion decouple. The second is whether the collective vibrational wave function is well localized near the bottom of the effective potential well. This chapter is investigating the second question. As a logical matter, if one finds that the collective wave function does not remain well localized *under the assumption that rotational and vibrational motion decouple*, then there are important corrections to the standard treatment *regardless of whether the assumption of decoupling is justified*. Therefore, by showing that the collective wave function is not localized as in the ideal limits, the assumptions that the standard quantization method is applicable will be justified *a posteriori*.

Having argued that the standard quantization of the collective coordinates is

applicable for the purposes here, one can focus on the heavy meson sector of the Lagrangian. This Lagrangian is the HQET heavy meson chiral Lagrangian in the Σ basis, Eq. (1.19), that was discussed in Sect. 1.2. The interaction term in this Lagrangian is

$$\mathcal{L}^{\rm int}_{\rm HQET} = \frac{ig}{2}{\rm Tr}\bar{H}_a H_b \gamma^\mu\gamma^5(\Sigma^\dagger\partial_\mu\Sigma)_{ba} + \ldots, \tag{3.6}$$

where the ellipsis denotes terms which are suppressed by inverse powers of the heavy quark mass, $1/m_H$. It should be noted that in this basis, the heavy fields have an unusual transformation under parity [113]. The field H_a transforms under parity as

$$H_a(x^0,\vec{x}) \to \gamma^0 H_b(x^0,-\vec{x})\gamma^0\Sigma^\dagger_{ba}(x^0,-\vec{x}). \tag{3.7}$$

This transformation has the interesting property that when the soliton and the heavy meson are located at the same point, $\Sigma^\dagger = -1$ in the transformation, while when they are separate, $\Sigma^\dagger = 1$. Thus, the heavy mesons act as though they have negative parity at long distances (as they must) but effectively as positive parity particles at short distances (when the anti-quark parity is also included).

Previously, the idealized $\lambda \to 0$ limit was uniform; *i.e.*, the ordering of the large N_c and heavy quark limits was irrelevant [106, 107]. It is hoped that in the current problem the ratio of the heavy quark mass to the ordinary baryon mass is equally irrelevant provided they are both large. If so, it is legitimate to calculate the effective potential assuming the heavy quark mass is infinite (but the nucleon mass is not). That calculation will be done here and subsequently verified that the result did not depend on this procedure. This will be demonstrated by showing that the same effective potential arises if the nucleon mass is taken to be infinite and the

heavy quark mass finite.

Since the complete spatially extended potential as a function of the relative separation distance between the particles is being considered, instead of the standard soliton ansatz, the following ansatz will be considered,

$$\begin{aligned}\Sigma(\vec{x}-\vec{x}_0(t)) &= A(t)\Sigma_0(\vec{x}-\vec{x}_0(t))A^{-1}(t),\\ \Sigma_0(\vec{x}-\vec{x}_0(t)) &= \mathrm{Exp}[i\vec{\tau}\cdot\frac{\vec{x}-\vec{x}_0}{|\vec{x}-\vec{x}_0|}F(|\vec{x}-\vec{x}_0|)]\end{aligned} \tag{3.8}$$

where $\vec{x}$ is the position of the heavy meson, $\vec{x}_0$ is the position of the soliton, and the soltion coordinate and the collective coordinates are time dependent while the heavy meson coordinate is not. This will fix the heavy meson to a specific location, which can be chosen to be the origin, and allows one to work in the rest frame of the heavy meson. Therefore the four-velocity of the heavy meson is $v^\mu = (1,\vec{0})$.

Even with this different choice for the soliton ansatz, the only term that produces an interaction between the heavy meson and the chiral soliton is

$$H_I = -\frac{ig}{2}\int d^3\vec{x}\ \mathrm{Tr}\bar{H}_a H_b\gamma^j\gamma^5(\Sigma^\dagger\partial_j\Sigma)_{ba}. \tag{3.9}$$

The summation is only over the spatial coordinates in the interaction as the spin trace with the temporal coordinate is zero. When the appropriate soliton ansatz is inserted into the interaction followed by some manipulation, the interaction term is written as

$$\begin{aligned}H_I = \frac{g}{2}\int d^3\vec{x}\ &\mathrm{Tr}\bar{H}_a H_b\gamma^j\gamma^5\ \times\\ &\Big(A\Big\{\frac{y^j}{|\vec{y}|}\hat{y}\cdot\vec{\tau}\Big(F'-\frac{\sin(2F)}{2|\vec{y}|}\Big)+\frac{\tau^j}{2|\vec{y}|}\sin(2F)+\epsilon^{jmk}y^k\tau^m\frac{\sin^2(F)}{|\vec{y}|^2}\Big\}A^{-1}\Big)_{ba},\end{aligned} \tag{3.10}$$

where $\vec{y} = \vec{x} - \vec{x}_0$ is the separation distance between the soliton and the heavy meson. This can then be further simplified by factoring out τ from each term.

$$\begin{aligned} H_I &= \frac{g}{2}\int d^3\vec{x}\ \mathrm{Tr}\bar{H}_a H_b \gamma^j\gamma^5 (A\tau^i A^{-1})_{ba}\ \times \\ &\qquad \left(\frac{y^j y^i}{|\vec{y}|}\left(F' - \frac{\sin(2F)}{2|\vec{y}|}\right) + \frac{\sin(2F)}{2|\vec{y}|}\,\delta_{ij} + \epsilon^{jik}y^k\frac{\sin^2(F)}{|\vec{y}|^2}\right) \\ &= \frac{g}{4}\int d^3\vec{x}\ \mathrm{Tr}\bar{H}_a H_b \gamma^j\gamma^5\,(\tau^m)_{ba}\ \mathrm{Tr}(A\tau^i A^{-1}\tau^m)\ \times \\ &\qquad \left(\frac{y^j y^i}{|\vec{y}|^2}\left(F' - \frac{\sin(2F)}{2|\vec{y}|}\right) + \frac{\sin(2F)}{2|\vec{y}|}\,\delta_{ij} + \epsilon^{jik}y^k\frac{\sin^2(F)}{|\vec{y}|^2}\right). \end{aligned} \tag{3.11}$$

By noting that the isospin operator of the heavy meson on the H field is,

$$I_H^m H_a = -H_b\frac{(\tau^m)_{ba}}{2}, \tag{3.12}$$

and the spin operator of the light degrees of freedom of the heavy meson on the H field is,

$$S_{lH}^j H_b = -H_b\frac{\sigma^j}{2}, \tag{3.13}$$

along with the fact that $H_b\gamma^j\gamma^5 = -H_b\sigma^j$ in the rest frame of the H field, the interaction Hamiltonian can be written as

$$\begin{aligned} H_I = -gI_H^m S_{lH}^j\ \mathrm{Tr}(A\tau^i A^{-1}\tau^m)\int d^3\vec{x}\ \mathrm{Tr}\bar{H}_a H_a\ \times \\ \left(\frac{y^j y^i}{|\vec{y}|^2}\left(F' - \frac{\sin(2F)}{2|\vec{y}|}\right) + \frac{\sin(2F)}{2|\vec{y}|}\,\delta_{ij} + \epsilon^{jik}y^k\frac{\sin^2(F)}{|\vec{y}|^2}\right). \end{aligned} \tag{3.14}$$

These simplifications are similar to those performed in Ref. [114], whereas here the effective potential to all distances is considered. The integral can now be performed by explicitly fixing the heavy meson to be located at the origin. This is equivalent to equating $\mathrm{Tr}\bar{H}_a H_a$ with $-\delta(\vec{x})$. Upon replacing the soliton position label, $\vec{x}_0$, with

the more standard $\vec{r}$, the effective potential reads:

$$H_I = V(\vec{r}) = g I_H^m S_{lH}^j \, \mathrm{Tr}(A\tau^i A^{-1}\tau^m) \times \left(\frac{r^j r^i}{r^2} \left(F' - \frac{\sin(2F)}{2r} \right) + \frac{\sin(2F)}{2r} \, \delta_{ij} - \epsilon^{jik} r^k \frac{\sin^2(F)}{r^2} \right). \tag{3.15}$$

The effective potential just derived in Eq. (3.15) has three major aspects which are interconnected with each other. First, the potential is dependent on the spin and isospin of the light quarks in the heavy meson. Secondly, the term, $\mathrm{Tr}(A\tau^i A^{-1}\tau^m)$, is related to the spin and isospin of the chiral soliton and is dependent on the collective coordinate quantization as well as the states being considered. The last part of the potential is the spatially dependent term. This term is a function of the separation distance, $\vec{r}$, as well as the profile function, $F(r)$. The profile function can be derived numerically from the chiral soliton sector of the Lagrangian. Traditionally, it is achieved by minimizing the mass of the soliton either in the presence of a pion mass [137] or without a pion mass [123], subject to the constraints that $F(0) = -\pi$ and $F(\infty) = 0$. Furthermore, if the profile function is expanded in powers of r and only terms of order r^2 are kept in the effective potential of Eq. (3.15), one can easily show that our potential reduces to the one considered by Jenkins, Manohar, and Wise [115]. Therefore in the limit that the heavy meson and chiral soliton are close together, the effective potential is the same as previously considered.

The portion of the potential that is dependent on the chiral soliton, *viz.* $\mathrm{Tr}(A\tau^i A^{-1}\tau^m)$ is dependent on the spin and isospin of the soliton, yet neither spin nor isospin are guaranteed to be valid quantum numbers of the operator. That is, in some cases the chiral soliton term allows mixing between nucleon and delta states within the heavy baryon system. To simplify this issue, the iso-scalar heavy

baryons, as in the Λ_H, will only be considered. This simplifies the problem because in order to create an iso-scalar from a heavy meson and a soliton, the soliton must have isospin-$\frac{1}{2}$. Additionally, large N_c forces chiral solitons to exhibit the property that they have the same spin and isospin. Therefore, the only soliton that can bind with a heavy meson to form an iso-scalar heavy baryon has spin-$\frac{1}{2}$ and isospin-$\frac{1}{2}$, or a nucleon. When the chiral soliton is confined to the nucleon sector, it can be shown that $\mathrm{Tr}(A\tau^i A^{-1}\tau^m)$ is equivalent to $-8I_N^m S_N^i/3$, where I_N^m and S_N^i are the isospin and spin of the nucleon, respectively. Making this replacement in the effective potential and summing over repeated indices leads to a potential operator that reads:

$$V(\vec{r}) = -\frac{8g}{3}(\vec{I_H}\cdot\vec{I_N})\Big((\vec{S_{lH}}\cdot\hat{r})(\vec{S_N}\cdot\hat{r})(F' - \frac{\sin(2F)}{2r}) + (\vec{S_{lH}}\cdot\vec{S_N})\frac{\sin(2F)}{2r} - (\vec{S_{lH}}\times\vec{S_N})\cdot\hat{r}\,\frac{\sin^2(F)}{r}\Big). \tag{3.16}$$

Having derived a potential operator, the problem reduces to finding the eigenvalues and eigenstates of this operator. In order to determine the eigenstates of this potential operator, let us consider states labelled by the total isospin, I, the total spin, s, and the spin of the light degrees of freedom, s_l. These states can be written as $|I, s, s_l\rangle$. For a total isospin-0, three states can be constructed; $|0, \frac{1}{2}, 0\rangle$, $|0, \frac{1}{2}, 1\rangle$, and $|0, \frac{3}{2}, 1\rangle$. From the potential, it is clear that total isospin is a good quantum number for the states, however, the spin of the light degrees of freedom is not obviously a good choice here as the cross product term changes the spin state. Therefore, instead of the simple state $|I, s, s_l\rangle$, the appropriate wave function which

should be considered has the form:

$$\Psi_{\Lambda 0} = [1 + D(r)\vec{r} \cdot (\vec{S_{lH}} \times \vec{S_N})]|0, \frac{1}{2}, 0\rangle \phi(\vec{r}) \tag{3.17}$$

for the $|0, \frac{1}{2}, 0\rangle$ state, and

$$\Psi_{\Lambda 1} = [1 + D'(r)\vec{r} \cdot (\vec{S_{lH}} \times \vec{S_N}) + E'(r)(\vec{S_{lH}} \cdot \vec{r})(\vec{S_N} \cdot \vec{r})]|0, \frac{1}{2}, 1\rangle \phi(\vec{r}) \tag{3.18}$$

for the $|0, \frac{1}{2}, 1\rangle$ and $|0, \frac{3}{2}, 1\rangle$ states. There is a degeneracy for the light quark spin-1 states because of the degeneracy between the pseudo-scalar and vector heavy mesons in the heavy quark limit. It can be shown that the wave function for the light quark spin-0 state is in fact the eigenfunction of the potential operator when

$$D(r) = \frac{-2(\cos(F) + 1)}{r \sin(F)} \tag{3.19}$$

with an eigenvalue of

$$V_{\Lambda 0}(r) = -\frac{g}{2} F'(r) + g\frac{\sin(F)}{r}. \tag{3.20}$$

The effective potential for the isospin-0 light quark spin-1 channel can be obtained in a similar manner. Here, the form given above is the eigenfunction when

$$D'(r) = \frac{-4(1 + \cos(F))}{r \sin(F)} \quad \text{and} \quad E'(r) = -\frac{4}{r^2} \tag{3.21}$$

with the eigenvalue

$$V_{\Lambda 1}(r) = -\frac{g}{2} F'(r) - g\frac{\sin(F)}{r}. \tag{3.22}$$

The previous discussion was based on taking the heavy meson mass to be arbitrarily large so that collective dynamics involved the soliton moving. It has been argued that the resulting dynamics ought to be independent of this assumption. To

demonstrate this, the effective potential with the soliton's position held fixed can be calculated with the methods described above with a few caveats. First, since the heavy meson is now moving, the kinetic energy term of the heavy meson needs to be explicitly considered. From HQET [138] the additional term in the Lagrangian for the heavy meson fields is

$$\mathcal{L}_{\text{kinetic}} = \text{Tr}\bar{H}_a \frac{(D_\perp^2)_{ba}}{2M_H} H_b, \tag{3.23}$$

where $D_\perp^\mu$ is the covariant derivative perpendicular to the velocity and is defined as $(D_\perp^\mu)_{ba} = (D^\mu)_{ba} - v^\mu (v \cdot D)_{ba}$. The velocity of the heavy meson is given by v, and D^μ is the covariant derivative defined by $(D^\mu)_{ba} = \partial^\mu \delta_{ba} - \frac{1}{2}(\Sigma^\dagger \partial^\mu \Sigma)_{ba}$. The Roman indices are the light quark flavor indices, as before. This term is the heavy meson analog to the kinetic $1/m_Q$ correction in the heavy quark Lagrangian Eq. (1.10). Second, even though the heavy meson is allowed to move, it is still desirable to be close to the heavy quark limit, therefore, the heavy meson's velocity will be small; $v^\mu = (1, \vec{\epsilon})$.

The effective potential can still be derived from the interaction term as written in Eq. (3.9) except the integral is now over x_0—the soliton's position rather than the heavy meson's position. The use of only the spatial directions in this equation is still justified since corrections to this are of order ϵ, which will remain small. The calculation proceeds as previously illustrated until Eq. (3.14). The substitution of the spin of the light quark in the heavy meson from the previous formula is still possible with corrections of $O(\epsilon)$. At this point, the integral can be performed analogously as before, but by fixing the soliton's position to be $x_0 = 0$. However,

unlike before, the term $\mathrm{Tr}\bar{H}H$ in the expression of the effective potential remains. This term is dependent on the heavy meson wave function. However, the heavy meson wave function can be expressed as an exponential, *i.e.*, $H \sim \mathrm{Exp}[if(x)]$, where $f(x)$ is some unknown function of the heavy meson's position. With the appropriate normalization, one can thereby set $\mathrm{Tr}\bar{H}H = -1$. Thus the same effective potential as in Eq. (3.15) has been (practically) derived. The careful observer will notice that the potential derived with the soliton held fixed is identical with Eq. (3.15) except for the sign of the last term. Nevertheless it will be shown that this potential will lead to the same physical system.

The eigenfunctions and eigenvalues of the new potential operator can be constructed just as before. However, when the effective potential having held the soliton fixed is used instead, $D(r)$ and $D'(r)$ in Eqs. (3.19) and (3.21) have the opposite sign. This sign difference compensates exactly the sign difference between the potentials discussed above. Thereby both methods lead to the same physical effective potentials in Eqs. (3.20) and (3.22). Since both methods lead to the same physical effective potentials, the commutativity of the large N_c and heavy quark limits in this problem has been demonstrated.

To complete the discussion of these wave functions, one needs to establish the correspondence between the $|I, s, s_l\rangle$ states and the physical Λ_H states. From the states' quantum numbers it is clear that the light quark spin-0 state, $|0, \frac{1}{2}, 0\rangle$, corresponds to the ground state of Λ_H, while the light quark spin-1 states are spin excitations of this ground state which have yet to be observed. The observed excited states to Λ_c, $\Lambda_c^+(2593)$ and $\Lambda_c^+(2625)$, would constitute radial excitations of the

light quark spin-0 state. However, even with these apparently clear assignments, the parity of the heavy baryon states is not immediately clear in this language. The wave functions for both the light quark spin-0 and spin-1 states written above do not appear to have definite parity. Thus when the orbital momentum between the heavy meson and the soliton is considered in the $l = 0$ state, the ground state wave function contains parts which are characteristic of both s- and p-wave states. The states achieve definite parity when one recalls that the heavy meson state itself is negative under parity when near the soliton and positive when far apart, as pointed out in Eq. (3.7) and the sentences following that equation. The wave functions in Eqs. (3.17) and (3.18) show that when the heavy meson and soliton are close together, the state has a positive parity (positive from the s-wave, positive from the heavy meson) while when they are far apart, the state still has positive parity (negative from the p-wave, negative from the heavy meson). Thereby, the ground states, and thus subsequent excitation, have the same parity as their physical particle states, which completes the assignment between wave functions and physical states. In this system, there is a subtlety associated with orbital momentum states since the orbital momentum is not a good quantum number. However, the "orbital momentum", l, used in the Schrödinger equation is a good quantum number, and will henceforth be used to label these states. This label can be thought of as the orbital momentum state when the heavy meson and soliton are close together. In previous studies, since they were only concerned with small motion of the potential away from the heavy meson and soliton sitting at the same place, these long distance effects on the parity of the states did not matter. Thus, in their work the states

could be clearly labelled by the orbital momentum between the heavy meson and the soliton.

The effective potential of a heavy meson and a nucleon in terms of the profile function, $F(r)$, for the isospin-0 light quark spin-0 and spin-1 channels has been derived. Note that these potentials are completely radial. These potentials include short- and long-distance behavior for the binding which inherently has not been considered before. It should be noted that when both of these potentials are examined at short distances, they reduce to the potentials and values at the origin that have been previously identified [113, 114, 115].

3.3 Determination of bound states

At this point, the constructed effective potentials can be used in a Schrödinger equation, and the bound states can be calculated. At the time of the previous studies the heavy meson-soliton coupling, g, was undetermined. In recent years this has been measured to be ≈ 0.59 from the decays of D^* meson into D mesons and pion emissions [108]. It can be assumed that this coupling is the same for B mesons (as it should be in the heavy quark limit) since an experimental determination via pion emission is not energetically possible. The physical mass of the spin-0 heavy meson was used (1864 MeV for D meson and 5279 MeV for B meson [109]), while the mass of the soliton was calculated from the profile function.

The short- and long-distance structure of the profile function, $F(r)$, was obtained by examining the differential equation that minimized the mass of the chiral

soliton. From there, the profile function was constructed by parameterizing the functional form consistent with the short- and long-distance behavior with two parameters. These two parameters where determined by an iterative method that minimized the mass of the soliton while keeping the nucleon-pion coupling, g_A, and the pion decay constant, f_π, constant. This procedure constructed the Skyrmion profile function plotted in Fig. 3.1 and fixed the Skyrme parameter, $e = 4.10$, and the soliton mass, $M = 949$ MeV.

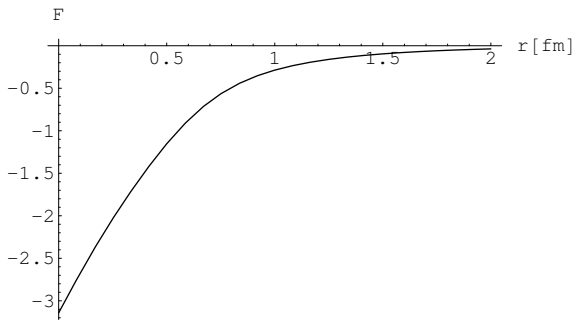

Figure 3.1: Calculated Skyrmion profile function, $F(r)$.

The Schödinger equation with the appropriate effective potential for this system was solved to test for the existence of bound states. Figure 3.2 shows the potential for the light quark spin-0 state with the harmonic oscillator approximation overlaid. When the equation was solved, the binding energy for the charm case was found to be 155 MeV while for the bottom case, the binding energy was found to be 177 MeV. In both cases a weakly bound radial excited state was also observed; 6.18 MeV for charm and 19.32 MeV for bottom. The observed ground states are more tightly bound than the ground state in the harmonic oscillator approximation. Therefore the inclusion of the entire potential increases the binding

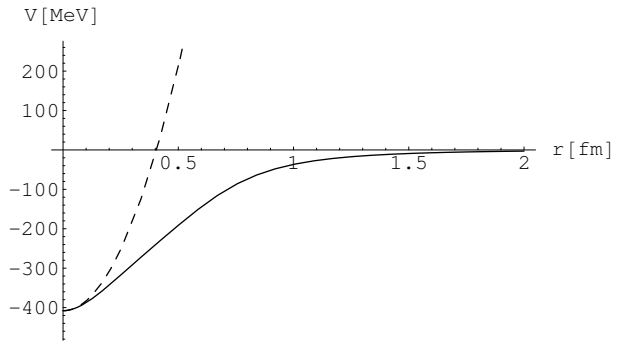

Figure 3.2: Light quark spin-0 state effective potential (solid curve) with harmonic approximation (dashed curve) as a function of separation distance.

energy and favors a stronger bound state. Furthermore, the wave function of the nucleon in the ground state is much broader with the extended potential compared with the wave function of the harmonic oscillator (see Fig. 3.3). This increase in the wave function breadth indicates that the nucleon is influenced by the long-distance part of the potential.

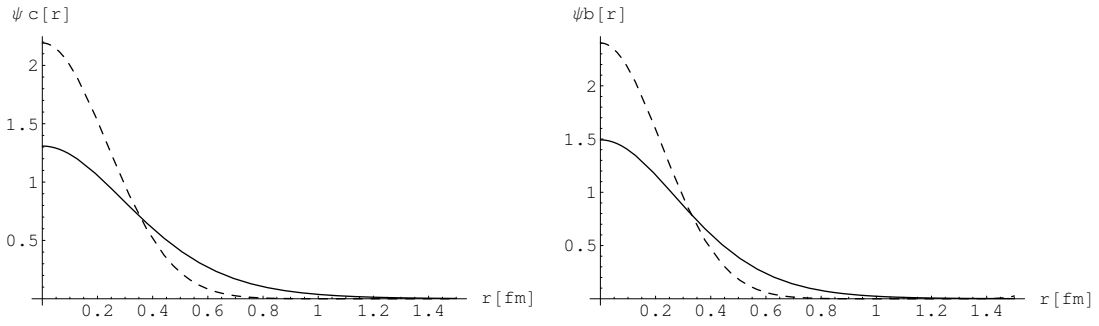

(a) Charm Wave Function (b) Bottom Wave Function

Figure 3.3: (a) Calculated normalized wave function for the ground state Λ_c from the complete potential (solid curve) and the harmonic approximation (dashed curve). (b) Calculated normalized wave function for the ground state Λ_b from the complete potential (solid curve) and the harmonic approximation (dashed curve).

It is clear that for this particular model, both the shape of the wave function and the binding energy are vastly different when the entire effective potential is

considered as compared to when the potential is assumed to be harmonic with the collective degree of freedom tightly localized. Large amplitude motion clearly occurs and the standard analysis appears to be invalid for this system.

For this system, orbital excited states can also be seen. Both the charm and bottom cases have an $l = 1$ excited state; the binding energy is 42.0 MeV (charm) and 68.0 MeV (bottom). Neither system appears to have a bound $l = 2$ state.

For the case when the light quark system carries spin-1, no bound states were found. The potential in this channel has a strong repulsive core with a very shallow attractive region which appears to be too weak to support bound states.

The previous calculations were performed using the assumption (valid in the heavy quark limit) that vector and pseudoscalar heavy mesons are degenerate. This is obviously not true in the physical case; that is, the D and the D^* or the B and the B^* have different masses. The calculation can be extended to include the physical mass splittings between the heavy meson states. When these splittings are included, there are still bound Λ_H states, however, the binding is weaker. The binding energy of the ground state is reduced by 88.7 MeV for charm and 35.9 MeV for bottom.

To reiterate, these results clearly illustrate that the effective potential is not strong enough to localize the collective variable in the harmonic region for these models. The underlying assumption that the system is sufficiently close to the large N_c and heavy quark limits to use the harmonic approximation is not justified. Clearly it is important to see whether the breakdown of the combined heavy quark and large N_c limit is generic for realistic nucleon and heavy quark masses. This is particularly true since the model considered has serious phenomenological flaws, as

will be discussed below. The key question is whether the standard treatment works for "realistic" models.

3.4 Towards the effective potential in realistic models

The model considered in the previous section is unsatisfactory in terms of phenomenology. In the first place the mass of the heavy baryons is well off from the empirical ones. The relevant issue is not how large the fractional error is for the mass since a large fraction of the mass is simply from the heavy quark itself. The relevant issue is the fractional error in the binding energy—*i.e.*, the difference between the mass of a nucleon plus a heavy meson from the mass of the heavy baryon. The experimental and model-calculated binding energies for both charm and bottom baryons are summarized in Table 3.1. Note the large difference between the experimental and calculated binding energies.

Method	$\boldsymbol{\Lambda_c}$	$\boldsymbol{\Lambda_b}$
Experiment	520 MeV	590 MeV
Full Potential (no mass splitting)	155 MeV	177 MeV
Full Potential (mass splitting)	67.3 MeV	141.1 MeV

Table 3.1: Table summarizing the binding energies for the Λ_c and Λ_b baryons.

Moreover, the model considered above has the feature that the interaction is identical under the exchange of a heavy meson to a heavy anti-meson. That is, our extended potential will give the same bound states for ordinary heavy baryons as for heavy pentaquark states. Clearly this is unphysical. While heavy pentaquark states are known to exist in the extreme heavy quark and large N_c limits as shown

in the previous chapter, there exists no symmetry of QCD in that limit which implies a degeneracy between pentaquarks and ordinary heavy baryons. Moreover, strong-interaction-stable heavy pentaquarks have not been detected despite intensive searches, suggesting that for realistic masses they do not exist.

If one wishes to make a more realistic model it is necessary to include additional interaction terms between the heavy meson and the soliton which split the ordinary heavy baryon from the pentaquark. Such an interaction should be strong enough to give heavy baryons with approximately the correct mass. Heretofore, only an interaction term between the pion fields and the heavy quark which was lowest order in the chiral expansion has been included. However, in the soliton there is no chiral power counting and thus no necessity to restrict the interaction to this term. The spirit of model building in Skyrme type models is to include a small number of terms to make the problem tractable. Although there is no systematic power counting, the hope is that one can get qualitatively sensible results by choosing coefficients for these which compromise between the various observables. The simplest model realistic enough to get the binding of the heavy baryons correct while pushing up the mass of the heavy pentaquarks above threshold will require one new interaction term.

The simplest term one can consider, which distinguishes between interactions between heavy mesons and anti-mesons, is coupling the light quark baryon current to the heavy quark vector current. Note that if a heavy anti-meson binds with a nucleon, the heavy quark current will switch sign compared with the heavy meson case while the baryon current (associated with the nucleon) will not. Therefore the

term

$$\mathcal{L}_{\text{baryon}} = g' \text{Tr} \bar{H}_a H_a \gamma_\mu B^\mu \tag{3.24}$$

can be added to the Lagrangian, with the baryon current, B^μ, given by the standard form,

$$B^\mu = \frac{\epsilon^{\mu\nu\alpha\beta}}{24\pi^2} \text{Tr}[(\Sigma^\dagger \partial_\nu \Sigma)(\Sigma^\dagger \partial_\alpha \Sigma)(\Sigma^\dagger \partial_\beta \Sigma)], \tag{3.25}$$

where the notation $\epsilon_{0123} = -\epsilon^{0123} = 1$ was used. By inserting the functional form for the solitons into this term, and working in the rest frame of the heavy (anti)meson, the interacting potential can be derived as :

$$V_{\text{baryon}}(\vec{r}) = g' B^0(r) = \frac{g'}{2\pi^2} \frac{\sin^2(F)}{r^2} F'(r). \tag{3.26}$$

The coupling constant, g', and its relative sign are unknown, but the sign will be chosen such that this potential is attractive for heavy meson-nucleon interactions while repulsive for heavy anti-meson-nucleon interactions. In the spirit of this class of model, the coupling g' will be tuned in order to get a reasonable mass for the heavy baryon (either Λ_b or Λ_c). Of course, this procedure is quite *ad hoc*, but Skyrme type models always require some *ad hoc* procedure. One useful check on whether the model obtained is sensible is whether the the coupling obtained has a natural size, *i.e.*, whether it is of $O(1)$.

When the Schödinger equation with the combined potential was used to calculate bound states, the coupling constants needed to have bound states with physical binding energies were determined to be -3.27 for Λ_c and -3.34 for Λ_b. These are natural in size. Furthermore, the two coupling constants obtained via fitting for the two types of heavy baryons are quite close to one another; they differ by only

2% suggesting that the procedure is robust for physical values. For simplicity, the heavy meson mass splittings were not included in this calculation.

Because of the lack of the heavy meson mass splitting, one would expect that the first excited state to be a superposition of the two physically observed excited states, $\Lambda_c^+(2593)$ and $\Lambda_c^+(2625)$. It is not unbelievable to surmise that this combined state would weight the two states by the relative spins of the states. This would lead to a mass of the combined state of 2614 MeV or an excitation energy of 328 MeV above the ground state. With the coupling constants considered here, the excitation energy from the combined potential was found to be 324 MeV and 316 MeV for the charm and bottom cases, respectively. This is in surprisingly good agreement with the expected excitation from the physically seen states.

With the inclusion of the baryon current term to the potential, the light quark spin-1 state becomes bound for the coupling constants considered here. The binding energies are weak–125 MeV for charm and 173 MeV for bottom–compared with their spin-0 counterparts, 521.6 MeV and 593.4 MeV for the Λ_c and Λ_b, respectively. This binding is driven solely by the size of the baryon current coupling. The presence of a bound state in the spin-1 channel does not invalidate nor should it limit this method. It is not unreasonable to believe that the strength of the additional potentials needed to be included to drive the binding energy down to physical values might also bind light quark spin-1 states. Therefore the lack of any observation of these states could be associated with the difficulty in detection and not in the lack of the presence of these states.

A harmonic approximation can also be made for the combined potential with

the provided coupling constants. The energy levels for the approximation are again different from that of the combined potential and the ground state is bound weaker. An examination of the shape of the wave function for the combined potential compared with the harmonic wave functions shows again that the wave functions for the combined potential are broader than the harmonic wave functions and extend beyond the harmonic region. One is again not driven to the effective potential minimum by the realistic masses suggesting that the physical states are not close to the extreme large N_c and heavy quark limits. These observations confirm the results from the previous section that the long-distance potential greatly influences heavy baryon formation.

Unlike with the original potential, the new combined potential is sensitive to the difference between regular heavy baryons and heavy pentaquarks. One can examine whether a bound pentaquark state is possible within the combined potential by flipping the sign of the coupling constant of the baryon current term. When this is performed, a very weakly bound pentaquark state can be found with a binding energy of 33.4 MeV for a charm type pentaquark, and 42.9 MeV for a bottom type pentaquark. These are rather small binding energies compared with the binding energies of the regular heavy baryons, and are small compared to the deeply bound pentaquark states suggested by the large N_c and heavy quark limits of the previous chapter. Furthermore, the potential for the heavy pentaquark is repulsive at short distance creating the attractive region and localization of the wave function away from the origin. Therefore, even in the ground state, the pentaquark formed here has a fixed separation between the heavy anti-meson and the nucleon. However, due to

the strong repulsion at short distance this is a very delicate state. If one turns off the potential which is identical for the heavy baryon and heavy pentaquark states, and tune the baryon current coupling such that heavy baryons are still bound with the appropriate binding energy, the heavy pentaquark effective potential is completely repulsive and thereby no heavy pentaquark state is bound. The coupling constants needed to achieve this condition were -5.52 for the charm case and -5.49 for the bottom case. These couplings are again neither unreasonably large nor small. This indicates that this model is capable of binding a heavy pentaquark state, but with minor changes, it is just as reasonable not to support a bound heavy pentaquark state. The relative ease for the state to become unbound furthers the point in Chapter 2 that heavy pentaquark binding with physically reasonable parameters is subject to the dynamical details of the model.

The inclusion of an additional interaction term based upon the coupling of the heavy quark current to the baryon current was motivated by the need to break the degeneracy between heavy baryon and heavy pentaquark states associated with the leading order HQET. This interaction was derived for all separation distances. The coupling of the interaction was determined by having the ground state binding energy correspond to the physical value. With this potential in place, the simple model considered here gives phenomenologically reasonable results concerning ordinary heavy baryons while simultaneously being reasonably consistent and inconsistent with a bound heavy pentaquark state.

3.5 Calculation of the Isgur-Wise Function

The Isgur-Wise function is a universal function in the heavy quark limit that describes the semileptonic decay of all heavy hadrons in an $SU(2N_H)$ multiplet (where N_H is the number of heavy flavors) [11, 12]. Heavy hadrons of the Λ type will be considered in this section. Thus the process in question is $\Lambda_b \to \Lambda_c e^- \bar{\nu}_e$. Previous work has shown that the Isgur-Wise function is completely determined in the combined large N_c and heavy quark limit [115]. In this limit the effective potential is purely harmonic in nature, and the Isgur-Wise function depends on only one parameter, the harmonic "spring constant" [116, 117]. Therefore it has been pointed out that if the excitation energy of heavy baryons were measured, the spring constant would be fixed and thus the Isgur-Wise function would be completely determined up to higher-order corrections.

Unfortunately, it has been shown thus far that for realistic parameters, the system does *not* remain in the harmonic region and the expansion appears to break down. Of course, from the wave functions which have already been calculated, the Isgur-Wise function can also be calculated, and again one would expect distinct results from the harmonic oscillator case.

The most interesting aspect of the Isgur-Wise function near the combined limit is related to the fact that this entire universal function is dependent on one measurable parameter. It is important to test the reliability of this result when one deviates from the ideal limit, *viz.*, for the real world. Ideally one could test this by using the empirical value of the excitation energy of the first excited state plus

the assumption that one is near the combined large N_c and heavy quark limits to compute the Isgur-Wise function; this ought then to be compared with the experimental Isgur-Wise function for an empirical test. However, the Isgur-Wise form factors have not been measured.

In the absence of such data, one can still get some idea of how robust the prediction is by using "realistic" models. Since these models indicate that that system is quite anharmonic, one does not expect a close agreement of the Isgur-Wise function with the harmonic approximation based on the energy of the first excited state. Instead of considering the entire Isgur-Wise function, the curvature at zero recoil, ρ, of the Isgur-Wise function will be focused upon. This is chosen as ρ is proportional to the mean radius squared in the heavy quark limit, and thereby provides a single number with which to compare and does so in a physically transparent way.

The Isgur-Wise function in momentum space from [115] is

$$\eta_0 = \int d^3\vec{p}\, \phi_c^*(\vec{p} + m_N\vec{v}')\, \phi_b(\vec{p}). \tag{3.27}$$

In the case of harmonic wave functions this reduces to

$$\eta_{HO}(z) = \frac{2\sqrt{2}\mu_b^{3/8}\mu_c^{3/8}}{(\sqrt{\mu_b}+\sqrt{\mu_c})^{3/2}} \exp\Big(\frac{-z^2}{2\sqrt{\kappa}}\Big), \quad \text{where} \quad z \equiv \frac{m_N|\vec{v}|}{(\sqrt{\mu_b}+\sqrt{\mu_c})^{1/2}}, \tag{3.28}$$

m_N is the mass of the nucleon, κ is the harmonic coupling, $\vec{v}$ is the transfer velocity, and μ_c and μ_b are the reduced mass of the heavy meson-nucleon system for either charm or bottom, respectively. One can also express the Isgur-Wise function in terms of position space wave function as

$$\eta_0 = \int d^3\vec{x}\ \psi_c^*(\vec{x})\psi_b(\vec{x})\, e^{im_N\vec{v}\cdot\vec{x}}. \tag{3.29}$$

These expressions for the Isgur-Wise function lead to the following leading order expressions for the curvature at zero recoil,

$$\rho_{HO} \equiv \frac{\partial^2 \eta_{HO}}{\partial z^2}(z=0) = -\frac{2\sqrt{2}\mu_b^{3/8}\mu_c^{3/8}}{\sqrt{\kappa}\,(\sqrt{\mu_b}+\sqrt{\mu_c})^{3/2}} \tag{3.30}$$

for the harmonic case, and

$$\rho \equiv \frac{\partial^2 \eta}{\partial z^2}(z=0) = -(\sqrt{\mu_b}+\sqrt{\mu_c})\int d^3\vec{x}\;\psi_c^*(\vec{x})\psi_b(\vec{x})\vec{x}^{\,2}\cos^2(\theta) \tag{3.31}$$

for the spatial wave function case.

The curvature at zero recoil, ρ, will be calculated in three different manners. First, ρ can be calculated by approximating the potential by a harmonic oscillator to generate a harmonic coupling, κ. Equation (3.30) can then be used for this value of κ, along with physical values of the mass variables, to calculate ρ. Second, the wave functions of the ground state of the complete potential can be used directly in Eq. (3.31) to calculate ρ. Of course, this is the proper way to calculate ρ and the Isgur-Wise function since the complete potential is being considered. One would expect a vast difference between the first two methods since differences in the wave function between the harmonic wave functions and the complete potential wave functions have been consistently observed. Lastly, even though one knows that the energy levels calculated by using the entire effective potential are not harmonic in nature, one could use the excitation energy of the first excited state to calculate κ as though it were derived from a harmonic oscillator, and then use this value of κ to calculate ρ using Eq. (3.30). That is, instead of deriving the harmonic coupling from an approximation to the actual potential, a new harmonic potential is constructed from the excitation energy of the complete potential. This new harmonic potential

is unrelated to the original harmonic potential and to the complete potential, except that the energy gap between the ground state and the first excited state of this new potential and the complete potential are identical. Of course, the third method has no underlying theoretical basis unless the system is harmonic (in which case it will agree with the first two). It is useful to consider it, however, because it simulates theoretically the empirical procedure outlined above.

When the curvature of the Isgur-Wise function at zero recoil, ρ, was calculated in these manners, using physical mass of the nucleon and the heavy baryons, the following results were obtained. The normalized wave functions are shown in Fig. 3.4, remembering that ρ is proportional to the expectation value of r^2. Method 1

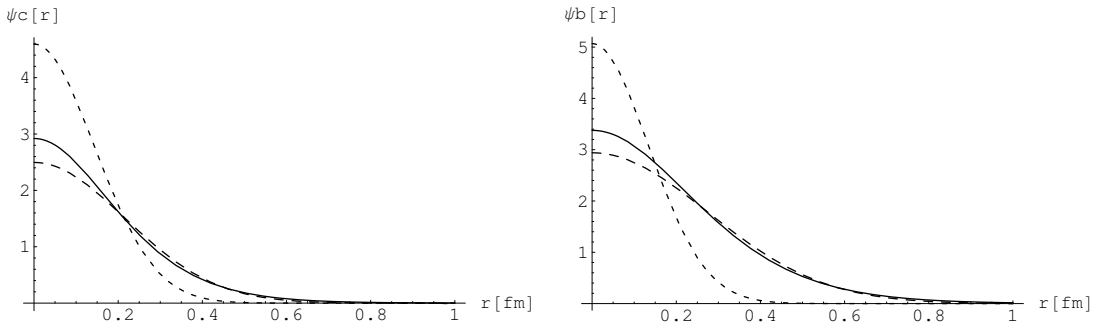

(a) Charm Wave Functions (b) Bottom Wave Function

Figure 3.4: (a) Calculated normalized wave functions for the ground state Λ_c from the complete potential (solid curve), the harmonic approximation (smaller dashed curve), and the harmonic approximation from the excitation energy (larger dashed curve). (b) Calculated normalized wave functions for the ground state Λ_b form the complete potential (solid curve), the harmonic approximation (smaller dashed curve), and the harmonic approximation from the excitation energy (larger dashed curve).

yielded $-53.8 \times 10^{-6}\text{MeV}^{-3/2}$ when g' was chosen to have the appropriate coupling constant for the bottom sector. Method 2 yields $-121 \times 10^{-6}\text{MeV}^{-3/2}$. Note that by using the complete wave functions, the curvature is a factor of 2 larger than the case

of using harmonic oscillator wave functions. Lastly, Method 3, using the excitation energy from the full potential and assuming it came from a harmonic oscillator potential, yields $-111 \times 10^{-6}\mathrm{MeV}^{-3/2}$ with the bottom case coupling constant. This result is different from Method 1 as one might have expected, but is quite similar to Method 2 (which gives the "correct" result). This is quite surprising since Method 3 can only be justified via the harmonic approximation which appears to be badly violated (as seen from the result of Method 1). Given the fact that Method 3 simulates the natural way to test the harmonic approximation empirically, it is important to test whether the success of Method 3 in getting close to the correct result is a mere numerical accident for this model or whether it is a robust feature. As will be demonstrated, it is quite robust.

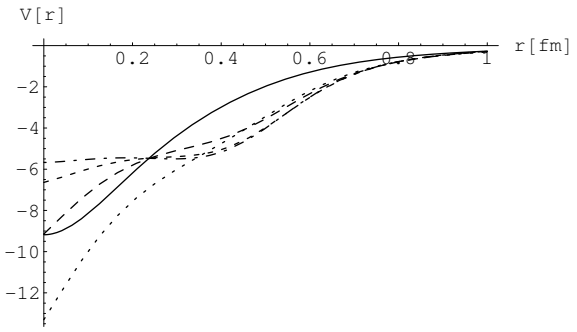

Figure 3.5: Variety of effective potentials: (a) solid curve; (b) long dashed curve; (c) short dashed curve; (d) dotted curve; (e) dot-dashed curved.

In order to test the extent to whether Method 3 generically reproduces the correct result of Method 2, one needs to consider a wide variety of models and compare the results. Since the effective potential only depends on the Skyrme profile function, a variety of profile functions (which we constructed on an *ad hoc* basis entirely for the purpose of testing the validity of Method 3) have been considered.

The curvature at zero recoil of the Isgur-Wise function was calculated for these effective potentials using the three methods detailed above. The effective potentials that were considered are shown in Fig. 3.5 while the results of the calculations of ρ are presented in Table 3.2. One can clearly see that with all effective potentials considered, the curvature at zero recoil calculated with harmonic wave functions is different from the calculations performed with the other two methods. However, for all the potentials considered, the latter two methods provide similar results. Although not depicted in Table 3.2, when an effective potential with a global minimum away from the origin is considered, Methods 2 and 3 give different results. This can be attributed to the wave function calculated with the complete effective potential being peaked away from the origin, where Method 3 assumes that the wave function is still peaked at the origin.

Potential	**Method 1**	**Method 2**	**Method 3**
a (Original)	-53.8	-121	-111
b	-83.3	-175	-171
c	-109	-216	-215
d	-101	-142	-139
e	-132	-225	-231

Table 3.2: The curvature at zero recoil, ρ, of the Isgur-Wise function calculated in three different manners in units of $10^{-6}\text{MeV}^{-3/2}$. The first line is the original profile function. All calculations were performed with the coupling constant, g', chosen to bind Λ_b with the appropriate binding energy.

The fact that Method 3 works so well, even when the system is quite anharmonic, appears to have some important consequences. In the first place, it means the prediction of ρ from the excited state energy (using the harmonic approximation) may be expected to hold reasonably well and, hence, one has some real predictive

power even if the system is rather anharmonic. The converse of this appears to be that the degree to which ρ is accurately predicted via Method 3 is a poor test of the degree to which the system is harmonic.

In fact, the situation is a bit more subtle than this. Qualitatively it is clear what is happening: the anharmonic nature of the potential lowers the excitation energy compared to that of a harmonic potential with the same curvature at the minimum. Fitting this excitation with a harmonic oscillator means that the fitted oscillator will have a smaller curvature (*i.e.*, spring constant) than the actual spring constant at the minimum. This has the effect of spreading out the wave function compared to the harmonic approximation based on the true curvature which in turn means a larger value of ρ; this acts to simulate the true wave function which is also wider than the naïve harmonic result. Thus, generically, the *sign* of the effect of anharmonicity on the excitation energy and ρ helps explain the viability of Method 3. The degree to which the method works quantitatively may still seem remarkable, however. The quantitative success is at least partially understandable analytically. It is straightforward to calculate the leading order effect of the anharmonicity on both the excitation energy of the lowest excited state [117]. As it happens, the shift in the excitation energy *exactly* compensates the shift in ρ to leading order in the anharmonicity, and the according inaccuracies due to using Method 3 only appear at next-to-next-to leading order. Thus, the system can be rather anharmonic and Method 3 can remain reasonably accurate. It is nevertheless remarkable how well Method 3 appears to work since the wave functions appear to be qualitatively quite different from the harmonic ones of Method 1.

In conclusion, an effective potential for the binding of the heavy (anti-)meson and nucleon to form regular and exotic heavy baryons for variations of the Skyrme model have been constructed. It has been demonstrated that this effective potential gives excitation energies and collective wave functions which are qualitatively different from those obtained with a harmonic oscillator approximation to the potential: the wave functions with realistic particle masses are not concentrated near the potential minimum, as expected from the large N_c and heavy quark limits. This indicates that the masses are not heavy enough to have heavy baryons exhibit the properties of these limits. Calculations with the full effective potential showed that heavy pentaquark states are possible in this class of model but the existence of bound pentaquarks depends sensitively on the details of the model studies. This result is consistent with the observations of Chapt. 2. It was also shown that despite strong anharmonicities the description of the Isgur-Wise function derived from the harmonic approximation works remarkably well provided that the effective harmonic coupling derived from the first excitation energy is used. The next chapter will move away from potential models. It will focus on an emergent symmetry of QCD associated with heavy quark physics.

Chapter 4

Doubly heavy hadrons and the domain of validity of doubly heavy diquark–anti-quark symmetry

4.1 Introduction

This chapter concerns an emergent symmetry of QCD which is relevant for heavy quarks. It has been known for some time that in the limit of arbitrarily large heavy quark masses that QCD has a symmetry which relates hadrons with two heavy quarks (anti-quarks) to analogous states with one heavy anti-quark (quark) [139]. This symmetry will be referred to as the doubly heavy diquark–antiquark (DHDA) symmetry. Presumably when the masses are finite, but very large, a remnant of this DHDA symmetry will survive in the form of an approximate symmetry. A key issue is how large must the masses be before such an approximate DHDA symmetry is manifest in a useful way. The issue is particularly relevant for charm quarks—both because the charm quark is the lightest of the heavy quarks and hence the approximation is most likely to fail and because doubly bottomed hadrons (or hadrons with a charm and a bottom) are more difficult to create and detect than doubly charmed ones.

The issue remained of only marginal importance in the absence of observed doubly heavy hadrons. However, in the past several years, the SELEX Collabora-

tion has reported the first sighting of doubly charmed baryons [140, 141, 142, 143]. Four states, $\Xi_{cc}^{+}(3443)$, $\Xi_{cc}^{++}(3460)$, $\Xi_{cc}^{+}(3520)$, and $\Xi_{cc}^{++}(3541)$ (which have been interpreted as two pairs of iso-doublets) are reported, as shown in Fig. 4.1. It should be noted that all four states were identified through their weak decay products. This is surprising as one would ordinarily expect the excited states to decay electromagnetically much more rapidly and thus wash out a signal for weak decays [144]. This issue creates a problem for any interpretation of the data. Additionally, most recently, BaBar has reported that they have not observed any evidence of doubly charmed baryons in $e^{+}e^{-}$ annihilations [145]. Thus one might question the existence of these states. However, despite these issues it is useful to ask whether the properties of these states could be understood at least qualitatively in terms of the DHDA symmetry assuming that the states are, in fact, real. Recently Refs. [146] and [147] argued that the splitting between the lower doublet and the upper doublet Ξ states can be understood semi-quantitatively (at the 30% level) in terms of an approximate DHDA symmetry.

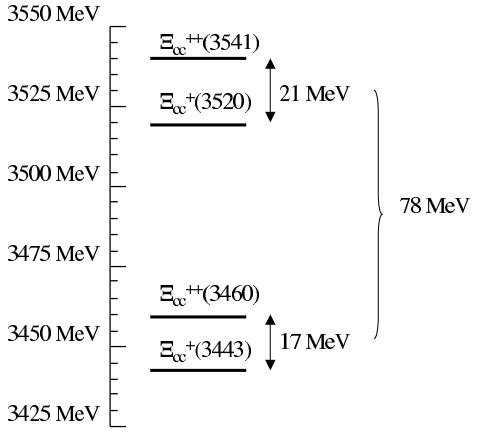

Figure 4.1: Spectrum of Ξ_{cc} that have been observed by the SELEX Collaboration. [140, 141, 142, 143]

This chapter critically examines the extent to which an approximate DHDA symmetry could be present for charm quarks. This is of importance both for the doubly charmed states found by SELEX and also for the existence of putative doubly charmed tetraquarks which are known to exist in the heavy quark limit [112] and in potential models [148]. Strong evidence is found to suggest that the charm quark mass is *not* heavy enough for the symmetry to emerge automatically of color Coulombic interactions. The key issue is the degree to which scales that separate in the heavy quark limit (and whose separations are critical to the derivation of the DHDA symmetry) in fact separate for doubly charmed systems. As will be detailed below, such a scale separation probably does not hold. Despite this, the analysis in this chapter will show that the presence of certain non-perturbative interactions *could* result in an approximate DHDA symmetry in the charm sector.

To begin the discussion, consider why one expects the DHDA symmetry. Physically, it arises from a diquark pair forming a tightly bound, nearly point-like, static object. The attraction between the two heavy quarks in the diquark comes from a color Coulombic interaction that is attractive in the color $\bar{\mathbf{3}}$ channel. If the mass of the quarks is large enough, the heavy quarks move slowly and act like non-relativistic particles in a Coulombic potential. As the size of a Coulombic bound state is inversely proportional to its mass (for fixed coupling), in the large mass limit the diquark becomes a heavy, small object with color $\bar{\mathbf{3}}$. To a good approximation it becomes a static point-like $\bar{\mathbf{3}}$ color source; in this sense it acts in essentially the same way as a heavy anti-quark. This symmetry was first discussed by Savage and Wise [139] in the context of relating the properties of doubly heavy baryons, QQq,

to those of heavy mesons, $\bar{Q}q$.

To the extent that one can treat the heavy diquark as formed, one can simply use standard HQET to describe the properties of the doubly heavy baryons. Since the diquark in the doubly heavy baryon essentially acts as an antiquark, one can directly relate the properties of this system to heavy mesons. Using the HQET effective Lagrangian from Eq. (1.4) and extended to include the diquark fields as in Ref. [139], a relationship valid at large m_Q for the mass difference of spin excited states between the doubly heavy baryons and heavy mesons was derived [1]:

$$m_{\Sigma^*} - m_{\Sigma} = \frac{3}{4}(m_{P^*} - m_P), \tag{4.1}$$

where Σ and Σ^* are the doubly heavy anti-baryons with $S = \frac{1}{2}$ and $S = \frac{3}{2}$, respectively, and P and P^* are the heavy mesons with $S = 0$ and $S = 1$, respectively. A discussion of the derivation of Eq. (4.1) is given in Appendix C.1. From the perspective of HQET, this relationship should hold to $O(\Lambda_H^2/m_Q)$ where Λ_H is a typical hadronic energy and is proportional to, but not necessarily identical to $\Lambda_{\rm QCD}$. At the time of the Savage and Wise paper, this relationship was a prediction of the theory: doubly heavy baryons had not been discovered. The SELEX data allows one to explore this relation with–even if dubious–real world data.

Before proceeding further, one should note that this analysis is based on the assumption that a spatially small and tightly bound diquark configuration exists and remains unexcited in the dynamics. The key question to address is the extent

[1]Equation (4.1) is different from that in Refs. [139] by a factor of $\frac{1}{2}$. This error was observed and corrected by Ref. [146] and [149].

to which this assumption is true.

To examine the issue of diquark excitations, a systematic treatment for the dynamics of two heavy quarks is needed. At a formal level the non-relativistic expansion of the heavy quark degrees of freedom with QCD (NRQCD) is the natural language to explore this issue. NRQCD was first developed by Bodwin, Braaten, and Lepage [150], where it was modeled after a similar treatment in the context of QED [151]. As discussed in Sect. 1.2, HQET describes the dynamics of a single heavy quark. It has two energy scales, m_Q and Λ_H, and creates an expansion in Λ_H/m_Q. On the other hand, NRQCD attempts to describe multi-heavy quark systems. This added dynamics requires the introduction of two new scales: the characteristic momentum, mv, and energy scale, mv^2, where v is the characteristic velocity of the two heavy quarks relative to each other. For relevant systems, this velocity is typically related to the strong coupling constant as $v \sim \alpha_s(mv)$. NRQCD relies on the hierarchy, $m \gg mv \gg mv^2$. This creates four characteristic regimes of (energy, momentum) transfer; namely (m, m), (mv, mv), (mv^2, mv), and (mv^2, mv^2) which are conventionally referred to as hard, soft, potential, and ultrasoft, respectively. Traditional NRQCD has been further simplified into two different effective theories, pNRQCD and vNRQCD. The pNRQCD approach to diquarks integrates out the soft momentum gluons to form heavy diquarks states with definite color, and uses these diquark states as the degrees of freedom [152, 153, 154]. On the other hand, the vNRQCD approach keeps the heavy quarks as explicit degrees of freedom while matching the effective theory at the hard scale [155]. In all forms of NRQCD, the separation of scales creates an expansion of powers of v.

On physical grounds, one expects that NRQCD at leading order for systems with two heavy quarks (or anti-quarks) ought to reduce to the HQET description of the dual problem—*i.e.*, the problem related by the DHDA symmetry. Recently, Ref. [146] derived the presence of DHDA symmetry in the context of pNRQCD while Ref. [147] confirmed this for vNRQCD by showing the equivalence between vNRQCD and pNRQCD. It should be noted that this derivation represents a qualitatively new domain for NRQCD. Traditionally, NRQCD is applied to systems with one heavy quark and one heavy anti-quark with no valance light quark degrees of freedom. The fact that the technique may be extended to problems with two heavy quarks plus additional light quark degrees of freedom is non-trivial. One central point, that should be stressed, is that the derivation is quite general and applies equally well to the problem of heavy tetraquarks as well as doubly heavy baryons. The key advantage to the NRQCD formalism is that corrections due to dynamical heavy quarks can be systematically incorporated by working at higher order.

While it is known that the DHDA symmetry must emerge in the heavy quark limit, it is not immediately clear how large the corrections to the symmetry results should be for the realistic case in which heavy quarks have large but finite mass. Clearly the fundamental issue is the interplay between the binding of two quarks into an approximately point-like object and the extent to which the diquark is point-like from the perspective of the light quarks and glue; thus both the details of the physics of the interactions between the two heavy quarks as well as between the heavy and light quarks are essential. Previous works in this area [146, 147] have concentrated their efforts on perturbative expansions of the interactions between the two heavy

quarks in the framework of NRQCD and have not dealt with heavy/light interactions. Since the interactions between the heavy and light quarks are intrinsically non-perturbative, it cannot be estimated directly via the techniques of NRQCD. The full expansion should be a combination of HQET and NRQCD which incorporates the mixing of perturbative and non-perturbative scales. The issue of how to attack the question of the scale of these corrections for charmed or bottom quarks is the motivation for this chapter. This is done in the context of the SELEX data with tools motivated by NRQCD. Even though the new combined expansion is not fully formulated in this chapter, strong arguments suggesting the need for such a theory when dealing with doubly heavy mesons are provided. This chapter explores this issue both in terms of systematic treatment of the problem based on power counting in effective field theories and in terms of more heuristic phenomenological reasoning.

This chapter is divided into two major sections. In the first, the consequences for the spectrum in the large quark mass limit are developed. In the second section, a finite quark mass is considered. This section will argue that the SELEX data are not consistent with the large mass limit; there is a need for a new expansion to describe this system; and an apparent DHDA symmetry beyond that which is justified by NRQCD can be seen by the SELEX data.

4.2 Consequences of DHDA symmetry in the large mass limit

Before addressing the key question of whether the charm quarks are too light for the DHDA symmetry to be manifest, it is useful to consider just what implica-

tions the DHDA symmetry have on the spectrum when the symmetry is manifest—namely, when the quarks are sufficiently heavy. The extreme heavy quark limit, where all relevant scales cleanly separate, is considered. It is unlikely that this extreme limit can be anything but a gross caricature of the physical world. Nevertheless, an understanding of the physics in this extreme regime is useful in understanding the applicable expansions. There has been extensive work using a variety of models in detailing the hadronic spectrum including Refs. [156] and [157] among others. The focus here will be considering the spectrum in the context of a possible DHDA symmetry. A regime with more modest masses intended to describe the physical world will be considered in the next section.

The first consequence to consider is qualitative—namely, the existence of exotic states. The DHDA symmetry in HQET was first used to relate doubly heavy baryons to heavy mesons [139]. However, the symmetry is independent of the light quarks in the problem. Formally, in NRQCD, the light quarks are governed by non-perturbative dynamics, and are thereby considered irrelevant when focusing on the heavy quarks in the large mass limit. As the DHDA symmetry applies in the heavy quark limit independent of the number and state of spectator light quarks, it is sufficient to consider an ordinary heavy baryon, Qqq. From DHDA symmetry, this state is directly related to a doubly heavy tetraquark state, $\bar{Q}\bar{Q}qq$. Thus in the heavy quark limit, when the DHDA symmetry is exact, the existence of heavy baryons implies the existence of doubly heavy tetraquarks.

The fact that doubly heavy tetraquarks must exist in the heavy quark limit has been shown previously. This was done both based on the simple argument discussed

here and in the context of an illustrative model based on pion exchange [112, 148]. It should be noted that while being in the regime of validity of DHDA requires the existence of doubly heavy tetraquarks, the converse is not true: doubly heavy tetraquarks could be formed via other mechanisms. Nevertheless, the general result is significant in that the tetraquark has manifestly exotic quantum numbers in the sense that it cannot be made in a simple quark model from a quark–anti-quark pair. As discussed in Chapt. 1, the observation of exotic hadrons has been a longstanding goal of hadronic physics. The prediction of the existence of an exotic particle directly from QCD–albeit in a peculiar limit of the theory–is of theoretical importance in that it demonstrates by direct construction that QCD can be compatible with exotics. As shown in Chapt. 2 other exotic particles, *viz.* heavy pentaquark, have already been shown to exist in the heavy quark limit combined with the large N_c limit.

Now the focus will be on more quantitative issues associated with the excitation spectrum. As noted in the introduction, the formal treatment of this problem incorporates NRQCD (for the interactions between the heavy quarks) and HQET (for the interactions of a single heavy quark). The DHDA symmetry requires each of these effective theories to be in its domain of validity. In the heavy quark limit where both expansions will work, one has

$$m_Q \gg m_Q v \gg m_Q v^2 \gg \Lambda_H \gg \frac{\Lambda_H^2}{m_Q} \tag{4.2}$$

where Λ_H is a typical hadronic scale proportional to $\Lambda_{\rm QCD}$ and v, the relative velocity of the heavy quark, is typically of order α_s and hence depends logarithmically on the quark mass. It should be noted that the NRQCD formalism is still valid for

$m_Q v^2 \sim \Lambda_H$ as indicated by Ref. [146]. However, none of the analysis in this work depends on $m_Q v^2$ being larger than Λ_H, and hence is consistent with the domain of validity on NRQCD. The formalism of NRQCD and its associated power counting rules remains valid for two heavy quarks in the color $\bar{\mathbf{3}}$ in the presence of additional light quark degrees of freedom and not just for heavy quark–anti-quark systems in the color singlet in heavy mass limit. This was shown in Ref. [146] and verified in Ref. [147].

It is important to note that these effective theories have different types of excitations with qualitatively different scales. Doubly heavy hadrons (in the formal limit of very large quark mass) have three characteristic types of excitation:

a. Excitations of order Λ_H^2/m_Q which correspond to the interaction of the spin of the diquark with the remaining degrees of freedom in the problem.
b. Excitations of order Λ_H which correspond to the excitations of the light degrees of freedom.
c. Excitations of order $m_Q v^2$ which correspond to the internal excitation of the diquark.

The first two types of excitations can be understood in terms of HQET while the third requires NRQCD. (Non-perturbative physics also strongly influences the second type of excitation.) The essential point is that as $m_Q \to \infty$ these three scales separate cleanly. Since these excitations all occur at disparate scales, they do not influence each other.

DHDA symmetry imposes many relations on the various types of excitations of various doubly heavy hadrons and their associated singly heavy ones. To enumerate these, it is useful to have a naming convention for the various doubly heavy

hadrons. The ground state of a doubly heavy baryon with two Q quarks will be generically called Ξ_{QQ} while the ground state of the tetraquark are named T_{QQ}. Through the DHDA symmetry, these states are analogous to heavy (anti-) mesons (*i.e.* the $\bar{D}$ and $\bar{B}$ mesons) and heavy baryons (*i.e.* Λ and Σ), respectively. The following convention will be used to indicate various types of hadron excitations:

* indicates an excitation of type (a);

$'$ indicates an excitation of type (b);

$^\sharp$ indicates an excitation of type (c).

In addition, the DHDA equivalence between associating baryons and mesons will be indicated.

Let us consider the phenomenological consequences of these types of excitations. In HQET, the $SU(2)$ heavy spin symmetry causes states which are only different by a spin flip to have the same mass. Excitations of type (a) are the type which will break this symmetry creating a mass difference between these states. As this is the leading term to create the mass splitting, HQET dictates that this splitting is $O(\Lambda_H^2/M_Q)$ with corrections of $O(\Lambda_H^3/M_Q^2)$. Additionally, there are corrections to this hyperfine splitting due to pNRQCD. These corrections are related to the soft gluons that have been integrated out to construct the diquark potential. The leading corrections contribute at two loops, as shown in Ref. [146], and are thus relative $O(\alpha_s^2)$. This implies a correction to the mass splitting of $O(\Lambda_H^2\alpha_s^2/M_Q)$, which is formally larger than the $O(\Lambda^3/M_Q^2)$ corrections of HQET in the infinite mass limit. Because $\frac{\Lambda_H}{M_Q}$ is the smallest scale, these excitations should be the lowest

excitations above the ground state.

Excitations of type (b) are the other excitations associated with the light degrees of freedom. These include orbital excitations between heavy and light components, as well as excitations within the light quark degrees of freedom. Due to the light quark mass, these excitations are in the non-perturbative regime of QCD, and can only be characterized by some general hadronic scale, Λ_H. Perturbative corrections to this are, in turn, meaningless. Traditional NRQCD has not been applied to systems with valance light quark degrees of freedom, and thus to date has ignored these excitations. Some form of light quark excitations may be able to be incorporated into NRQCD, but since they occur at a scale of Λ_H, they would be highly suppressed. HQET, on the other hand, combines these into the definitions of heavy fields from the outset, and thereby neglects them for the rest of the problem. These excitations should be qualitatively the second smallest scale.

Excitations of type (c) are internal diquark excitations. These excitations correspond to the excited levels of the color Coulombic potential that binds the diquark. In the extreme heavy quark limit, the binding potential is $V(r) = -\frac{2}{3}\frac{\alpha_s}{r}$, where the factor of $\frac{2}{3}$ comes from color considerations. This leads to energy levels and energy differences of:

$$E_n = -\frac{1}{9}\frac{\alpha_s^2 M_Q}{n^2}; \quad \Delta E = \frac{1}{12} M_Q \alpha_s^2 = \frac{1}{12} M_Q v^2. \tag{4.3}$$

The last step is justified since at the heavy quark scale, $\alpha_s(M_Q v) \sim v$. This verifies that type (c) excitations are $O(M_Q v^2)$. This type of excitation should be present in both the doubly heavy baryon and tetraquark sectors as the light quark interactions

are suppressed since they are $O(\Lambda_H)$. The corrections to these relations can be found by considering the corrections to the color Coulombic potential. In the context of NRQCD, it has been shown by Ref. [158] that these corrections are $O(M_Q v^4)$ at the heavy quark scale. This leads to mass relations such as:

$$m_{\Xi_{cc}^\sharp} - m_{\Xi_{cc}} = m_{T_{cc}^{\Lambda\sharp}} - m_{T_{cc}^\Lambda} = m_{T_{cc}^\sharp} - m_{T_{cc}} = \frac{1}{12} M_Q v^2 + O(M_Q v^4). \tag{4.4}$$

Since diquark excitations are $O(M_Q v^2)$, these are the largest excitations discussed here.

In addition to these excitations, DHDA symmetry will relate heavy mesons ($\bar{Q}q$ states) to doubly heavy baryons (QQq states) and relate heavy baryons (Qqq states) to doubly heavy tetraquarks ($\bar{Q}\bar{Q}qq$ states) which otherwise have the same quantum numbers. Therefore the following relations can be made:

$$\begin{aligned} D &\Leftrightarrow \Xi_{cc}; \\ D^* &\Leftrightarrow \Xi_{cc}^*; \\ \Lambda &\Leftrightarrow T_{cc}^\Lambda; \\ \Sigma, \Sigma^* &\Leftrightarrow T_{cc}, T_{cc}^*, T_{cc}^{**} \end{aligned} \tag{4.5}$$

where D and D^* are standard spin-0 and spin-1 D-mesons; Ξ_{cc} and Ξ_{cc}^* are spin-$\frac{1}{2}$ and spin-$\frac{3}{2}$ doubly heavy baryons; Λ is isospin-0 spin-$\frac{1}{2}$ heavy baryon; Σ and Σ^* are isospin-1 spin-$\frac{1}{2}$ and spin-$\frac{3}{2}$ heavy baryons; T_{cc}^Λ is an isospin-0 spin-0 doubly heavy tetraquark; T_{cc}, T_{cc}^*, T_{cc}^{**} are isospin-1 spin-0, spin-1, and spin-2 doubly heavy tetraquarks.

The DHDA symmetry can then be used to relate the mass splittings [139]. Equation (4.1) identifies the corrections to the mass splitting, but not to the DHDA

symmetry itself. DHDA symmetry relies on the interactions between the heavy diquark and the light quark(s). These types of interactions, which are intrinsically non-perturbative, are not well understood in either NRQCD or HQET, as argued above. Therefore, to understand the corrections to the symmetry, a new power counting scheme that combines the scales of NRQCD and HQET and is consistent with the other scales in the problem is necessary to account for these interactions systematically. At this time, such a fully systematic expansion has not been formulated. Yet one can attempt to get a reasonable estimation of the corrections by considering the effects of the diquark structure compared with a point-like diquark on the DHDA symmetry. This consideration is exactly the form factor of the diquark relative to the scale of the light quark wave function. The form factor can be calculated by taking the Fourier transform of the square of the diquark wave function. In the limit of infinite heavy quarks, the diquark is in a Coulombic wave function so the calculation is straightforward. Assuming that the momentum transferred is $O(\Lambda_H)$, the form factor can be expanded to give the leading correction to DHDA symmetry as follows:

$$F(q) \propto \frac{1}{(1+\frac{a_0^2}{4}q^2)^2} \sim 1 - \frac{1}{2}a_0^2 q^2 \sim 1 - \frac{1}{2}\frac{\Lambda_H^2}{M_Q^2(\frac{2}{3}\alpha_s)^2}, \tag{4.6}$$

where a_0 is the corresponding "Bohr radius" of the Coulombic bound state of the diquark. Thus the corrections due to DHDA are $O(\Lambda_H^2/(M_Q^2\alpha_s^2))$. However, these corrections are formally smaller than the type (a) mass splitting correction of $O(\alpha_s^2)$. Equation (4.1) can be translated into the previous notation, and extend the relations

to include the tetraquark splittings to have:

$$\begin{aligned} m_{\Xi_{cc}^*} - m_{\Xi_{cc}} &= \frac{3}{4}(m_{D^*} - m_D) + O(\Lambda_H^2 \alpha_s^2 / M_Q) \\ m_{T_{cc}^{**}} - m_{T_{cc}^*} &= \frac{2}{3}(m_{\Sigma_c^*} - m_{\Sigma_c}) + O(\Lambda_H^2 \alpha_s^2 / M_Q) \\ m_{T_{cc}^*} - m_{T_{cc}} &= \frac{1}{3}(m_{\Sigma_c^*} - m_{\Sigma_c}) + O(\Lambda_H^2 \alpha_s^2 / M_Q) \\ m_{T_{cc}} - m_{T_{cc}^\Lambda} &= (m_{\Sigma_c} - m_{\Lambda_c}) + O(\Lambda_H^2 \alpha_s^2 / M_Q). \end{aligned} \tag{4.7}$$

A detail derivation of these relations can be found in Appendix C.2.

To summarize, the doubly heavy baryons and tetraquarks will have three types of excitations which are distinct in the heavy quark limit. From these the hadronic spectrum for these particles can be constructed based upon these excitations and their relative size to one another. Additionally, these spectra are related to the hadronic spectra of heavy mesons and heavy baryons via the DHDA symmetry. These spectra are presented in Figs. 4.2 and 4.3.

4.3 DHDA symmetry and the physical world

The previous section concentrated on the limit of arbitrarily large quark mass to determine what one might expect from the structure of the spectrum if the symmetry were fully justified. The usefulness of DHDA symmetry has been demonstrated in relating the spectra of doubly heavy baryons to heavy mesons and doubly heavy tetraquarks to heavy baryons in this limit. One can try to use this tool to interpret the corresponding spectra with a finite massive heavy quark. As the heavy quark mass is decreased from infinity, one expects that the correction terms outlined above to increase until at a certain low enough quark mass they become as domi-

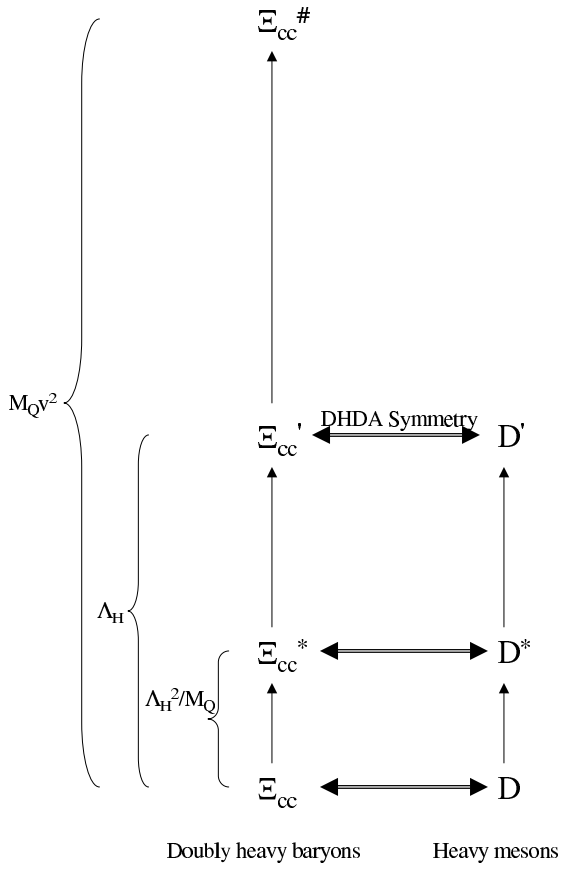

Figure 4.2: Hadronic spectrum for doubly heavy baryons related to heavy mesons.

nant as the leading order, resulting in a breakdown of the expansion. The claimed discovery of doubly charmed baryons by the SELEX collaboration provides the first experimental data to confront the heavy hadronic spectrum described above. An understanding of the SELEX data can provide an insight into whether DHDA symmetry persists in the real world.

A priori the SELEX data, along with real world parameters, might suggest one of three possible scenarios into the validity of DHDA symmetry for doubly charmed states. First, upon examining the data, one could find that the data support a claim that the charm mass is heavy enough to be considered near the ideal large mass limit discussed in the previous section. If this were the case, the spectrum can

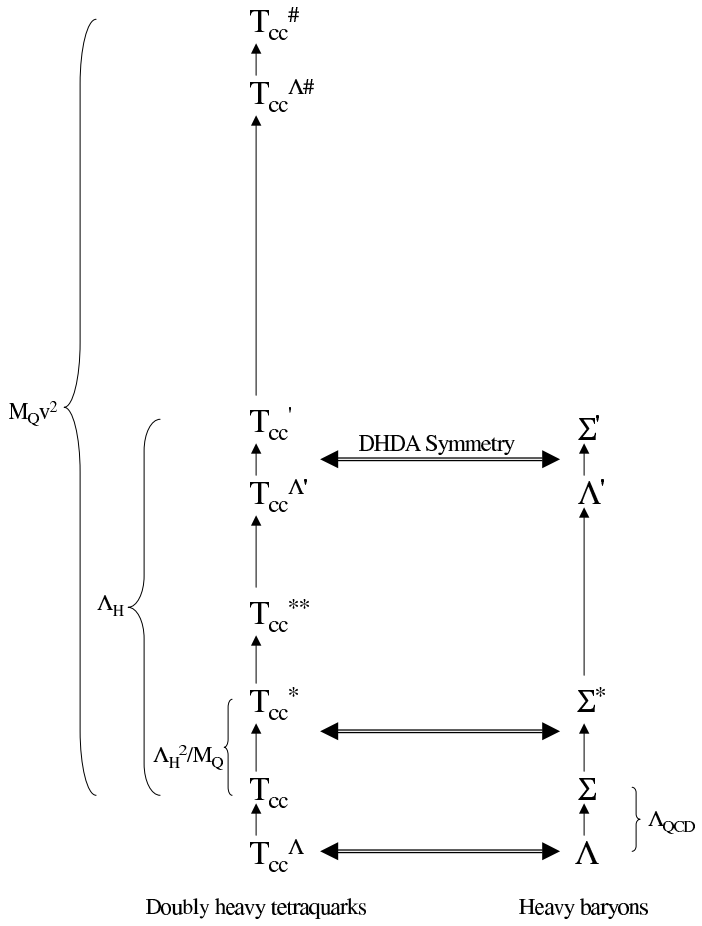

Figure 4.3: Hadronic spectrum for doubly heavy tetraquarks related to heavy baryons.

be easily interpreted in terms of an approximate DHDA symmetry. Secondly, the opposite could be true; namely that the SELEX data would be inconsistent with an approximate DHDA symmetry. This would indicate that the charm quark mass is simply too light for the symmetry to be manifest. The last possibility is perhaps the most intriguing: that data could suggest that charm quark mass is not heavy enough for the preceding argument to hold in full, but that data might still be consistent with some aspects of an approximate DHDA symmetry. This last option is not unreasonable as the DHDA symmetry relies on the heavy diquark to be viewed as point-like with respect to the light degrees of freedom. The infinite mass limit

ensures the validity of this assumption, but a small-sized diquark might be achieved even with a relatively modest heavy quark mass. For this possibility to be realized, dynamics beyond the simple Coulombic interaction must play a central role. To determine which of these possibilities is most consistent with the SELEX data, the size of each of the previously-mentioned excitations, as well as their corrections, will be examined and compared with experimentally determined parameters from the SELEX data.

Before doing this, one should note a general word of caution. The fact that the excited doubly charmed states were seen only via their weak decays presents a challenge to *any* simple interpretation of the data. The problem is that the electromagnetic lifetime of the excited states as estimated by any simple model should be short enough to wash out any detection of excited states via their weak decay [144]. Any simple interpretation of the SELEX results cannot simultaneously explain the type of excitation that is observed as well as the lack of an electromagnetic decay channel. Therefore the focus here will be placing limitations on the type of excitation.

The excited state seen by SELEX shown in Fig. 4.1 could be interpreted as either a type (a) spin excitation or a type (c) diquark excitation. Type (b) light quark excitations are ruled out as they occur on the scale of hadronic physics which is much larger than the reported excitation. Either interpretation, as will be discussed, explains aspects of the data, but neither provides a complete explanation.

4.3.1 Scenario I: Spin excitation

Consider the case where the excited states are type (a) spin excitations. From the discussion of the infinite mass case, one would expect that even for a finite quark mass, these excitations would be the lowest lying occurring at $O(\Lambda_H^2/M_Q)$. According to the SELEX data, the excitation energy is 78 MeV. With this identification, the DHDA mass splitting relations, Eqs. (4.1) and (4.7), are satisfied with only a 30% deficiency as has been pointed out elsewhere [146, 147]. This size of error is also consistent with the equations' corrections of $O(\Lambda_H^2\alpha_s^2/M_Q)$. This appears to correspond to a success of DHDA symmetry.

At this point, Refs. [146] and [147] have only verified that Eq. (4.1) is approximately satisfied. This could be satisfied because DHDA symmetry is the underlying phenomenon or because of a numerical accident. In order to determine between these two scenarios, one needs to consider the other aspects of the spectrum and DHDA symmetry. That is, are type (c) excitations larger than type (a) excitations as expected when a finite quark mass is considered, and is the spatial extent of the diquark small enough to consider it point-like?

The former condition will be tackled first. Assuming, first, that the system really is in the extreme heavy quark limit, the diquark excitation energy can be calculated from Eq. (4.3) using the color coloumbic potential. From Eq. (4.3), one can calculate the expected excitation energy of the diquark for a charm quark mass of 1.15 GeV and a velocity of .53. This gives an excitation energy of 26.9 MeV! This is clearly not larger than the assumed 78 MeV spin excitation. This is a sign that

the scale separation arising from the color Coulombic interactions, expected for an infinite quark mass, is not present for the charm quark.

Furthermore, the assumptions that lead to the DHDA symmetry need to be examined. The key issue in determining whether DHDA symmetry could hold is the size of the diquark with regards to the light valance quark(s). This can be formally addressed by looking at the size of the diquark to determine if it is nearly point-like. The size of the diquark can be characterized by the RMS radius of the state. Again, assuming the extreme heavy quark limit, the RMS radius can be calculated from the Coulombic wave function; this yields a size of the ground state diquark to be 1.64 fm. Clearly this is not point-like on the scale of hadronic physics. The large size of the ground state of the diquark also indicates that the excited state would be even larger. This invalidates the previous diquark excitation energy calculation, while emphasizing the absurdity of assuming that the diquark is bound deeply by the color Coulombic interaction. Moreover, this further indicates that the diquark must be under the influence of interactions in addition to the color Coulombic potential. However, perhaps for the DHDA symmetry, the actual physical size of the diquark is not what is important but rather if the light quarks observe it as approximately point-like on hadronic scales. This distinction can be seen by examining the form factor corrections that were considered in the previous section. To expect the DHDA symmetry, these form factor corrections would need to be small compared with 1. For the values for the charm quark, the correction can be calculated from Eq. (4.6) to be $3.02\frac{\Lambda_H^2}{\mathrm{GeV}^2}$, which for a typical hadronic scale of $\Lambda_H \sim 1$ GeV is not much smaller than 1 for momenta of typical hadronic scales. (For smaller values of Λ_H

this relation becomes borderline, at best.) Thus both indicators show that the real world charm quark is not heavy enough to justify the point-like nature of the doubly heavy diquark which is necessary for the DHDA symmetry.

It should be noted that the bottom quark has a mass large enough to begin to approach the regime where the heavy mass limit scaling could hold. The type (c) excitation is 32.8 MeV, with the type (a) excitation being 34.3 MeV calculated from the B-meson mass splitting. Additionally, the characteristic size is 0.79 fm, and the correction to the DHDA symmetry is $.69\frac{\Lambda_H^2}{\mathrm{GeV}^2}$. All of these numbers show that for the bottom quark the scale hierarchy is as expected and corrections could be relatively small, even if the scale separation is not complete. However, presently doubly bottom baryons have not been observed experimentally.

It has been shown that a naive approach to DHDA symmetry results in the conclusion that the charm quark is by no means heavy enough to believe that this symmetry is manifest in the real world–at least if it is to arise due to color Coulombic interactions. In other words, the relatively small charm quark mass causes the corrections to the heavy massive limit to become large enough to question the expansion for the excited states. However, this does not completely rule out the possibility that DHDA could hold approximately and that these excitations are of type (a). The color Coulombic interactions are not the only interactions the charm quarks could experience as part of a diquark or a doubly heavy baryon. Since the charm quarks are not heavy enough to fall into the color Coulombic region, it is reasonable to surmise that these other non-perturbative interactions could conspire in such a manner that would facilitate an approximate DHDA symmetry. However, these ad-

ditional non-perturbative interactions are not systematically included in NRQCD. Therefore, in order to describe this system, a new expansion that combines the perturbative and non-perturbative scales of NRQCD and HQET in a systematic manner is needed. At present, such an expansion has not yet been formulated. Nevertheless, by examining the properties of the interactions needed to maintain DHDA symmetry, a general picture of the new theory could be made.

Before proceeding with a discussion of the conditions that DHDA symmetry imposes on additional non-perturbative interactions, an additional comment on the color Coulombic potential is needed. First, when working in the large mass limit, the regime of $m_Q v^2 \gg \Lambda_H$ was implied. However, with a finite massive quark this condition could be weakened to include $m_Q v^2 \sim \Lambda_H$. Under this condition, the type (b) and type (c) excitations may mix since they are at the same energy scale. Nevertheless, the key issue here is whether type (a) and type (c) excitations separate. The possible inclusion of type (b) excitations with type (c) does not effect whether they are separated from type (a), and hence do not effect the results discussed here. Secondly, the color Coulombic potential is only the leading-order term in NRQCD; sub-leading terms might need to be included when a finite massive quark is considered. However, since a need for a new expansion which includes the mixture of perturbative and non-perturbative effects has been seen, it is not clear whether the sub-leading terms suggested by NRQCD are the only sub-leading terms in the combined expansion. In both of these cases though, additional interactions beyond the simple color Coulombic potential are included. It is not impossible that these, just like the ones hypothetically postulated above, could conspire so that the

DHDA symmetry would be manifest in an approximate manner in the real world. Again, a description of the conditions to obtain an approximate DHDA symmetry will provide insight into these additional interactions whether they are NRQCD based or well beyond the scope of NRQCD and HQET.

There are two key places where the analysis based on the color Coulombic potential fails to give rise to the DHDA symmetry with real world parameters. The assessment of these failures will provide conditions on the additional interactions to re-establish DHDA symmetry. The first is the characteristic size of the diquark. It has already been shown that for the Coulombic potential, the size of the diquark is large enough not to be considered even remotely point-like from the point of view of hadronic dynamics. Secondly, the hierarchy of scales used to derive the result breaks down badly. Additional dynamics beyond the color Coulombic potential would need to create a diquark with a size much smaller than the characteristic hadronic size and to re-establish the spin excitations as the lowest-lying excitations as one originally assumed.

An examination of the restrictions placed on the characteristic size of the diquark reveals the following. The characteristic size of the diquark, which will be denoted as L, must be smaller than the size in a Coulombic potential, denoted as L_c, and it must be small enough to allow the DHDA corrections to be small. The correction term of Eq. (4.6) can be rewritten in terms of this characteristic size as $\frac{1}{6}L^2\Lambda_H^2$. Thus for the correction to be small, $L \ll \sqrt{6}/\Lambda_H \equiv L_{DHDA}$. L_c must be larger than L_{DHDA} since L_c already violates DHDA symmetry and thus cannot be smaller than L_{DHDA}. Therefore, in order for the diquark to be considered nearly

point-like, both

$$L \ll L_c \quad \text{and} \quad L \ll L_{DHDA} \tag{4.8}$$

must be simultaneously satisfied. In order to ensure this, in terms of size, L_{DHDA} could be much smaller than L_c, or L_{DHDA} could be of comparable size to L_c. Consider the former possibility. $L_{DHDA} \ll L_c$ is equivalent to $\frac{\sqrt{6}}{\Lambda_H} \ll \frac{3}{2m_Q\alpha_s}$. This implies that $m_Q\alpha_s \ll .6\Lambda_H$. This relationship is never satisfied since $\alpha_s \sim 1/\ln(m_Q)$ and $m_Q \gg \Lambda_H$. Thus for DHDA symmetry to occur the latter condition must hold. It gives: $L_{DHDA} \sim L_c$ implying $m_Q\alpha_s \sim .6\Lambda_H$. As α_s at the charmed quark mass scale *is* around .6, this relation can only be satisfied if $m_Q \sim \Lambda_H$. It should be noted however, that an interaction providing a characteristic size of the diquark which is consistent with Eq. (4.8) is possible. For the purposes of the discussion here, one needed to show that at least one kinematic region was possible, and the region where $m_Q \sim \Lambda_H$ satisfies these conditions even though it should not be unique.

A couple of comments should be made about this condition. The first is that it naively appears not to occur even for the charm quark case. If one takes Λ_H to be of the scale of Λ_{QCD} it seems to be much smaller than m_c. However, one should note that the $\sim$ indicates "of the same scale as" under the assumption that the coefficients which arise in the expansion are "natural," *i.e.*, of order unity. If the dynamics are such that some of the coefficients multiplying Λ_H are anomalously large, the condition $m_Q \sim \Lambda_H$ could hold effectively. The second key point is simply that if this does occur the system is clearly beyond the perturbative regime. It should also be noted that this should *not* be seen as a generic condition invalidating NRQCD.

Rather, it implies the expansion has broken down *for this particular system.* There is non-trivial evidence that this is in fact the case; namely if one assumes the expansion is working, one gets inconsistent results as already seen here. The central question addressed here is not whether the expansion has broken down, but rather whether one can still have a small diquark even if the expansion has broken down. If it indeed is the case that the condition $m_Q \sim \Lambda_H$ is effectively met, then there is a possible characteristic size of the charmed diquark for which DHDA symmetry could be valid. This region is simply a size that is much smaller than the length associated with the Coulombic potential and smaller than the typical hadronic size.

Thus far a possible kinematic region for which approximate DHDA symmetry may be possible has been identified. However, to test whether this can occur in practice, one needs to see whether plausible dynamics can drive the system into such a regime. To this end, a "reasonable" dynamical model for the interaction between the heavy quarks is considered. This model is not intended to be an accurate description of hadronic physics. The goal is simply to see whether a simple model with natural scales can put the system in the regime where DHDA symmetry emerges at least approximately. The existence of a model which does this shows that an approximate DHDA symmetry could be present in charm physics despite the fact that the charm quark mass is not heavy enough to be considered in the extreme limit.

To illustrate the kind of model which brings us into this regime, a linear confining potential with a string tension of $1\frac{\text{GeV}}{\text{fm}}$ is considered. The value of the string tension is not experimentally determined, but here it is chosen to achieve

the desired results of a small diquark size with large diquark excitation. Such a potential with the same string tension can be used to get a reasonable description of the J/Ψ [159]. One might not believe that such a model is applicable at all distances to which it will be attempted to be applied. Indeed, one may reasonably question whether any two-body potential description is sensible. Nevertheless the scales of the model are at least instructive. Any confining potential that can be introduced will cause the characteristic size of the diquark to be reduced; thus the conditions on the diquark size may be satisfied. Specifically, the characteristic length is 0.5 fm when the linear confining potential above is used to bind charmed quarks. This is substantially smaller than the Coulombic wave function and might be small enough so that approximate DHDA might emerge. Moreover, the small size of the bound state helps to justify the two-body potential description *a posteriori*; the effects of the light quark between the heavy ones should be suppressed due to the small size. Unfortunately, this calculation is not part of a systematic calculation, and it is not immediately clear how to reliably estimate the size of the correction to the leading-order DHDA estimate for the splitting.

Calculations of the energy spectrum of Coulombic plus linear confining potentials in this channel reveals that the radial excitation energy is 630 MeV–far above the 100 MeV energy associated with expected spin excitations. Thus this linear confining potential satisfies both of the conditions needed to believe that an approximate DHDA symmetry could be realized for charmed quarks.

A region has therefore been found where an approximate DHDA symmetry could be realized approximately and the lowest-lying excitations are type (a) spin

excitations. The color Coulombic interactions cannot be the only relevant interactions the heavy quarks experience (as is assumed in the heavy quark mass limit). Of course the question of whether the dynamics as such is realized in nature remains an open question. It would be very fortuitous if this model of non-peturbative interactions mimics the actual non-peturbative dynamics.

Even though a consistent argument for the observed excited states to be spin excitation has been presented, there remains a phenomenological issue with the parity of the excited state. Type (a) excitations do not change the parity of the excited state relative to the ground state. Ground state baryons have positive parity, thus the spin excited state should also have positive parity. Experimentally, the parity of the excited states has not been determined. The SELEX collaboration have argued that the orbital angular momentum of the ground state is consistent with $L = 0$ (positive parity), while the excited state is consistent with $L > 0$ (either positive or negative parity). Furthermore, SELEX observed an orbital excited state $\Xi_{cc}(3780)$ which has negative parity and decays via pion emission to $\Xi_{cc}(3520)$ suggesting that this state could have negative parity. If this parity assignment holds, the interpretation that the excited states were spin excitations made here and in Refs. [146, 147], would be ruled out.

4.3.2 Scenario II: Diquark Excitation

Now let us consider the case where the excitation is interpreted as a type (c) diquark excitation. Type (c) excitations could result in a parity flip from the

ground state. This would resolve the parity problem found with the spin excitation interpretation. As will be discussed below, if this scenario is correct one is almost certainly outside the regime of validity of DHDA as well as outside the regime of validity of NRQCD. Moreover, it is likely to be very difficult to make such a scenario work phenomenologically.

In order for diquark excitations to be smaller than the spin excitations, there must be a breakdown of the heavy quark mass limit; the system must reside in a non-perturbative regime. Thus if the DHDA symmetry is present, it is not due to NRQCD, HQET, or the heavy quark limit. Therefore, as with the previous case, the diquark can be under the influence of non-perturbative interactions beyond the color Coulombic interactions. It was shown that if these additional confining interactions maintained an approximate DHDA symmetry, the diquark excitations were much larger than the observed 78 MeV excitation. Again one can illustrate this with a linearly rising potential between the heavy quarks. In order for the diquark excitations to be comparable to the observed splitting, the linear confining interactions must have a string constant of $\sim 50\frac{\mathrm{MeV}}{\mathrm{fm}}$, which is very small compared to the natural scales in the problem. The small size of the linear confining interactions results in the diquark having a larger size, and makes the assumptions that it is point-like even less believable. For the string constant of 50 $\frac{\mathrm{MeV}}{\mathrm{fm}}$ considered here, the ground state of the diquark has an RMS radius of 1.2 fm, and the first excited state has an RMS radius of 5.8 fm. These numbers are extremely large compared to typical hadronic sizes.

The preceding model calculation suggests that if the excitation were the ex-

citation of the diquark, the DHDA symmetry cannot be valid even approximately. It also raises a fundamental issue of self-consistency. A large spatially extended diquark allows the light quark to come between the two heavy quarks allowing for three-body interactions to play a significant dynamical role. To the extent that this occurs, it is meaningless as a phenomenological matter to separate the diquark excitation from excitations of the entire system. Thus, excitations of type (b) and (c) would strongly mix and the entire structure of scale separation would break down.

It should be noted that this analysis was based on a very simple and not terribly plausible model. However, it does incorporate the natural scales of the problem and shows that the excited state wave functions are *much* too large to be taken seriously. It is also clear that it would be very hard to construct any potential model which restricts the diquark size to be much less than a fermi while having an excitation energy of 78 MeV. To illustrate this point, one can consider a harmonic confining potential instead of the linear potential. One would expect that this potential would confine the excited state and reduce its size more than the linear potential. Calculating the size of the diquark under these conditions for an excitation energy of 78 MeV results in a ground state RMS radius of 1.3 fm and an excited state RMS radius of 2.5 fm. Even though the diquark size is smaller, it is still very large in terms of hadronic physics. Furthermore, if one were able to drive the size of the excited state to a reasonable hadronic size, say, 1 fm, the ground state would be even smaller. Such a small ground state size is then consistent with spin excitations discussed previously. It therefore seems difficult for this scenario to be correct.

Together these two scenarios make it very difficult to understand the data in a simple way. If the parity of the states is correctly interpreted by SELEX, there does not appear to be any simple phenomenologically reasonable interaction yielding either small diquark excitations or DHDA symmetry. However, if one sets the parity designation aside, Scenario I (the assignment of type (a) spin excitations) seems to be the more plausible interpretation.

4.4 Conclusion

This chapter has explored the implications of the DHDA symmetry both in the extreme heavy quark limit as well as with physical quark masses. It has shown that the DHDA symmetry suggests that doubly heavy tetraquark states should be stable to strong decays in the heavy quark limit. Though there may be some inconsistencies associated with the SELEX experiment, the DHDA symmetry and the heavy quark limit were used in an attempt to explain the data. It was shown that it is unlikely the charm quark is heavy enough for one to expect to observe the DHDA symmetry because of the heavy quark limit. Models including non-perturbative physics were considered which could lead to an approximate DHDA symmetry away from the heavy quark limit. Therefore, the work in this chapter suggests that despite DHDA being first formulated using HQET, and then later verified to be derivable from NRQCD, a new systematic expansion–which may be a hybrid of HQET and NRQCD–is needed for a complete understanding of the applicability of DHDA symmetry to physical systems.

Chapter 5

The status of the conjectured viscosity/entropy density bound

5.1 Introduction

In the previous chapters, various systems of heavy quarks have been considered. This chapter will also prominently feature a system of heavy quarks. However, the outlook will be rather different. Here, heavy quarks will play a role in investigations of a fundamental question: are there intrinsic limits on viscosity and entropy density for all fluids? As will be seen here, a gas of mesons containing heavy quarks in a peculiar limit of QCD plays a key role in this analysis. This chapter, however, will discuss the broader question of whether a fundamental bound on the ratio of viscosity to entropy density, η/s, exists.

Kovtun, Son, and Starinets (KSS) have proposed a conjecture that there is a universal bound for the ratio of shear viscosity, η, to entropy density, s, [160]:

$$\frac{\eta}{s} \geq \frac{\hbar}{k_B}\frac{1}{4\pi}, \tag{5.1}$$

where $\hbar$ and k_B are Plank's constant and Boltzmann's constant, respectively. (For the remainder of this chapter units with $\hbar = 1$ and $k_B = 1$ will be used.) KSS found that Eq. (5.1) is saturated by certain strongly coupled field theories which have a super-gravity dual [160], and conjectured that η/s has a universal lower limit. Physically interesting and accessible fluids, such as water, liquid nitrogen,

and helium-4 satisfy the bound [161]. The bound appears to be well justified for the class of field theories originally considered by KSS [160], but it is not obvious from first principles that it should apply more universally (hence its status as a conjecture).

The original form of the KSS conjecture states that the bound should be universal and apply to *all* fluids, including non-relativistic fluids [160]. However, a non-relativistic system can be constructed which can violate the bound via the Gibbs mixing entropy associated with the system's many species [162]. To avoid the many species problem, KSS has subsequently suggested two other domains of validity for their bound. They stipulate that either the bound is valid for "all systems which can be obtained from a sensible relativistic quantum field theory by turning on temperatures and chemical potentials" [163] or for a "single component nonrelativistic gas of particles with either spin zero or spin 1/2" [161]. It is in the context of the former where a gas of heavy mesons plays a critical role.

If the bound could be shown to be correct in any of its proposed forms, or indeed in some readily specifiable alternative form, it would represent a truly major advance in our understanding of quantum many-body physics. Indeed, even as a conjecture it has been invoked in discussing systems as diverse as ultra-cold gases of trapped atoms [164] and the quark-gluon plasma (QGP) [165, 166, 167, 168]. Since KSS first conjectured their bound, the ratio of shear viscosity to entropy density has been investigated in a variety of systems [164, 169, 170, 171, 172, 173, 174, 162, 175]. The smallest reported measurement of η/s has been associated with the QGP at RHIC [165, 166, 167, 168]. (A more recent analysis of the data from RHIC may

actually be consistent with a violation of the proposed bound [176].) Since the η/s bound may (or may not) have a rather extensive scope, it is important to understand in which types of systems one should expect the bound to hold.

At the beginning, it is useful to briefly review the argument of KSS that led to their proposed bound. The argument makes use of the AdS/CFT duality from string theory [177, 178, 179, 180]. It is argued that in higher dimensional gravity theories, black branes (higher-dimensional analogs of black holes) have finite temperature field theory duals (specifically, $\mathcal{N} = 4$ supersymmetric Yang-Mills theories at large N_c and infinite 't Hooft coupling $g^2 N_c$) that possess hydrodynamic properties such as viscosity. These hydrodynamic properties can be related to gravitational properties of the black branes, and the correspondence can be used to compute transport properties [160]. Using these methods the ratio η/s can be computed. A number of theories in this class have been studied in the large N_c limit at infinite 't Hooft coupling. All of them have saturated the inequality of Eq. (5.1) [160]. A general argument has been given that all theories in this class at large N_c and infinite 't Hooft coupling must saturate the bound [161]. Moreover, one generally expects that as one weakens the coupling of an interacting system, the viscosity should increase. One might, therefore, expect that as the 't Hooft coupling is decreased from infinity, the ratio η/s should increase. This has been seen in an explicit calculation for the first correction due to finite 't Hooft coupling for one particular theory [181]. Thus, it seems quite plausible that η/s is bounded as in Eq. (5.1), at least for those large N_c field theories which have super-gravity holographic duals.

However, the AdS/CFT correspondence is not directly relevant to any physical

systems. Hence it is rather a large leap to believe that the bound conjectured in this unphysical theory would apply beyond it. The interesting question therefore is whether the bound holds for some general class of theories beyond AdS/CFT, and if so for which class of theories. Note that apart from the field-theoretic calculations based on AdS/CFT, there is no reliable method to calculate η/s for *any* strongly coupled quantum fluid, yet it is this class of fluids for which one expects the smallest values of η/s. The optimistic view is that there could exist a very general property of some large class of quantum fluids; namely the η/s bound, which was unnoticed prior to the AdS/CFT calculations in large measure because there was no tractable way to compute the entropy and viscosity properties for strongly coupled theories. One way to probe whether there is a bound which applies to the class of theories that describe the real world is to ask whether there are any known fluids which violate the putative bound. In Ref. [161], KSS examined a number of real life fluids, including liquid helium, liquid nitrogen, and water, under a variety of conditions and found no examples where the bound was violated. Typically, the ratio η/s for these fluids was found to be orders of magnitude larger than the bound. This empirical data appears to be one of the strongest pieces of evidence for the existence of a bound.

If the bound is as universal and fundamental to physics as claimed, one would hope to be able to derive it using a more physically relevant theory, such as quantum mechanics. Though some have tried to use heuristic arguments based in quantum mechanics to justify the bound [161, 182], a rigorous proof from quantum mechanics has not been achieved. Moreover, it has been shown by Ref. [162] that it is possible to

construct a system in the context of quantum mechanics which actually violates the bound. A detailed description can be found in Appendix D. In this counterexample, the KSS bound is evaded by considering a non-relativistic gas of many species of particles. The many different species causes the entropy to increase because of the Gibbs mixing entropy, while keeping the viscosity unaffected. Therefore, for a sufficiently large number of species, the ratio η/s can be made sufficiently small to violate the KSS bound.

This particular non-relativistic gas can be considered as a counterexample to the general claim made by KSS. It seems that one cannot justify their bound from quantum mechanics alone. However, KSS has suggested two other key domains of validity for their bound. First, KSS claimed that one needed a "sensible," or UV complete, quantum field theory for the bound to be applicable [163]. This variation was an attempt to overcome the Gibbs mixing entropy problem. The manner in which sensible quantum field theories restrict the number of species is a subtle issue which is discussed in Appendix E. Additionally, KSS claimed that the bound should hold only for a "single component nonrelativistic gas of particles with either spin zero or spin 1/2" [161]. By restricting the number of allowable species, this variant of the conjecture clearly attempts to avoid the problem with the Gibbs mixing entropy that allowed the construction of the other counterexamples.

This chapter will address these two variants of the KSS conjecture by examining counterexamples to each of the claims. In Sect. 5.2, the need for a sensible quantum field theory will be investigated in the context of a peculiar heavy meson gas. It will be shown that despite the arguments of Appendix E, this system

can violate the bound because of the Gibbs mixing entropy associated with a large number of heavy meson species. Section 5.3 will then present a counterexample to the claim that the bound should hold for a single species fluid. Again the system considered is rather peculiar.

5.2 Heavy meson gas

This section will investigate a gas comprised of heavy mesons which was first considered by Ref. [162]. It will be shown that for a particular choice of parameters, the KSS bound on viscosity and entropy density can be violated. Since the constituents of the gas are mesons, this system would constitute a counterexample for the claim that the bound should hold for "sensible," or UV complete, quantum field theories.

Consider a gas comprised of heavy mesons. Each meson consists of a heavy quark and a light anti-quark. For the discussion that follows, it is sufficient to assume that the gas is comprised solely of pseudoscalar heavy mesons without the need to include the vector meson states; this assumption will be justified below. The heavy meson gas of interest is rather peculiar as it consists of many different species of heavy mesons. The many species can be produced by fixing the number of light quark flavors to some small value with one being adequate, and choosing a large number of heavy quark flavors, N_f. Furthermore, in a particular kinematic regime, *viz.* that of a dilute, low temperature gas, the viscosity of this fluid is calculable,

ala Maxwell [183] as

$$\eta = C\frac{\sqrt{mT}}{\sigma}, \tag{5.2}$$

where σ is the cross section, $\sqrt{mT}$ is the thermal momentum, and C is a proportionally constant of $O(1)$. In this regime, the entropy can be approximated by that of an ideal gas with a contribution from the Gibbs mixing entropy. The Gibbs mixing entropy is associated with the many species in the gas and is equal to $n\log(N_f)$ where n is the density of the gas; thus with a sufficiently large number of species, this will dominate the entropy of the gas. Combining these, the ratio η/s can be expressed as

$$\frac{\eta}{s} \sim \frac{\sqrt{mT}}{n\sigma \log N_f}. \tag{5.3}$$

To proceed, a parameterization for the quantities in Eq. (5.3) needs to be constructed. First, if one wishes to push the extent to which Eq. (5.1) is a lower bound for this fluid, a large number of species is desired. Since the Gibbs mixing entropy depends on the logarithm of the number of species, the number of species should grow exponentially, say as e^{ξ^4} where ξ is a scaling parameter, to have a meaningful contribution. However, if N_f becomes large, there is a chance that QCD will break down because it would no longer be asymptotically free. This problem can be overcome if N_c, the number of colors, increases at the same rate as N_f; hence $N_c \sim e^{\xi^4}$. Therefore this heavy meson gas becomes even more peculiar because it requires the large N_c limit.

Second, the scaling of the cross section is important. As mentioned in Sect. 1.3, the meson-meson interactions are suppressed in the large N_c limit, which would

suggest a small cross section. However, that discussion was relevant only for light mesons. The cross section is actually dependent on the quantity mV, the mass of the meson and the interparticle potential, not simply the potential. From the arguments of Sect. 1.3, the potential, V, still scales like $1/N_c$, but now the mass can be made large (since the gas is of heavy mesons) so that the cross section becomes independent of the parameter ξ.

Lastly, the kinematic regime of a dilute, low temperature gas which allows a calculable viscosity needs to be maintained. This is ensured as long as $n^{-\frac{1}{3}} \gg (mT)^{-\frac{1}{2}}$. This can be maintained by choosing n and $\sqrt{mT}$ to depend on ξ as $1/\xi^4$ and $1/\xi$, respectively. To summarize, the parameters of the heavy meson gas must depend on the parameter ξ as follows:

$$\begin{aligned} &N_c = e^{\xi^4} \quad N_f = e^{\xi^4} \quad m_h = m_{h0}\, e^{\xi^4} \quad m_l \sim m_{l0} \\ &\Lambda_{\mathrm{QCD}} = \Lambda_{\mathrm{QCD}_0} \qquad n = n_0 \xi^{-4} \qquad T = T_0 \frac{e^{-\xi^4}}{\xi^2}, \end{aligned} \tag{5.4}$$

where m_l is the light quark mass, and m_{h0}, m_{l0}, n_0, and T_0 are quantities which are independent of ξ. With these relations, the ratio η/s scales with ξ as $1/\xi$. Therefore with an arbitrarily large value of ξ, η/s can be made arbitrarily small.

It was assumed that the heavy meson gas is dominantly composed from spin-0 pesudoscalar mesons, as opposed to spin-1 vector mesons for an arbitrarily large ξ. Because of the scaling relations chosen in Eq. (5.4), the heavy meson gas is clearly in the heavy quark limit. In this limit, the pseudoscalar, H, and vector, H^*, heavy mesons are nearly degenerate. Therefore, one may naively expect both spin states to be present in the heavy meson gas. However, as has been discussed on several

occasions here, the two spin states have a typical mass splitting on the order of $\frac{\Lambda_{\rm QCD}^2}{m_h}$. From the parameter scaling relations in Eq. (5.4), it is not hard to see that this mass splitting scales like $\sim e^{-\xi^4}\Lambda_{\rm QCD}^2/m_{h0}$. One would expect a heavy meson gas to contain both the pseudoscalar and the vector form of the heavy mesons, with their populations determined by a Boltzmann distribution. Hence consider the ratio of the populations of the vector mesons to the pseudoscalar mesons. From the Boltzmann distribution, this ratio is given by

$$\frac{N_{\rm vec}}{N_{\rm pseudo}} \sim \frac{e^{-\beta M_{H*}}}{e^{-\beta M_H}} = e^{-\beta(M_{H*}-M_H)}, \tag{5.5}$$

where β is the inverse temperature. Using Eq. (5.4), one sees that

$$\frac{N_{\rm vec}}{N_{\rm pseudo}} \sim e^{-\xi^2 \frac{\Lambda_{\rm QCD}^2}{m_{h0}}}, \tag{5.6}$$

which for large values of ξ reduces this ratio to zero. Therefore, at large ξ the gas is predominantly composed of pseudoscalar heavy mesons, and one is well justified in neglecting the heavy vector mesons.

One final observation about the heavy meson gas. The heavy meson gas considered here is metastable. The details of which are not important, but it is sufficient to note that the heavy meson gas could decay either by clumping together into tetraquark, hexaquark, or larger states or by rearranging into a baryon of only heavy quarks and a light anti-baryon. It can be shown that this decay occurs over long time scales with large ξ. Thus this peculiar heavy meson gas is metastable. Therefore, the counterexample is only for metastable fluids. Hence, for the KSS conjecture to be valid, it may only apply to *stable* UV complete theories.

5.3 Single species gas

KSS postulated that perhaps their universal bound on viscosity and entropy density should only be applicable to fluids comprised of a single species. This is an obvious attempt to elude the counterexamples which use many species and the Gibbs mixing entropy to evade the KSS bound. However, as will be shown here, a single species system can be constructed which can violate the bound. The system is very peculiar because it involves the construction of a two-body potential which contains many resonant states. The inclusion of these resonant states acts equivalently to the many species of the other counterexamples to drive up the entropy in the presence of more resonances.

Note at the outset that the evidence in support of this variant of the conjecture is quite limited. The AdS/CFT duality arguments do not apply. Since these calculations were done in the large N_c limit, it is hard to understand how they could justify a bound that fails for a large number of species and only works when the number of species is small enough. Moreover, much of the empirical evidence in favor of a KSS bound does not apply to variants of this sort. The term "single-species" in this context refers to systems whose constituents are either elementary or are in their ground state and do not access higher excited states. As a result, liquid water is not covered in this variant of the conjecture: water molecules in a liquid state can access rotational modes, making water a multi-species fluid from this perspective. This limits the applicability of this variant of the bound mostly to mono-atomic fluids, such as liquid helium. Since the vast majority of real world

fluids are not in this class, the fact that no known violation of the bound exists for real fluids provides only modest support for the bound.

The structure of this section is as follows. An example of a stable quantum-mechanical system composed of only one kind of spin-0 particle that can violate the KSS bound will be presented. To demonstrate that this system violates the bound, the system will first be defined in Sect. 5.3.1 by choosing a particular two-body interaction potential. The properties of the fluid in a non-relativistic regime are determined by the interaction potential along with the temperature and the density. The basic idea is to construct a two-body interaction of finite range which has an extremely large number of two-body resonant states right above threshold. Sect. 5.3.2 will show that the entropy for such a system has a lower bound, while Sect. 5.3.3 indicates that by a judicious choice of parameters, the entropy can be made arbitrarily large, even though there is only a single species of particles making up the fluid. Finally, in Sect. 5.3.4, it will be argued that the shear viscosity of such a system is not expected to become uncontrollably large as the parameters are adjusted to make the entropy grow arbitrarily. Thus it appears that the ratio of η/s can be made arbitrarily small within this class of theory.

5.3.1 Constructing the System

In this section, a single-species fluid composed of identical, stable, spin-0 particles will be defined. These identical spin-0 particles are considered to be the fundamental particles of the fluid. A finite-range two-body interaction that supports

no bound states (two-body or many-body) while supporting an arbitrary number of arbitrarily low-lying resonant states in the scattering amplitude will be chosen. The resonant states may be long-lived (depending on the choice of parameters of the potential), but it is important that they are indeed resonant states, and *not* bound states, so that there is no question that the fluid is of a single species.

Before discussing a detailed form of interaction which can generate this situation, it is important to note at the outset the interaction will require an exceptional degree of fine-tuning. The principal reason for this is that one requires that the range of the interaction remains fixed as resonances are added. This requirement will be imposed because one wishes to keep the density of the fluid fixed as resonances are added in order to avoid having many particles simultaneously within the range of interaction. This creates a strong constraint as an exponentially large number of nearly degenerate s-wave resonances near threshold for a system of fixed spatial extent is required. A useful way to envision making a system of finite size with multiple nearly degenerate two-body resonances is to start by constructing a system with numerous nearly degenerate two-body s-wave bound states and then add a repulsive potential to push them into the continuum.

However, it is not trivial to create a large number of nearly degenerate bound states with the same quantum numbers due to level repulsion. One way to proceed is by using a central potential which has numerous nested spherical-shell-shaped wells; the number of wells will be denoted as N. Clearly, if the spatial size of the interaction is kept fixed as one goes to a regime of large N (as is needed to achieve many bound states), the width of each well in the radial coordinate, r, must be

very small. To understand the tuning of parameters that is required, it is easiest to start by considering a system with a single well at a fixed position—with the position corresponding to the positions of one of the nested wells. The parameters are picked such that the single-well system has a single two-particle bound state. This can be achieved by tuning either the width or the depth of the well, or both.

Arbitrarily narrow wells can always be constructed to have a single bound state with fixed binding energy by making the well deep enough. In taking the width in the radial direction to be small (as one is forced to), in essence one is fine-tuning the depth of the potential, V_0, so that the binding energy is a very small fraction of V_0. For a generic well, it is not possible to do this for more than one bound state level. The bound state wave functions will be localized in the radial coordinate around the well. Note that there is a considerable level of parameter-tuning necessary to achieve this.

Now suppose one considers a system with all N of the wells present simultaneously. The parameters would need to be further tuned so that the bound states in each of the N wells are nearly degenerate. To the extent that bound state wave functions for the single well case were well localized—*i.e.*, have a spreading in r which is much less than spacing between levels — the full system will have N nearly degenerate bound states, each with an energy near that of the single well case. However, if that condition is not met, there will be significant level repulsion and the condition of near degeneracy will be destroyed. The characteristic spread of the wave functions is $(mB)^{-1/2}$ where m is the particle mass, and B is the binding energy. Accordingly, to include a large number of wells within a fixed radius while

keeping the levels nearly degenerate requires that the binding energy be tuned to be large.

There is a final level of tuning required. It has been shown that considerable tuning is required to get N nearly degenerate deeply bound states in a system with N nested wells with fixed range. However, a system with N resonances is desired. One can do this by adding a finite-range repulsive step function potential which will push the bound states just above threshold yielding resonances. As noted above, the bound states need to be very deeply bound. Accordingly, to get resonances just above threshold, one must tune the strength of the repulsive interaction to very high accuracy to cancel out the binding, leaving behind barely unbound resonances. However, in principle there is nothing to prevent one from arranging a system with all of this fine-tuning done as accurately as one wishes, yielding as many resonances as one wants as close to threshold as desired.

An example of a two-body central potential that has the desired properties is

$$V(r) = -b\sum_{k=1}^{N}\delta(r - \frac{kL}{N}) + V_0\theta(r - (L + \frac{L}{N})), \tag{5.7}$$

where r is the distance between fundamental particles, L is the range of the potential, b is the strength of each of the N delta functions, and the delta functions are raised on a potential step of height V_0. The additional factor of L/N in the step potential is intended to extend the range of the potential just beyond the last delta function. This ensures that the potential is identical in the neighborhood of each delta function. The δ functions in the potentials should be thought of as very deep, narrow potential wells—where the details of how this is done becomes irrelevant

provided the width is much smaller than all other scales in the problem. One can imagine tuning the parameters in the interaction of Eq. (5.7) (that is, choosing b and V_0) so that any "would-be" bound states become barely unbound, turning into low-energy, long-lived resonances. Appendix F provides some numerical evidence that it is possible to tune the parameters of the two-body interaction of Eq. (5.7) to create an arbitrary number of nearly degenerate low-energy resonances.

Qualitatively, one expects that the many different resonant states will behave as if they were the different species in a multi-species fluid. However, since these states are resonant states and not bound states, they eventually decay back into the fundamental particles, meaning this really is an interacting single-species gas rather than a multi-species gas. Furthermore, since the fundamental particles are absolutely stable, this system describes a stable fluid.

For the system to be of a single species, it is critical that the system does not have any three- or higher-body bound states. Given the singular nature of delta functions, one might worry that the Hamiltonian for three-body or higher-body Hilbert spaces might be unbounded from below, yielding arbitrarily deeply bound states. By regulating the delta functions and treating them as finite width wells, it should become readily apparent that this will not occur in the zero width limit with fixed resonance positions. Yet, it is not immediately apparent whether or not the system, as given, supports three- or higher-body bound states. To ensure that such states are excluded from this system, a three-body repulsive potential is also

imposed. The chosen three-body interaction $V_3(\vec{r_1}, \vec{r_2}, \vec{r_3})$ is

$$\begin{aligned} V_3(\vec{r_1}, \vec{r_2}, \vec{r_3}) &= V_3\Theta(R - \max[l_1, l_2, l_3]), \\ l_1 &= |\vec{r_1} - R_{CM}|, \\ l_2 &= |\vec{r_2} - R_{CM}|, \\ l_3 &= |\vec{r_3} - R_{CM}|, \\ R_{CM} &= \frac{m_1\vec{r_1} + m_2\vec{r_2} + m_3\vec{r_3}}{m_1 + m_2 + m_3}, \end{aligned} \tag{5.8}$$

where V_3, the strength of the three-body interaction, is a constant set to be larger than any other energy scale in the problem, $\vec{r_1}$, $\vec{r_2}$, and $\vec{r_3}$ are the position vectors of the three interacting particles, R is the range of the three-body interaction, R_{CM} is the location of the center of mass, and l_1, l_2, and l_3 are the distances from the center of mass to the location of each particle. The range of the three-body interaction range R is chosen to be larger than the range of the two-body interaction L. This interaction forces the interaction between the fundamental particles and any resonant state to be that of hard sphere scattering. Once a two-particle resonance is formed, the three-body potential above prevents the resonance from being disturbed by interactions with other particles and prevents the formation of three-particle resonant states.

5.3.2 Constructing a bound on the entropy

The calculation of the entropy of a strongly coupled many-body system can be quite difficult. Instead a variational argument will be used. This argument will show that entropy of the entire system for a gas of many particles interacting through

Eq. (5.7) can bounded from below. In the next section, a variational ansatz will be chosen for which the bound is calculable and show that the lower bound of the entropy can be made arbitrarily large.

Since the fluid under consideration has a finite temperature, one can work in the canonical ensemble. Recall that in this ensemble, with natural units ($k_B = 1$), the entropy is given by

$$S = \frac{E}{T} + \log(Z), \tag{5.9}$$

where E is the energy of the system, T is the temperature, and Z is the partition function. By increasing the step height in Eq. (5.7), the system can be tuned to have only resonant scattering states, and no two-body bound states. Similarly by choosing the strength of the repulsive three-body potential in Eq. (5.8) large enough, one can ensure that there are no three- or higher-body bound states. This means that all of the possible configurations of the fluid must have positive energy. Therefore, the entropy is bounded by

$$S \geq \log(Z). \tag{5.10}$$

So by calculating the partition function, a bound on the entropy can be made. However, just as with the entropy, the partition function is difficult to calculate directly, but the partition function is also bounded from below.

Recall that in the canonical ensemble the partition function is given by

$$Z = \mathrm{Tr}\left(\exp[-\beta \hat{H}]\right), \tag{5.11}$$

where $\hat{H}$ is the Hamiltonian operator for the system and β is the inverse temperature. In order to compute the partition function, one typically needs to use a complete

basis for the Hilbert space of the system. Since the Hamiltonian is Hermitian, the operator $\exp[-\beta\hat{H}]$ is positive semi-definite. This implies that the partial trace over any arbitrary subspace of the Hilbert space will be smaller than the complete partition function. The partition function over this subspace will be termed Z_{sub}. Choosing such a subspace amounts to choosing a variational ansatz for the class of configurations of the fluid: a calculation of the partition function within the variational ansatz is equivalent to the partition function of some subspace of the complete Hilbert space. Furthermore, the relation of the partition functions holds for the logarithm of the partition function as well,

$$\log(Z) \geq \log(Z_{\text{sub}}). \tag{5.12}$$

Combining Eqs. (5.10) and (5.12) yields

$$S \geq \log(Z_{\text{sub}}). \tag{5.13}$$

This shows that the entropy of the entire system is bounded from below by $\log(Z_{\text{sub}})$. By working with a variational ansatz for which the partition function Z_{sub} is calculable, one can compute a lower bound on the entropy of the fluid.

5.3.3 Calculating the partition function

In this section, a variational ansatz for the system for which the calculation of the lower bound for the entropy is tractable is chosen. The particular configuration of the system that will be considered is picked entirely for computational ease and is a highly unlikely one. This merely ensures that the true entropy may be well above this computed lower bound.

Consider dividing the volume occupied by the fluid into cells. For the variational ansatz, one can choose each cell to have exactly two particles. The total wave function for this ansatz can be constructed out of the wave function for each cell as:

$$\Psi_{\text{total}}(\vec{r_1}, \vec{r_2}, \ldots) = \hat{S} \prod_{\text{cells } i} \Psi_i(r_{2i-1}, r_{2i}) \tag{5.14}$$

where Ψ_{total}, the wave function of the entire fluid, is a function of the position of every fundamental particle in the fluid, $\hat{S}$ is an operator which symmetrizes the wave function under the exchange of any two particles to impose the exchange symmetry of bosons, and Ψ_i is the (two-particle) wave function of each individual cell, and they are summed over all of the cells. An illustration of the cell decomposition of the fliud is given in Fig. 5.1. To make the computation of the entropy easier, the configurations are further restricted so that wave function for each cell has the relative coordinate and center of mass coordinate completely uncorrelated. With this choice, the wave function for a cell can be written as

$$\Psi_{\text{cell}}(\vec{r}, \vec{R}) = \Psi_{\text{rel}}(\vec{r})\Psi_{\text{CM}}(\vec{R}), \tag{5.15}$$

where $\vec{r}$ is the relative coordinate, $\vec{R}$ is the center of mass coordinate, Ψ_{rel} is the wave function associated with the relative coordinate, and Ψ_{CM} is the wave function associated with the center of mass. This ansatz is subject to one further condition: namely, the following (Dirichlet) boundary conditions:

$$\begin{aligned} \Psi_{\text{rel}}(\vec{r})\big|_{r \geq r_{\max}} &= 0, \\ \Psi_{\text{CM}}(\vec{R})\Big|_{R \geq R_{\max}} &= 0, \end{aligned} \tag{5.16}$$

where $r_{\max}$ and $R_{\max}$ are the maximum relative coordinate and center of mass coordinate, respectively, that is allowed by a given cell. The maximum relative coordinate

is chosen to be beyond the range of the two-body interaction, thereby $r_{\max} > L$. These boundary conditions ensure for this particular ansatz the fundamental particles only interact within a given cell, and that each cell is isolated from all other cells. This isolation implies that the two-body interaction plus the boundary conditions give the dominant contribution to the partition function within the subspace that is considered. A pictorial view of the constraints of the boundary conditions can be seen in Fig. 5.2. This highly restrictive ansatz is certainly an unlikely configuration of the fluid, but it is a valid variational ansatz; such configurations are present in the complete Hilbert space.

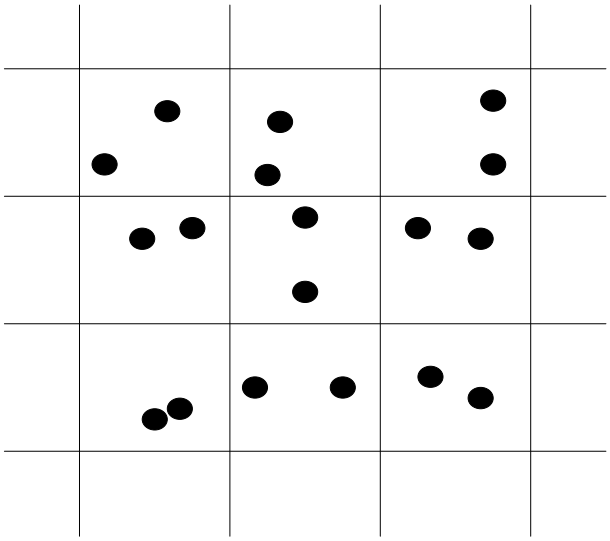

Figure 5.1: As a variational ansatz, one pictures the fluid's volume to be divided into cells with exactly two particles in each cell.

Having chosen an ansatz for the wave function of the fluid, the corresponding partition function can be computed. The arguments of the preceding subsection

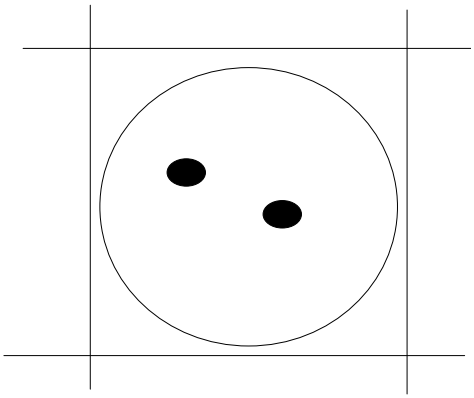

Figure 5.2: A close-up view of one particular cell with the drawn circle representing the constraints on the particles' wave function imposed by the boundary conditions.

showed that since the fluid considered has only positive energy states, the entropy of the entire system will be larger than the logarithm of the partition function calculated in this ansatz. Each cell has been isolated by imposing boundary conditions, and it is sufficient to calculate the partition function of only one cell to exhibit the bound. Since each cell is identical, the total entropy within the ansatz is the entropy of one cell times the number of cells. Accordingly the entropy density of the fluid is bounded by:

$$s \geq \frac{n}{2} S_{cell} \tag{5.17}$$

where n is the total density (implying that $n/2$ is the density of cells, and the factor of $\frac{1}{2}$ is due to our choice of two particles per cell).

In order to show that the entropy density of the fluid is arbitrarily large, one only has to show that the logarithm of the partition function $\log(Z_{\rm sub})$ for one particular cell in the fluid can be made arbitrarily large. To calculate the partition function, the energies of the states within each cell are needed. Since

the two-body interaction has a finite range, the relative coordinate wave function within the cell has two different forms: one within the range of the interaction, Ψ_{in}, and one beyond the range of the interaction, Ψ_{out}. The inner wave function can be calculated numerically from a non-relativistic Schrödinger equation and the potential in Eq. (5.7). The outer wave function is that of a free state restricted by the boundary conditions, and can be written as

$$\Psi_{\text{out}}(r) = A\sin(k(r_{\text{max}} - r)), \tag{5.18}$$

where A is a normalization factor, k is the momentum of the state such that $k = \sqrt{2\mu E}$ with μ as the reduced mass, and E is the energy of the state. The momentum, and thereby the energy, of the quantum states within the cell can be calculated by matching the logarithmic derivative at the boundary between the two wave functions. The matching leads to the equation

$$\left.\frac{\Psi'_{\text{in}}(r)}{\Psi_{\text{in}}(r)}\right|_{r=L} = -k\cot(k(r_{\text{max}} - r))|_{r=L}\,. \tag{5.19}$$

The solutions of these equations give the energies of the states within each cell. Relating this condition to the two-body s-wave scattering phase shifts yields the condition:

$$kr_{\text{max}} = -\delta(k) + n\pi, \tag{5.20}$$

where n is an arbitrary integer. Since the phase shifts pass rapidly through π at each resonance, it should be apparent that there is one low-lying energy state within this ansatz for every resonance.

The parameters of the two-body interaction can be tuned in such a manner that all of the resonant states have nearly degenerate, arbitrarily low energies. If the

resonance energies are fine-tuned to be very small compared to the temperature of the system, their contribution to the partition function is only slightly suppressed by a Boltzmann factor and each resonance contributes nearly unity to the $Z_{\rm sub}$. From the resonant contributions it is easy to see that

$$\log(Z_{\rm sub}) > \log(N) - E_H/T \tag{5.21}$$

where E_H is the energy of the highest-lying resonance. The logarithm of the partition function of the restricted system thus scales as $\log(N)$. The illustration that this scaling can be realized is provided by the results of numerical calculations in Appendix F.

The bound established in the preceding subsection shows that the system's entropy density, s, is larger than $\log(Z_{\rm sub})$. By increasing the number of resonant states while keeping E_H fixed, the lower bound on the entropy also increases. Since the number of resonant states in the two-body interaction can become arbitrarily large, so can the lower bound on the entropy density.

5.3.4 Viscosity and Stability

To complete the argument that the single-species fluid considered here can violate the single species variant of the KSS conjecture, one needs to argue that the shear viscosity η does not grow with the number of two-body resonant states, N (or, more precisely, grows slower than logarithmically). Furthermore, it is important to show the resulting fluid is stable in order to rule out variants of the conjecture for both stable and metastable fluids.

The shear viscosity is difficult to calculate for virtually any strongly-interacting system. For fluids which the Boltzmann equation is applicable, there are simplifying arguments that allow one to calculate the shear viscosity [183]. However, due to the presence of long-lived resonant states, the fluid described here does not satisfy the assumptions of the Boltzmann equation. Therefore, an analytical calculation of the shear viscosity is not known.

Heuristically, the resonant states in the system described in this section can be thought of *approximately* as bound states. It has been shown in the context of the models of Ref. [162], which are outlined in Appendix D, that the shear viscosity of a system of bound states need not scale uncontrollably with additional components to the fluid. Therefore, it is difficult to believe that the shear viscosity for the approximate bound states would scale vastly differently than that of a dilute many-component fluid. The actual difference between the shear viscosity of the two systems should depend on how well the bound state approximation is valid, which depends on the resonant state lifetimes. The resonant states of the fluid have been constructed to have very long lifetimes. As a result, for the purposes of understanding the shear viscosity, the approximation that the resonant states can be considered bound states should be quite accurate. Therefore the shear viscosity of a fluid of long-lived resonant states should scale similarly to the viscosity of a fluid of bound states. Moreover, the shear viscosity of a fluid typically diverges only when it approaches either a non-interacting ideal gas, or behaves like the cold limit of a fluid without a defined melting temperature, such as glass. It is hard to see how a strongly interacting system, such as the one described in this paper, with a large

number of long-lived resonant states should approach either one of these limits with the addition of resonant states. Therefore, the shear viscosity should remain finite as the entropy is made arbitrarily large, violating the η/s bound. While this is not a mathematically rigorous argument, it is very hard to see how it can fail.

In discussing shear viscosity, the system was approximated as though it contained bound states. However, at a fundamental level there are no bound states, and the fluid is still composed of only one species. If one wanted to compute η/s for this system numerically, for instance, the relevant degrees of freedom to simulate would be those of the fundamental particles together with their interactions, and *not* of the resonances. Since these fundamental particles are absolutely stable, by construction, the fluid is stable.

5.4 Conclusion

The preceding arguments show that the entropy, and therefore the entropy density increases with the number of resonant states. It has been argued that although the calculation of the shear viscosity for the fluid described is not tractable, there are strong heuristic reasons to believe that it will not diverge when one chooses parameters to force the entropy to diverge. To the extent one accepts these arguments, one must conclude that the ratio η/s can be made arbitrarily small by increasing the number of resonant states, violating the conjectured bound on η/s.

The number of resonant states needed to actually violate the bound could be extremely large, but the two-body interaction that has been discussed here can

be tuned in such a manner as to produce an arbitrary number of resonant states. That is, there does not appear to be a limit inherent in the structure of quantum mechanics on the number of resonant states that can be constructed within a finite ranged potential.

It is noted that if a conjecture is false for stable fluids in some class of theories, it must be false for metastable fluids as well. As a result, the single species fluid that has been described in this chapter actually provides a counterexample to all theories of fluids of a single species, both for stable and metastable fluids.

Combining the arguments here and those of Ref. [162], it appears that one need not expect the KSS bound to hold for a vast class of fluids. It may be true empirically that most fluids do respect the bound, but that appears to be a matter of coincidence rather than being driven there by some fundamental principle of the universe. By the current arguments and those of Ref. [162], the bound cannot be derived from quantum mechanics (either for a single species or many species) for both stable and metastable fluids. The heavy meson gas described here and in Ref. [162] indicates that the bound can be violated for a metastable fluid of QCD. Should the KSS bound actually be universal, it presumably comes from some physical descriptions beyond quantum field theory (*e.g.*, string theory, super gravity, or the like).

Appendix A

Bound States of heavy pentaquarks in quantum mechanics

Consider a smoothly varying potential $V(r)$ that vanishes as $r \to \infty$. If $V(r)$ is nonsingular and has an attractive region, it must possess a minimum at some r_0. In the neighborhood of r_0 the potential is approximately harmonic [*i.e.*, $V(r) \simeq \frac{k}{2}(r - r_0)^2$]. Therefore, if the wave function is for some reason localized near the minimum, then the system can be approximated as a harmonic oscillator. For large reduced mass μ the kinetic energy operator is small, and minimizing the wave function's curvature forces its localization near $r = r_0$, as desired. The harmonic oscillator potential has an infinite number of bound states, separated by multiples of $\omega = \sqrt{k/\mu}$. Furthermore, for large values of μ, the harmonic oscillator wave function, given by

$$\Psi_n(\xi) = \frac{1}{(2^n n!)^{1/2}} \left(\frac{\mu\omega}{\pi}\right)^{1/4} H_n(\xi) e^{-\xi^2/2}, \quad \xi = \sqrt{\mu\omega}(r - r_0) \tag{A.1}$$

where H_n are the Hermite polynomials, is self-consistently localized about the minimum. Thus one sees that multiple bound states must exist for sufficiently large μ. If the potential is singular (but not more singular than $1/r^2$, so that a ground state exists), the large size of μ localizes the wave function deep in the potential near the singularity, again allowing plenty of room for bound states.

Appendix B

Details of numerical results for heavy pentaquark models

This appendix focuses on the numerical results associated with binding of a heavy pentaquark in a modified one-pion exchange potential. Table B.1 lists the parameters used in the calculation. Table B.2 summarizes the potentials that were used. Table B.3 presents the energies of bound states for a B meson binding with a nucleon, while Table B.4 presents the same for a D meson.

Quantity Name	Quantity Value
g_A	1.27
f_π	131 MeV
g_H	$\pm$ 0.59
m_π	138 MeV
m_N	938.92 MeV
m_B	5279 MeV
m_D	1867 MeV
Δ_B	46 MeV
Δ_D	141 MeV

Table B.1: Constants used in bound-state calculations for heavy pentaquarks.

$$
\begin{aligned}
V_\pi(\vec{x}) &= \begin{cases} (I^2 - I_N^2 - I_H^2)[S_{12}V_T(r) + (K^2 - S_N^2 - S_H^2)V_c(r)] & r > r_0 \\ V_1(r) \text{ or } V_2(r) & r < r_0 \end{cases} \\
V_c(r) &= \frac{g_A g_H}{2\pi f_\pi^2} \frac{e^{-m_\pi r}}{3r} m_\pi^2 \\
V_T(r) &= \frac{g_A g_H}{2\pi f_\pi^2} \frac{e^{-m_\pi r}}{6r} \left(\frac{3}{m_\pi^2 r^2} + \frac{3}{m_\pi r} + 1 \right) m_\pi^2 \\
V_1(r) &= V_0 \ (V_0 = -62.79 \text{ MeV or} - 276 \text{ MeV}) \\
V_2(r) &= -252.659 \, \frac{\text{MeV}}{\text{fm}^2} \, r^2 + 541.321 \, \frac{\text{MeV}}{\text{fm}} \, r - 309.822 \, \text{MeV}
\end{aligned}
\tag{B.1}
$$

Table B.2: Potentials used in heavy pentaquark calculations. The labels are: total isospin I, nucleon isospin I_N, heavy meson isospin I_H, tensor force S_{12}, tensor potential $V_T(r)$, nucleon spin S_N, light quark in heavy meson spin S_l, sum of nucleon spin and light quark spin K, central potential $V_c(r)$. Numerical values are such that potentials are measured in MeV, distances in MeV^{-1}, unless noted otherwise. Both $V_1(r)$ and $V_2(r)$ are central potentials. The parameters in $V_2(r)$ were fixed by making the potential differentiable at r_0 and bind deuterium with the appropriate energy.

Channel			I	A		B		C		D	
J	S	P		+	−	+	−	+	−	+	−
$\frac{1}{2}$	$\frac{1}{2}$	−	0	1.30	1.35	3.89	1.92, 3.62	139.38, 142.14	–	14.49, 16.01	15.46, 16.15
			1	–	–	0.35	0.27	–	139.38, 140.76	15.32, 15.60	15.04, 15.46
$\frac{1}{2}$	$\frac{1}{2}$	+	0	–	–	–	–	14.9, 32.39	4, 19.32, 46.5	–	–
			1	–	–	–	–	12.72, 18.22, 26.91	9.45	–	–
$\frac{1}{2}$	$\frac{3}{2}$	−	0	1.30	1.31	3.89	3.67	140.76	140.76	15.87	15.32
			1	–	–	–	0.26	140.76	140.76	15.04	15.32
$\frac{1}{2}$	$\frac{3}{2}$	+	0	–	–	–	–	32.15	3.35, 45.95	–	–
			1	–	–	–	–	12.12, 27.19	8.36, 22.08	–	–
$\frac{3}{2}$	$\frac{1}{2}$	−	0	1.42	1.31	3.89	3.67	140.76	140.76	15.87	15.32
			1	–	–	–	0.26	140.76	140.76	15.04	15.32
$\frac{3}{2}$	$\frac{1}{2}$	+	0	–	–	–	–	15.32, 18.49, 32.43	4.65	–	–
			1	–	–	–	–	12.80	17.25, 17.66, 22.91	–	–
$\frac{3}{2}$	$\frac{3}{2}$	−	0	1.42	1.25	3.89	3.67	140.76	140.76	15.87	15.32
			1	–	–	–	0.20	140.76	140.76	15.04	15.32
$\frac{3}{2}$	$\frac{3}{2}$	+	0	–	–	–	–	18.22, 32.29	–	–	–
			1	–	–	–	–	4.18, 23.18	–	–	–

Table B.3: B meson bound-state energies for each channel, where + and − refer to relative sign of g_A and g_H. All energies in MeV. Column A: constant potential, $V_0 = -62.79$ MeV and $r_0 = 1$ fm; B: quadratic potential; C: constant potential, $V_0 = -276$ MeV and $r_0 = 1$ fm; D: constant potential, $V_0 = -62.79$ MeV and $r_0 = 1.5$ fm.

Channel J	S	P	I	A +	A −	B +	B −
$\frac{1}{2}$	$\frac{1}{2}$	−	0	113.99, 110.4	–	7.36, 9.00	8.45, 9.27
			1	–	114.82, 115.78	8.40, 8.79	8.16, 8.63
$\frac{1}{2}$	$\frac{1}{2}$	+	0	2.91	16	–	–
			1	–	–	–	–
$\frac{1}{2}$	$\frac{3}{2}$	−	0	117.3	116.2	9.00	8.45
			1	115.23	115.23	8.45	8.45
$\frac{1}{2}$	$\frac{3}{2}$	+	0	2.10	15.87	–	–
			1	–	–	–	–
$\frac{3}{2}$	$\frac{1}{2}$	−	0	117.3	116.20	9.00	8.45
			1	115.37	115.78	8.45	8.45
$\frac{3}{2}$	$\frac{1}{2}$	+	0	2.91	–	–	–
			1	–	–	–	–
$\frac{3}{2}$	$\frac{3}{2}$	−	0	117.3	116.20	9.00	8.45
			1	115.09	115.09	8.45	8.45
$\frac{3}{2}$	$\frac{3}{2}$	+	0	2.53	–	–	–
			1	–	–	–	–

Table B.4: D meson bound-state energies for each channel, where + and − refer to the relative sign of g_A and g_H. All energies in MeV. Column A: constant potential, $V_0 = -276$ MeV and $r_0 = 1$ fm; B: constant potential, $V_0 = -62.79$ MeV and $r_0 = 1.5$ fm.

Appendix C

Description of calculation leading to mass splitting relations

In Chapt. 4, formulae for relating the spin state mass splittings between various hadrons, Eqs. (4.1) and (4.7), were presented without derivation. This appendix will detail the calculations leading to these equations. The calculations leading to Eq. (4.1) were first presented by Savage and Wise in their investigation relating heavy mesons and doubly heavy baryons [139]. The techniques of their calculation will then be extended to examine the similar relationships between the heavy baryon and the doubly heavy tetraquark states found in Eq. (4.7).

C.1 Heavy meson – doubly heavy baryon relations

Section 1.2 presented some general aspects of HQET. There it was pointed out that the effective Lagrangian for HQET to $O(1/m_Q)$ was,

$$\mathcal{L}_{\text{quark}} = \bar{Q}_i \, iv \cdot D Q_i - \frac{\alpha_2(\mu) g(\mu)}{m_Q} \sum_{i,j} \bar{Q}_i \frac{\sigma_{ij} \cdot B}{2} Q_j, \tag{C.1}$$

where the label Q_i with an explicit spin index has replaced h_v, the kinetic term has been omitted, and the color magnetic moment term has been expressed in terms of the color magnetic field. As mentioned before, this is the Lagrangian for a single heavy quark. A doubly heavy diquark in a vector state can easily be included into

this theory by adding the following terms to the Lagrangian[1]:

$$\mathcal{L}_{\text{diqaurk}} = \bar{V}_i \, iv \cdot DV_i - \frac{\alpha_2(\mu) g(\mu)}{m_Q} \frac{i}{2} \sum_{i,j,k} \epsilon_{ijk} V_i^\dagger B_j V_k, \tag{C.2}$$

where V_i is the vector diquark field. One should observe initially that the leading order terms between the quark and the diquark sector have the same structure. By incorporating the two quark spin states and the three vector spin states into one multiplet, the leading order Lagrangian exhibits a $SU(5)$ symmetry. This symmetry is referred to by Savage and Wise as a superflavor symmetry [139], and it is exactly the DHDA symmetry discussed in Chapt. 4. If one extends the DHDA, or superflavor, symmetry to the $O(1/m_Q)$ corrections terms in HQET, the color magnetic moment coupling constants $\alpha_2(\mu)$ is required to be the same for both the quark and the diquark sectors. (The coupling constant $g(\mu)$ is obviously the same for both sectors as this is the universal strong coupling constant.) Therefore, the similar portions of the quark and diquark color magnetic moment terms can be factored out so that those terms can be rewritten as

$$\mathcal{L}_Q = -\frac{\alpha_2(\mu)}{m_Q} g(\mu) \sum_{i,j} \bar{Q}_i \frac{\sigma_{ij} \cdot B}{2} Q_j = -\frac{\alpha_2(\mu) g(\mu)}{m_Q} \mathcal{O}_Q, \tag{C.3}$$

$$\mathcal{L}_V = -\frac{\alpha_2(\mu) g(\mu)}{m_Q} \frac{i}{2} \sum_{i,j,k} \epsilon_{ijk} V_i^\dagger B_j V_k = -\frac{\alpha_2(\mu) g(\mu)}{m_Q} \mathcal{O}_V. \tag{C.4}$$

The dissimilar parts of these terms, $\mathcal{O}_Q$ and $\mathcal{O}_V$, are the color magnetic moment operators for the quark and the vector diquark sectors, respectively.

The final piece needed to derive Eq. (4.1) is the superflavor generator. With the heavy quark and the doubly heavy diquark vector within the same group element,

[1] when a factor of 1/2 is corrected for in Ref. [139]

one can define a generator of this superflavor as

$$S^{(a)} = \int d^3x \{V_+^{(a)} Q_1^{(a)\dagger} + V_-^{(a)} Q_2^{(a)\dagger}\}, \tag{C.5}$$

where $Q_{1,2}^\dagger$ creates a heavy quark, $V_{+,-}$ destroys a heavy diquark, and (a) is a label for the flavor of the heavy quark. Overall this generator will convert a + state diquark into a quark oriented up or convert a − state diquark into a down state quark. Since the work here will focus on only one heavy quark flavor the label, (a), will be subsequently dropped.

Equation (4.1) is an expression that relates heavy mesons and doubly heavy baryons. The only mechanism to find relations between these two sectors is through the superflavor generator. Furthermore, it is important to have a complete set of relations without the duplication of equations. Therefore the superflavor generator will be applied to the states $|+\uparrow\rangle$ and $|+\downarrow\rangle$,[2] where the first label refers to the vector orientation and the second the light quark orientation, yielding

$$\begin{aligned} S|+\uparrow\rangle &= S|\Xi_{cc}^*, 3/2\rangle = |\uparrow\uparrow\rangle = |D^*, 3/2\rangle \\ S|+\downarrow\rangle &= S\{|\Xi_{cc}^*, 1/2\rangle + \sqrt{2}|\Xi_{cc}, 1/2\rangle\} = |\downarrow\uparrow\rangle = \sqrt{\frac{3}{2}}\{|D^*, 0\rangle + |D\rangle\}. \end{aligned} \tag{C.6}$$

In addition, being labelled by the spin orientation, the hadronic states above are also labelled by the hadron name and the hadron's overall spin orientation, such as $|\Xi_{cc}^*, 3/2\rangle$ refers to the doubly heavy baryon Ξ_{cc}^* with it's spin in the $+3/2$ state. In further calculations, this hadronic spin orientation is not relevant so this label will be suppressed.

Having established relations between the meson and baryon states, it is nec-

[2]Applying it to the states $|-\uparrow\rangle$ and $|-\downarrow\rangle$ would only lead to redundant relations.

essary to determine how the color magnetic moments between the quark and the vector sectors are related. To begin this, it is noted that the color magnetic moment operators, $\mathcal{O}_Q$ and $\mathcal{O}_V$, can be divided between the contribution from the three component of the color magnetic field and the remaining contributions. Therefore,

$$\begin{aligned} \mathcal{O}_Q &= \mathcal{O}_{Q;3} + \mathcal{O}_{Q;\perp} \quad \text{and} \\ \mathcal{O}_V &= \mathcal{O}_{V;3} + \mathcal{O}_{V;\perp}, \end{aligned} \tag{C.7}$$

where

$$\mathcal{O}_{Q;3} = \sum_{i,j} Q_i^\dagger \frac{\sigma_{ij}^3 B_3}{2} Q_j, \tag{C.8}$$

$$\mathcal{O}_{Q;\perp} = \sum_{i,j} Q_i^\dagger \frac{1}{2} (\sigma_{ij}^1 B_1 + \sigma_{ij}^2 B_2) Q_j, \tag{C.9}$$

$$\mathcal{O}_{V;3} = \frac{i}{2} \sum_{i,j} \epsilon_{ij3} V_i^\dagger B_3 V_j, \quad \text{and} \tag{C.10}$$

$$\mathcal{O}_{V;\perp} = \frac{i}{2} \sum_{i,j} (\epsilon_{ij1} V_i^\dagger B_1 V_j + \epsilon_{ij2} V_i^\dagger B_2 V_j). \tag{C.11}$$

From these relations, one can show the following double commutation relation holds,

$$[S^\dagger, [S, \mathcal{O}_{Q;3}]] = -S^\dagger \mathcal{O}_{Q;3} S = -\mathcal{O}_{V;3}. \tag{C.12}$$

This equation provides the necessary relationship between the color magnetic moment for the quarks and the vector diquark.

By using both Eqs. (C.6) and (C.12), one can calculate the expectation value of the color magnetic moment for the meson states on the right-hand side of Eq. (C.6) and relate them to the baryon states' expectation value. For the D^* case this leads

to

$$\begin{aligned}\langle D^*|\mathcal{O}_Q|D^*\rangle &= \langle \Xi^*_{cc}|S^\dagger \mathcal{O}_Q S|\Xi^*_{cc}\rangle \\ &= \langle \Xi^*_{cc}|S^\dagger(\mathcal{O}_{Q;3}+\mathcal{O}_{Q;\perp})S|\Xi^*_{cc}\rangle = \langle \Xi^*_{cc}|S^\dagger \mathcal{O}_{Q;3} S|\Xi^*_{cc}\rangle \\ &= \langle \Xi^*_{cc}|\mathcal{O}_{V;3}|\Xi^*_{cc}\rangle = \langle \Xi^*_{cc}|(\mathcal{O}_{V;3}+\mathcal{O}_{V;\perp})|\Xi^*_{cc}\rangle \\ &= \langle \Xi^*_{cc}|\mathcal{O}_V|\Xi^*_{cc}\rangle.\end{aligned} \tag{C.13}$$

The second equals sign in lines two and three are justified because in each case both the bra and ket were states with the same quark (or diquark) orientation and the $\perp$ operators change this orientation; hence their contribution is zero. A similar expression can be derived from the second expression in Eq. (C.6).

$$\begin{aligned}\frac{3}{2}(\langle D^*|\mathcal{O}_Q|D^*\rangle + \langle D|\mathcal{O}_Q|D\rangle) &= \langle \Xi^*_{cc}|S^\dagger \mathcal{O}_Q S|\Xi^*_{cc}\rangle + 2\langle \Xi_{cc}|S^\dagger \mathcal{O}_Q S|\Xi_{cc}\rangle \\ &= \langle \Xi^*_{cc}|\mathcal{O}_V|\Xi^*_{cc}\rangle + 2\langle \Xi_{cc}|\mathcal{O}_Q|\Xi_{cc}\rangle.\end{aligned} \tag{C.14}$$

Equations (C.13) and (C.14) can be solved for the Ξ^*_{cc} and the Ξ_{cc} matrix elements in terms of the D^* and the D matrix elements. Since the mass difference between the spin states is due solely from the color magnetic moment at leading non-vanishing order, the mass difference can be expressed in terms of the difference between the color magnetic moments just derived. This leads naturally to the expected Savage and Wise relation of Eq. (4.1),

$$\begin{aligned}m_{\Xi^*_{cc}} - m_{\Xi_{cc}} &= \langle \Sigma^*|\mathcal{O}_V|\Sigma^*\rangle - \langle \Sigma|\mathcal{O}_V|\Sigma\rangle \\ &= \frac{3}{4}(\langle D^*|\mathcal{O}_Q|D^*\rangle - \langle D|\mathcal{O}_Q|D\rangle) \\ &= \frac{3}{4}(m_{D^*} - m_D).\end{aligned} \tag{C.15}$$

C.2 Mass splittings of tetraquark states

The method to derive the relations of the mass splittings between spin states of the doubly heavy tetraquark and the spin states of heavy baryons is the same as the previous section. For these systems though there are more states. Remember there are three heavy baryon states: Λ, Σ, and Σ^*. The Λ has the light quark pair in a singlet state, so overall it has a spin of 1/2. The Σ and Σ^* have the light quark pair in a triplet state; hence Σ has a spin of 1/2, and Σ^* has a spin of 3/2.

There are now four tetraquark states labelled as T^Λ, T, T^*, and T^{**}. The T^Λ state is the tetraquark analog of the Λ with the light quark pair in a singlet state, hence the overall spin is 1. The other three tetraquarks have a triplet light quark component resulting in an overall spin of 0, 1, and 2 for states T, T^*, and T^{**}, respectively.

As was done before, the derivation of the mass splitting relations begins with applying the superflavor generator to the collection of states with the heavy diquark pair oriented in the +1 direction and the light quark pair oriented in each of its possible orientations. Therefore when the light quarks are in a singlet state, there is only one possible light quark orientation leading to the equation,

$$S|+0\rangle = S|T^\Lambda\rangle = |\uparrow 0\rangle = |\Lambda\rangle. \tag{C.16}$$

There are three possible orientations for a light quark pair triplet state. By applying

the superflavor operator to them leads to

$$S|++\rangle = S|T^{**}\rangle = |\uparrow +\rangle = |\Sigma^*\rangle, \tag{C.17}$$

$$S|+0\rangle = \frac{1}{\sqrt{2}}S(|T^{**}\rangle + |T^*\rangle) = |\uparrow 0\rangle = \sqrt{\frac{2}{3}}|\Sigma^*\rangle + \sqrt{\frac{1}{3}}|\Sigma\rangle, \tag{C.18}$$

$$S|+-\rangle = S(\frac{1}{\sqrt{6}}|T^{**}\rangle + \frac{1}{\sqrt{2}}|T^*\rangle + \frac{1}{\sqrt{3}}|T\rangle) = |\uparrow -\rangle = \frac{1}{3}|\Sigma^*\rangle - \frac{2}{3}|\Sigma\rangle. \tag{C.19}$$

The difference in the mass between the different states stems form the color magnetic moment operator. Similar to above, the expectation value of the color magnetic moment for the heavy baryon states from the right-hand side of Eqs. (C.16) and (C.17) will be calculated. The relations of Eqs. (C.7) and (C.12) still hold. Therefore, for the Λ state one gets

$$\langle\Lambda|\mathcal{O}_Q|\Lambda\rangle = \langle T^\Lambda|S^\dagger\mathcal{O}_Q S|T^\Lambda\rangle = \langle T^\Lambda|\mathcal{O}_V|T^\Lambda\rangle, \tag{C.20}$$

while the Σ states result in

$$\begin{aligned}\langle\Sigma^*|\mathcal{O}_Q|\Sigma^*\rangle &= \langle T^{**}|S^\dagger\mathcal{O}_Q S|T^{**}\rangle \\ &= \langle T^{**}|\mathcal{O}_V|T^{**}\rangle,\end{aligned} \tag{C.21}$$

$$\begin{aligned}\frac{2}{3}\langle\Sigma^*|\mathcal{O}_Q|\Sigma^*\rangle + \frac{1}{3}\langle\Sigma|\mathcal{O}_Q|\Sigma\rangle &= \frac{1}{2}\langle T^{**}|S^\dagger\mathcal{O}_Q S|T^{**}\rangle + \frac{1}{2}\langle T^*|S^\dagger\mathcal{O}_Q S|T^*\rangle \\ &= \frac{1}{2}\langle T^{**}|\mathcal{O}_V|T^{**}\rangle + \frac{1}{2}\langle T^*|\mathcal{O}_V|T^*\rangle,\end{aligned} \tag{C.22}$$

$$\begin{aligned}\frac{1}{3}\langle\Sigma^*|\mathcal{O}_Q|\Sigma^*\rangle + \frac{2}{3}\langle\Sigma|\mathcal{O}_Q|\Sigma\rangle &= \frac{1}{6}\langle T^{**}|S^\dagger\mathcal{O}_Q S|T^{**}\rangle + \frac{1}{2}\langle T^*|S^\dagger\mathcal{O}_Q S|T^*\rangle + \frac{1}{3}\langle T|S^\dagger\mathcal{O}_Q S|T\rangle \\ &= \frac{1}{6}\langle T^{**}|\mathcal{O}_V|T^{**}\rangle + \frac{1}{2}\langle T^*|\mathcal{O}_V|T^*\rangle + \frac{1}{3}\langle T|\mathcal{O}_V|T\rangle.\end{aligned} \tag{C.23}$$

One can solve these equations for the tetraquark matrix elements in terms of baryon matrix elements. As before, the mass difference between spin states is the same as

the difference between these matrix elements. The final step to derive the relations in Eq. (4.7) is simply to calculate the difference between the matrix elements of two different tetraquark states. This leads to

$$\begin{aligned} m_{T^{**}} - m_{T^*} &= \langle T^{**}|\mathcal{O}_V|T^{**}\rangle - \langle T^*|\mathcal{O}_V|T^*\rangle \\ &= \frac{2}{3}(\langle \Sigma^*|\mathcal{O}_Q|\Sigma^*\rangle - \langle \Sigma|\mathcal{O}_Q|\Sigma\rangle) \\ &= \frac{2}{3}(m_{\Sigma^*} - m_\Sigma), \end{aligned} \tag{C.24}$$

$$\begin{aligned} m_{T^*} - m_T &= \langle T^*|\mathcal{O}_V|T^*\rangle - \langle T|\mathcal{O}_V|T\rangle \\ &= \frac{1}{3}(\langle \Sigma^*|\mathcal{O}_Q|\Sigma^*\rangle - \langle \Sigma|\mathcal{O}_Q|\Sigma\rangle) \\ &= \frac{1}{3}(m_{\Sigma^*} - m_\Sigma), \end{aligned} \tag{C.25}$$

$$\begin{aligned} m_T - m_{T^\Lambda} &= \langle T|\mathcal{O}_V|T\rangle - \langle T^\Lambda|\mathcal{O}_V|T^\Lambda\rangle \\ &= \langle \Sigma|\mathcal{O}_Q|\Sigma\rangle - \langle \Lambda|\mathcal{O}_Q|\Lambda\rangle \\ &= m_\Sigma - m_\Lambda. \end{aligned} \tag{C.26}$$

These equations are identical to Eq. (4.7) when one remembers that the notation used there represents the mass of each state.

Appendix D

Non-relativistic gas

Reference [162] considers a non-relativistic quantum many-body system with a large number of species for which the computation of the ratio η/s is analytically tractable up to corrections which can be made arbitrarily small. By imposing a particular set of scaling relations on the parameters of the system, it is possible to demonstrate that η/s can violate the KSS bound in the limit of a large number of species. This argument is reviewed here.

Consider a gas composed of a number (N_s) of distinct species of spin-0 bosons of degenerate mass, m, which can interact via a two-body potential. The two-body potential is identical for all species, but is limited to a finite range, R. The gas is in thermal equilibrium at a temperature T, and has the same density for each species, $n_a = n/N_s$, where n is the overall density of the system. The system is in a low temperature and low density regime such that

$$R^{-2}, a^{-2} \gg mT \gg n^{2/3}, \tag{D.1}$$

where a is the scattering length, and mT is the thermal momentum squared. This regime can be maintained by using the following scaling of the density and temperature:

$$n = \frac{n_0}{\xi^4} \qquad T = \frac{T_0}{\xi^2}, \tag{D.2}$$

where n_0 and T_0 are independent of the dimensionless scaling parameter ξ. With a

sufficiently large value for ξ, Eq. (D.1) can be easily satisfied.

In this density and temperature regime, the entropy for the system is simply that of a classical ideal gas, with small corrections. The key point is that the temperature is high enough relative to $n_0^{2/3}/m$ for the classical expression to hold, while the density is low enough to neglect the interactions. The entropy density can then be written in terms of the scaling in Eq. (D.2) as

$$s \simeq n_0 \left(\log\left(\frac{(mT_0)^{3/2}}{n_0} \right) + \frac{5}{2} + \log(\xi) + \log(N_s) \right), \tag{D.3}$$

where the term $\log(N_s)$ is associated with the Gibbs mixing entropy of the N_s different species.

Furthermore, in this density and temperature regime, the thermal wavelength is much shorter than the inter-particle spacing, meaning that the many-body dynamics are essentially classical. Moreover, the low density implies that the many-body dynamics are dominated by binary collisions, implying that the system is in the regime of validity for the Boltzmann equation [183]. The low temperature further implies that the two-body collisions are dominated by s-wave scattering, with a cross section essentially unchanged from its zero momentum value. That is, two-body scattering in this system can be approximated as isotropic and energy independent, which is formally the same as classical hard sphere scattering.

The shear viscosity is analytically calculable in such a system [183], and it is given by $\eta = C_{\rm hs}\sqrt{mT}/d^2$, where d is the diameter of the hard spheres, and $C_{\rm hs} \approx .179$ is a coefficient that is numerically calculable [1]. Identifying the scattering

[1]The coefficient, C_{hs}, can be calculated in the Chapman Enskog expansion as outlined in

length a as the effective hard sphere diameter, we can now calculate the ratio η/s:

$$\frac{\eta}{s} \simeq \frac{C_{\rm hs}\xi^3\sqrt{mT_0}}{a^2 n_0\left(\log\left(\frac{(mT_0)^{3/2}}{n_0}\right)+\frac{5}{2}+\log(\xi)+\log(N_s)\right)}. \tag{D.4}$$

Corrections to Eq. (D.4) are suppressed by powers of $1/\xi$ and should become irrelevant for sufficiently large ξ.

The derivation of Eq. (D.4) required the system to be in a low density and low temperature regime such that a classical approximation for both the shear viscosity and the entropy density can be made. This limit does not place any constraints on the number of species of particles in the fluid. Accordingly, one can demand that the number of species scale exponentially with the scaling parameter:

$$N_s = \exp(\xi^4) \tag{D.5}$$

As the temperature and density decrease, the number of species increases simultaneously. When Eqs. (D.4) and (D.5) are combined, the large ξ scaling of the ratio is

$$\frac{\eta}{s} \simeq \frac{1}{\xi}\frac{C_{\rm hs}\sqrt{mT_0}}{a^2 n_0} \tag{D.6}$$

up to power law corrections in $1/\xi$. Clearly, in this combined limit, the ratio η/s can violate the conjectured bound simply by making ξ sufficiently large. This violation stems completely from the large Gibbs mixing entropy associated with the exponentially large number of species.

Having argued that the non-relativistic gas described above can violate a version of the KSS bound, it is important to understand whether this fluid is stable or

Ref. [183] and is $5/(16\sqrt{\pi})$ to leading order.

metastable. The argument in the preceding section does not depend on the inter-particle potential and thus will continue to hold for any choice of the interparticle potential. If we choose the interparticle potential to be purely repulsive, the particles making up the fluid cannot lower their energies by forming bound states. Therefore, with this choice, the system that has been described above is a stable fluid with an arbitrarily small value of the ratio η/s. This is sufficient to demonstrate that this system is a counterexample to *both* stable and metastable non-relativistic fluids.

what happens when the inter-particle interaction is attractive? One might worry that with such a potential, the fluid could lower its energy by forming bound states, or by "clumping" together; that is, by forming macroscropic regions of higher density where the attraction is enhanced and the free energy is lowered. If either situation is possible, the fluid would then be either unstable or metastable. In order to distinguish between these two cases, one needs to compare $\tau_{\rm met}$, the characteristic time for the phase to change macroscopically, with $\tau_{\rm fl}$, the characteristic time scale of the fluid. It can be shown that in the scaling regime of Eq. (D.2), $\tau_{\rm meta}/\tau_{\rm fl}$ diverges as ξ^5 or faster, ensuring that when ξ is large the system is metastable.

The type of metastability with the decay mechanism which yields the fastest possible decay parametrically is for systems which can form two-body bound states. As is well known, in a non-relativistic gas three-body collisions are necessary to allow the formation of two-body bound states due to energy and momentum conservation. Therefore, the decay time $\tau_{\rm met}$ scales with the time between three-body collisions in the system. The characteristic time scale of the fluid $\tau_{\rm fl}$ scales with the time scale for two-body collisions. Therefore the ratio $\tau_{\rm meta}/\tau_{\rm fl}$ has roughly the same scaling

as τ_3/τ_2, where τ_3 and τ_2 are the three-body and two-body collision time scales, respectively.

The time between two-body collisions is essentially just the mean free time of particles in the fluid. The mean free time $\tau_{\rm mf}$ is related to the mean free path $l_{\rm mf}$ by

$$\tau_{\rm mf} = l_{\rm mf}/v, \tag{D.7}$$

where v is the rms velocity of particles in the fluid. In dilute classical gases, the mean free path l can be related to the density and the interaction cross section,

$$n l_{\rm mf}\, \sigma \sim 1. \tag{D.8}$$

The rms velocity v can be related to the thermal momentum associated with the fluid: $mv \sim \sqrt{mT}$, where m is the mass of the particle, and T is the temperature of the fluid. Combining these equations and the scaling relations of Eq. (D.2), we see that the mean free time scales like

$$\tau_{\rm mf} = \frac{1}{n\sigma}\sqrt{\frac{m}{T}} \sim \xi^5 \frac{1}{n_0 R^2}\sqrt{\frac{m}{T_0}}, \tag{D.9}$$

where we have used the relation $\sigma \sim R^2$, with R being the characteristic range of the interaction.

In addition to $\tau_{\rm mf}$, we must examine the characteristic time that two particles spend interacting during a collision, $\tau_{\rm int}$. Equation (D.2) implies that scattering is at low momentum. As a result, $\tau_{\rm int}$ does not scale with ξ since it is essentially a function of the details of the two-body potential and does not depend on v. The fraction of the time between two-body collisions during which the particles are interacting is $f \sim \tau_{\rm int}/\tau_2 \sim \xi^{-5}$.

To form a two-body bound state, a three-body collision is necessary. That is, while two particles are in the process of interacting, a third particle must collide with them. In terms of the quantities defined previously, the time scale for such events is simply $\tau_3 = \tau_2/f$. As a result, one sees that $\tau_{\rm meta}/\tau_{\rm fl} \sim \tau_3/\tau_2 \sim \xi^5$, as claimed above. Other mechanisms take longer parametrically: if the most rapid decay involves the formation of an N-body state, an analogous calculation yields $\tau_{\rm meta}/\tau_{\rm fl} \sim \xi^{5(N-1)}$.

To summarize, the arguments in this Appendix show that the variants of the KSS bound associated with quantum mechanics can be violated by a fluid with a large number of species. Depending on the choice of an interaction potential, the fluid that has been described can be either stable or metastable. While the example used to demonstrate the violation of the bound is highly artificial and unlikely to be realizable even approximately in a real world setting, as a mathematical matter it is a legitimate counterexample. The implication is that the most well-supported and most widely applicable variant of the KSS conjecture is not tenable.

Appendix E

A many species pion gas

This appendix examines how the restriction of the KSS bound to apply to only sensible, or UV complete, theories. The issue is whether it restricts the number of species preventing the increase of the Gibbs mixing entropy and thus preventing the types of counterexamples considered in Ref. [162]. The pion gas illustrates this issue nicely.

Consider a non-relativistic gas which is predominantly composed of one type of pion of mass m_π, for instance, the π^+. Such a gas undoubtedly has its origins in QCD, a UV-complete quantum field theory. To describe such a gas in the context of QCD, one can consider the theory at a finite temperature T, and a chemical potential μ_u for the up quark u of the form $\mu_u \overline{u}\gamma_0 u$. (It is unnecessary to also impose a chemical potential for the down quarks.) If the system is in the regime $T \ll m_\pi$ and $\Lambda \gg \mu_u > m_\pi$ where Λ is a typical hadronic scale of order 1 GeV, then it is essentially a non-relativistic gas of π^+ mesons. Now suppose that this is generalized to a many-species pion gas. To do this, QCD needs to be generalized to include N_f degenerate flavors of quarks with N_f large and even. Furthermore, a common chemical potential μ_c can be added for half of the flavors:

$$\sum_{j=1}^{N_f/2} \mu_c \overline{q}_j \gamma_0 q_j \tag{E.1}$$

while keeping $T \ll m_\pi$. This will create a non-relativistic system containing $N_f^2/4$

types of pions (each one with a quark of type q_j with $j \leq N_f/2$ and an anti-quark of type $\overline{q}_k$ with $k > N_f/2$). By carefully tuning μ_c while increasing N_f, the total density of pions can be kept fixed while increasing the number of species. This appears to allow one to create the conditions in which the Gibbs entropy dominates the ratio of η/s and causes a violation of the KSS bound.

However, there is a catch: Recall that for small g, the beta function for QCD is given by

$$\beta(g) = -\frac{g^3}{16\pi^2}\left(\frac{11N_c}{3} - \frac{2N_f}{3}\right) . \tag{E.2}$$

Asymptotic freedom requires that $11N_c > 2N_f$. By increasing N_f in order to violate the bound in Eq. (5.1), the underlying theory is pushed outside of the domain of "sensible" theories. Of course, one might try to evade this by increasing N_c at the same time as N_f is increased; by fixing the ratio N_c/N_f as the large N_f limit is taken, asymptotic freedom can be maintained. However, recall that the cross section for $\pi - \pi$ scattering scales as $1/N_c^2 \sim 1/N_f^2$ [20]. For a weakly interacting fluid, the shear viscosity is expected to scale with the inverse of the cross section [183]. Thus, by increasing N_c along with N_f to maintain asymptotic freedom and keep the theory sensible, one finds that $\eta \sim N_f^2$. On the other hand, the Gibbs mixing entropy grows only with $\log(N_f)$, so $\eta/s \sim N_f^2/\log(N_f)$ for large N_f. As a result, in a pion gas in the large number of species limit, the decrease in the cross section associated with the N_c scaling necessary to maintain asymptotic freedom overwhelms the increase in Gibbs mixing entropy due the to the N_f scaling, and η/s is driven to infinity in the combined $N_f \sim N_c \to \infty$ limit. Hence, the KSS bound can not be violated for

a large number of species of pions if the theory is kept "sensible."

Appendix F

Numerical results from single species fluid model

In this appendix, numerical results in support of the argument that the partition function increases with the number of resonant states N are presented. The effects of the states associated with the center of mass motion on the partition function and the effects of states associated with confining the wave functions in each cell as these states are independent of N, are neglected. The parameters of the potential Eq. (5.7) were chosen as follows (in arbitrary units):

$$r_{\max} = 1.0001; \quad L = 1; \quad m = \frac{1}{2}; \quad \hbar = k_B = 1. \tag{F.1}$$

Discussed in Sec. 5.3.3, one has to tune b and V_0 to produce narrow resonances, as N is increased. In Table F.1, the partition function and its logarithm are calculated for different values of N with suitably tuned values of b and V_0 at fixed temperature, are shown. The values for b were chosen to ensure the resonant states

N	b	V_0	T	Z_{sub}	$\ln(Z_{\text{sub}})$
5	100	$2,500.5$	1600	5.06	1.62
10	200	$10,001.8$	1600	10.46	2.35
15	350	$30,626.2$	1600	15.46	2.74
20	480	$57,601.9$	1600	20.98	3.04
30	700	$122,505$	1600	30.09	3.40

Table F.1: Numerical results showing the increase in the partition function Z_{sub} calculated using the variational ansatz. N is the number of resonant states; b is the strength of each delta function well in two-body interaction; V_0 is the strength of energy plateau that creates resonant states in the delta function wells; T is the chosen temperature.

were nearly degenerate, *i.e.*, the larger b value, the smaller the spread in energy of the resonant states. The values of V_0 were chosen such that all states were barely resonant states and not bound states, while the temperature, T, was chosen large compared with the highest resonant state energy but smaller than the lowest-lying state associated with the artificial confinement to within a cell.

Note that the partition function and its logarithm scales with larger number of resonant states as expected by Eq. (5.21). To further illustrate this, the partition functions and their logarithms are plotted in Figs. 3 and 4, along with linear and logarithmic best-fit curves, respectively.

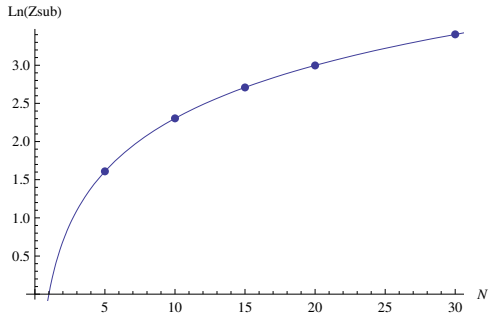

Figure F.1: Graph of the calculated partition function and a linear best-fit to the data.

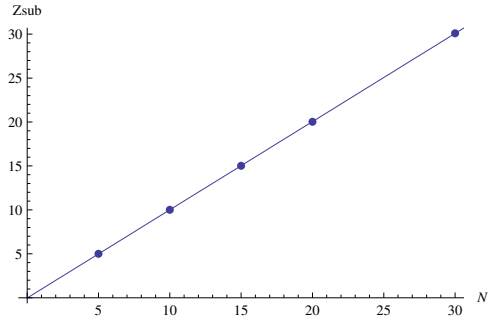

Figure F.2: Graph of calculated logarithm of the parition function and a logarithmic best-fit to the data.

This numerical data supports the argument that by increasing the number of

resonances in the potential of Eq. (5.7), it is possible to increase the lower bound on the partition function of the system, and thereby increase the lower bound on the entropy.

Bibliography

[1] D. J. Gross and Frank Wilczek. *Phys. Rev. Lett.*, 30:1343–1346, 1973.

[2] Steven Weinberg. *Phys. Rev. Lett.*, 31:494–497, 1973.

[3] H. Fritzsch, Murray Gell-Mann, and H. Leutwyler. *Phys. Lett.*, B47:365–368, 1973.

[4] D. J. Gross and Frank Wilczek. *Phys. Rev.*, D8:3633–3652, 1973.

[5] H. David Politzer. *Phys. Rev. Lett.*, 30:1346–1349, 1973.

[6] H. David Politzer. *Phys. Rept.*, 14:129–180, 1974.

[7] Thomas D. Cohen, Paul M. Hohler, and Richard F. Lebed. *Phys. Rev.*, D72:074010, 2005.

[8] Thomas D. Cohen and Paul M. Hohler. *Phys. Rev.*, D74:094003, 2006.

[9] Thomas D. Cohen and Paul M. Hohler. *Phys. Rev.*, D75:094007, 2007.

[10] Aleksey Cherman, Thomas D. Cohen, and Paul M. Hohler. 2007.

[11] Nathan Isgur and Mark B. Wise. *Phys. Lett.*, B232:113, 1989.

[12] Nathan Isgur and Mark B. Wise. *Phys. Lett.*, B237:527, 1990.

[13] Howard Georgi. *Phys. Lett.*, B240:447–450, 1990.

[14] Benjamin Grinstein. *Nucl. Phys.*, B339:253–268, 1990.

[15] Estia Eichten and Brian Russell Hill. *Phys. Lett.*, B234:511, 1990.

[16] Mark B. Wise. 1994.

[17] Mark B. Wise. *Phys. Rev.*, D45:2188–2191, 1992.

[18] Gerard 't Hooft. *Nucl. Phys.*, B72:461, 1974.

[19] Gerard 't Hooft. *Nucl. Phys.*, B75:461, 1974.

[20] Edward Witten. *Nucl. Phys.*, B160:57, 1979.

[21] S. K. Choi et al. *Phys. Rev. Lett.*, 91:262001, 2003.

[22] Darin E. Acosta et al. *Phys. Rev. Lett.*, 93:072001, 2004.

[23] V. M. Abazov et al. *Phys. Rev. Lett.*, 93:162002, 2004.

[24] B. Aubert et al. *Phys. Rev.*, D71:071103, 2005.

[25] K. Abe et al. 2005.

[26] K. Abe et al. 2004.

[27] G. Gokhroo et al. *Phys. Rev. Lett.*, 97:162002, 2006.

[28] K. Abe et al. 2007.

[29] T. Nakano et al. *Phys. Rev. Lett.*, 91:012002, 2003.

[30] V. V. Barmin et al. *Phys. Atom. Nucl.*, 66:1715–1718, 2003.

[31] A. E. Asratyan, A. G. Dolgolenko, and M. A. Kubantsev. *Phys. Atom. Nucl.*, 67:682–687, 2004.

[32] V. Kubarovsky et al. *Phys. Rev. Lett.*, 92:032001, 2004.

[33] A. Airapetian et al. *Phys. Lett.*, B585:213, 2004.

[34] S. Chekanov et al. *Phys. Lett.*, B591:7–22, 2004.

[35] M. Abdel-Bary et al. *Phys. Lett.*, B595:127–134, 2004.

[36] A. Aleev et al. *Phys. Atom. Nucl.*, 68:974–981, 2005.

[37] J. Barth et al. *Phys. Lett.*, B572:127–132, 2003.

[38] S. Stepanyan et al. *Phys. Rev. Lett.*, 91:252001, 2003.

[39] J. Z. Bai et al. *Phys. Rev.*, D70:012004, 2004.

[40] B. Aubert et al., 2004. hep-ex/0408064.

[41] K. Abe et al., 2004. hep-ex/0409010.

[42] Stephen R. Armstrong. *Nucl. Phys. Proc. Suppl.*, 142:364–369, 2005.

[43] S. Schael et al. *Phys. Lett.*, B599:1–16, 2004.

[44] Yu. M. Antipov et al. *Eur. Phys. J.*, A21:455–468, 2004.

[45] M. J. Longo et al. *Phys. Rev.*, D70:111101, 2004.

[46] Dmitry O. Litvintsev. *Nucl. Phys. Proc. Suppl.*, 142:374–377, 2005.

[47] Kevin Stenson. *Int. J. Mod. Phys.*, A20:3745–3748, 2005.

[48] K. Abe et al., 2004. hep-ex/0411005.

[49] Christopher Pinkenburg. *J. Phys.*, G30:S1201–S1206, 2004.

[50] I. Abt et al. *Phys. Rev. Lett.*, 93:212003, 2004.

[51] S. Nussinov, 2003. hep-ph/0307357.

[52] R. A. Arndt, I. I. Strakovsky, and R. L. Workman. *Phys. Rev.*, C68:042201, 2003.

[53] J. Haidenbauer and G. Krein. *Phys. Rev.*, C68:052201, 2003.

[54] Robert N. Cahn and George H. Trilling. *Phys. Rev.*, D69:011501, 2004.

[55] A. Sibirtsev, J. Haidenbauer, S. Krewald, and Ulf-G. Meissner. *Phys. Lett.*, B599:230–235, 2004.

[56] W. R. Gibbs. *Phys. Rev.*, C70:045208, 2004.

[57] M. Battaglieri et al. *Phys. Rev. Lett.*, 96:042001, 2006.

[58] K. H. Hicks, 2005. hep-ex/0510067.

[59] T. Nakano. *Int. J. Mod. Phys.*, A20:1543–1547, 2005.

[60] Dmitri Diakonov, Victor Petrov, and Maxim V. Polyakov. *Z. Phys.*, A359:305–314, 1997.

[61] Thomas D. Cohen. *Phys. Lett.*, B581:175–181, 2004.

[62] Dmitri Diakonov and Victor Petrov. *Phys. Rev.*, D69:056002, 2004.

[63] Nissan Itzhaki, Igor R. Klebanov, Peter Ouyang, and Leonardo Rastelli. *Nucl. Phys.*, B684:264–280, 2004.

[64] P. V. Pobylitsa. *Phys. Rev.*, D69:074030, 2004.

[65] Michal Praszalowicz. *Phys. Lett.*, B583:96–102, 2004.

[66] Michal Praszalowicz. *Acta Phys. Polon.*, B35:1625–1642, 2004.

[67] John R. Ellis, Marek Karliner, and Michal Praszalowicz. *JHEP*, 05:002, 2004.

[68] P. Schweitzer. *Eur. Phys. J.*, A22:89–95, 2004.

[69] R. L. Jaffe. *Eur. Phys. J.*, C35:221–222, 2004.

[70] F. Csikor, Z. Fodor, S. D. Katz, and T. G. Kovacs. *JHEP*, 11:070, 2003.

[71] Shoichi Sasaki. *Phys. Rev. Lett.*, 93:152001, 2004.

[72] N. Mathur et al. *Phys. Rev.*, D70:074508, 2004.

[73] N. Ishii et al. *Phys. Rev.*, D71:034001, 2005.

[74] Toru T. Takahashi, Takashi Umeda, Tetsuya Onogi, and Teiji Kunihiro. *Phys. Rev.*, D71:114509, 2005.

[75] B. G. Lasscock et al. *Phys. Rev.*, D72:014502, 2005.

[76] Ting-Wai Chiu and Tung-Han Hsieh. *Phys. Rev.*, D72:034505, 2005.

[77] F. Csikor, Z. Fodor, S. D. Katz, T. G. Kovacs, and B. C. Toth. *Phys. Rev.*, D73:034506, 2006.

[78] C. Alexandrou and A. Tsapalis. *Phys. Rev.*, D73:014507, 2006.

[79] Kieran Holland and K. Jimmy Juge. *Phys. Rev.*, D73:074505, 2006.

[80] Iain W. Stewart, Margaret E. Wessling, and Mark B. Wise. *Phys. Lett.*, B590:185–189, 2004.

[81] Marek Karliner and Harry J. Lipkin. *Phys. Lett.*, B575:249–255, 2003.

[82] M. Shmatikov. *Phys. Lett.*, B349:411–415, 1995.

[83] A. Aktas et al. *Phys. Lett.*, B588:17, 2004.

[84] J. M. Link et al. *Phys. Lett.*, B622:229–238, 2005.

[85] Margaret E. Wessling. *Phys. Lett.*, B603:152–158, 2004.

[86] Margaret E. Wessling, 2005. hep-ph/0505213.

[87] C. Gignoux, B. Silvestre-Brac, and J. M. Richard. *Phys. Lett.*, B193:323, 1987.

[88] Harry J. Lipkin. *Phys. Lett.*, B195:484, 1987.

[89] F. Stancu. *Phys. Rev.*, D58:111501, 1998.

[90] M. Genovese, J. M. Richard, F. Stancu, and S. Pepin. *Phys. Lett.*, B425:171–176, 1998.

[91] Robert L. Jaffe and Frank Wilczek. *Phys. Rev. Lett.*, 91:232003, 2003.

[92] Robert Jaffe and Frank Wilczek. *Phys. Rev.*, D69:114017, 2004.

[93] Elizabeth Ellen Jenkins and Aneesh V. Manohar. *JHEP*, 06:039, 2004.

[94] Dan Pirjol and Carlos Schat. *Phys. Rev.*, D71:036004, 2005.

[95] Thomas D. Cohen and Richard F. Lebed. *Phys. Rev. Lett.*, 91:012001, 2003.

[96] Thomas D. Cohen and Richard. F. Lebed. *Phys. Rev.*, D67:096008, 2003.

[97] Thomas D. Cohen and Richard F. Lebed. *Phys. Rev.*, D68:056003, 2003.

[98] Thomas D. Cohen and Richard F. Lebed. *Phys. Rev.*, D70:096015, 2004.

[99] Thomas D. Cohen and Richard F. Lebed. *Phys. Rev.*, D72:056001, 2005.

[100] Thomas D. Cohen, Daniel C. Dakin, Abhinav Nellore, and Richard F. Lebed. *Phys. Rev.*, D70:056004, 2004.

[101] Thomas D. Cohen, Daniel C. Dakin, Richard F. Lebed, and Daniel R. Martin. *Phys. Rev.*, D71:076010, 2005.

[102] Roger F. Dashen, Elizabeth Ellen Jenkins, and Aneesh V. Manohar. *Phys. Rev.*, D49:4713–4738, 1994.

[103] Thomas D. Cohen, Daniel C. Dakin, Abhinav Nellore, and Richard F. Lebed. *Phys. Rev.*, D69:056001, 2004.

[104] Thomas D. Cohen and Richard F. Lebed. *Phys. Lett.*, B578:150–155, 2004.

[105] Thomas D. Cohen and Richard F. Lebed. *Phys. Lett.*, B619:115–123, 2005.

[106] Chi-Keung Chow and Thomas D. Cohen. *Nucl. Phys.*, A688:842–870, 2001.

[107] Chi-Keung Chow and Thomas D. Cohen. *Phys. Rev. Lett.*, 84:5474–5477, 2000.

[108] A. Anastassov et al. *Phys. Rev.*, D65:032003, 2002.

[109] W.-M. Yao et al. Review of Particle Physics. *Journal of Physics G*, 33:1, 2006.

[110] Vladimir B. Kopeliovich. *Phys. Part. Nucl.*, 37:623–645, 2006.

[111] Thomas D. Cohen and Daniel C. Dakin. *Phys. Rev.*, C68:017001, 2003.

[112] Aneesh V. Manohar and Mark B. Wise. *Nucl. Phys.*, B399:17–33, 1993.

[113] Elizabeth Ellen Jenkins, Aneesh V. Manohar, and Mark B. Wise. *Nucl. Phys.*, B396:27–37, 1993.

[114] Zachary Guralnik, Michael E. Luke, and Aneesh V. Manohar. *Nucl. Phys.*, B390:474–500, 1993.

[115] Elizabeth Ellen Jenkins, Aneesh V. Manohar, and Mark B. Wise. *Nucl. Phys.*, B396:38–52, 1993.

[116] Z. Aziza Baccouche, Chi-Keung Chow, Thomas D. Cohen, and Boris A. Gelman. *Nucl. Phys.*, A696:638–666, 2001.

[117] Z. Aziza Baccouche, Chi-Keung Chow, Thomas D. Cohen, and Boris A. Gelman. *Phys. Lett.*, B514:346–354, 2001.

[118] Chi-Keung Chow, Thomas D. Cohen, and Boris Gelman. *Nucl. Phys.*, A692:521–545, 2001.

[119] Boris A. Gelman, 2002. hep-ph/0203246.

[120] T. H. R. Skyrme. *Proc. Roy. Soc. Lond.*, A262:237–245, 1961.

[121] Edward Witten. *Nucl. Phys.*, B223:433–444, 1983.

[122] J. Wess and B. Zumino. *Phys. Lett.*, B37:95, 1971.

[123] Gregory S. Adkins, Chiara R. Nappi, and Edward Witten. *Nucl. Phys.*, B228:552, 1983.

[124] E. Guadagnini. *Nucl. Phys.*, B236:35, 1984.

[125] Aneesh V. Manohar. *Nucl. Phys.*, B248:19, 1984.

[126] Jr. Callan, Curtis G. and Igor R. Klebanov. *Nucl. Phys.*, B262:365, 1985.

[127] Jr. Callan, Curtis G., Kent Hornbostel, and Igor R. Klebanov. *Phys. Lett.*, B202:269, 1988.

[128] Gustavo Burdman and John F. Donoghue. *Phys. Lett.*, B280:287–291, 1992.

[129] Tung-Mow Yan et al. *Phys. Rev.*, D46:1148–1164, 1992.

[130] Yong-seok Oh and Byung-Yoon Park. *Z. Phys.*, A359:83–90, 1997.

[131] Yong-seok Oh and Byung-Yoon Park. *Mod. Phys. Lett.*, A11:653–662, 1996.

[132] Yong-seok Oh and Byung-Yoon Park. *Phys. Rev.*, D53:1605–1615, 1996.

[133] Yong-seok Oh and Byung-Yoon Park. *Phys. Rev.*, D51:5016–5029, 1995.

[134] Dong-Pil Min, Yong-seok Oh, Byung-Yoon Park, and Mannque Rho. *Int. J. Mod. Phys.*, E4:47–122, 1995.

[135] Yong-seok Oh, Byung-Yoon Park, and Dong-Pil Min. *Phys. Rev.*, D50:3350–3367, 1994.

[136] Yong-seok Oh, Byung-Yoon Park, and Dong-Pil Min. *Phys. Lett.*, B331:362–370, 1994.

[137] Gregory S. Adkins and Chiara R. Nappi. *Nucl. Phys.*, B233:109, 1984.

[138] Aneesh V. Manohar and Mark B. Wise. *Camb. Monogr. Part. Phys. Nucl. Phys. Cosmol.*, 10:1–191, 2000.

[139] Martin J. Savage and Mark B. Wise. *Phys. Lett.*, B248:177–180, 1990.

[140] M. Mattson et al. *Phys. Rev. Lett.*, 89:112001, 2002.

[141] M. A. Moinester et al. *Czech. J. PHys.*, 53:B201–B213, 2003.

[142] A. Ocherashvili et al. *Phys. Lett.*, B628:18–24, 2005.

[143] J. A. Russ, 2003. www-selex.fnal.gov/documentation/fnal.gov.

[144] Jie Hu and Thomas Mehen. *Phys. Rev.*, D73:054003, 2006.

[145] B. Aubert et al. *Phys. Rev.*, D74:011103, 2006.

[146] Nora Brambilla, Antonio Vairo, and Thomas Rosch. *Phys. Rev.*, D72:034021, 2005.

[147] Sean Fleming and Thomas Mehen. *Phys. Rev.*, D73:034502, 2006.

[148] J. P. Ader, J. M. Richard, and P. Taxil. *Phys. Rev.*, D25:2370, 1982.

[149] D. Ebert, R. N. Faustov, V. O. Galkin, and A. P. Martynenko. *Phys. Rev.*, D66:014008, 2002.

[150] Geoffrey T. Bodwin, Eric Braaten, and G. Peter Lepage. *Phys. Rev.*, D51:1125–1171, 1995.

[151] W. E. Caswell and G. P. Lepage. *Phys. Lett.*, B167:437, 1986.

[152] A. Pineda and J. Soto. *Nucl. Phys. Proc. Suppl.*, 64:428–432, 1998.

[153] Nora Brambilla, Antonio Pineda, Joan Soto, and Antonio Vairo. *Nucl. Phys.*, B566:275, 2000.

[154] Nora Brambilla, Antonio Pineda, Joan Soto, and Antonio Vairo. *Rev. Mod. Phys.*, 77:1423, 2005.

[155] Michael E. Luke, Aneesh V. Manohar, and Ira Z. Rothstein. *Phys. Rev.*, D61:074025, 2000.

[156] S. Fleck and J. M. Richard. *Prog. Theor. Phys.*, 82:760–774, 1989.

[157] V. V. Kiselev and A. K. Likhoded. *Phys. Usp.*, 45:455–506, 2002.

[158] Aneesh V. Manohar and Iain W. Stewart. *Phys. Rev.*, D62:074015, 2000.

[159] E. Eichten, K. Gottfried, T. Kinoshita, K. D. Lane, and Tung-Mow Yan. *Phys. Rev.*, D17:3090, 1978.

[160] Pavel Kovtun, Dam T. Son, and Andrei O. Starinets. *JHEP*, 10:064, 2003.

[161] P. Kovtun, D. T. Son, and A. O. Starinets. *Phys. Rev. Lett.*, 94:111601, 2005.

[162] Thomas D. Cohen. *Phys. Rev. Lett.*, 99:021602, 2007.

[163] Dam T. Son and Andrei O. Starinets. *Ann. Rev. Nucl. Part. Sci.*, 57:95–118, 2007.

[164] Thomas Schafer. *Phys. Rev.*, A76:063618, 2007.

[165] A. Adare et al. *Phys. Rev. Lett.*, 98:172301, 2007.

[166] Tetsufumi Hirano and Miklos Gyulassy. *Nucl. Phys.*, A769:71–94, 2006.

[167] Tetsufumi Hirano, Ulrich W. Heinz, Dmitri Kharzeev, Roy Lacey, and Yasushi Nara. *Phys. Lett.*, B636:299–304, 2006.

[168] J. L. Nagle. *Eur. Phys. J.*, C49:275–279, 2007.

[169] Sibasish Laha et al., 2007. hep-ph/0702086.

[170] Antonio Dobado and Felipe J. Llanes-Estrada. *Eur. Phys. J.*, C49:1011–1013, 2007.

[171] Jiunn-Wei Chen, Yen-Han Li, Yen-Fu Liu, and Eiji Nakano. *Phys. Rev.*, D76:114011, 2007.

[172] Hui Liu, Defu Hou, and Jiarong Li, 2006.

[173] Eric Gourgoulhon and Jose Luis Jaramillo. *Phys. Rev.*, D74:087502, 2006.

[174] Jiunn-Wei Chen and Eiji Nakano. *Phys. Lett.*, B647:371–375, 2007.

[175] Antonio Dobado and Felipe J. Llanes-Estrada. *Eur. Phys. J.*, C51:913–918, 2007.

[176] Paul Romatschke and Ulrike Romatschke. *Phys. Rev. Lett.*, 99:172301, 2007.

[177] Juan Martin Maldacena. *Adv. Theor. Math. Phys.*, 2:231–252, 1998.

[178] S. S. Gubser, Igor R. Klebanov, and Alexander M. Polyakov. *Phys. Lett.*, B428:105–114, 1998.

[179] Edward Witten. *Adv. Theor. Math. Phys.*, 2:253–291, 1998.

[180] Ofer Aharony, Steven S. Gubser, Juan Martin Maldacena, Hirosi Ooguri, and Yaron Oz. *Phys. Rept.*, 323:183–386, 2000.

[181] Alex Buchel, James T. Liu, and Andrei O. Starinets. *Nucl. Phys.*, B707:56–68, 2005.

[182] Boris A. Gelman, Edward V. Shuryak, and Ismail Zahed, 2004. nucl-th/0410067.

[183] R. L. Liboff. *Kinetic theory: classical, quantum, and relativistic descriptions.* Springer-Verlag, New York, USA, 3rd edition, 2003. The Boltzmann equation, viscosity and dilute gases are described in any standard textbook on kinetic theory. This is just one example.